DESIGN OF TEMPORARY SUBSEA INSTALABLE PRESSURE CAP

DESIGN AV TEMPORÆRT UNDERVANNS INSTALLERBART TRYKKLOKK

Lars Ola Birger Rimmereid

Design of Temporary Subsea Installable Pressure Cap

A Master Thesis by Lars Ola Birger Rimmereid

In cooperation with

AkerSolutions

PREFACE

This master thesis is the final part of a master degree program in Machinery and Product Development at the Norwegian university of life science (UMB). The time duration of the thesis was from January to May 2013 and it gives 30 credits. It is performed in collaboration with the Subsea Tie-In product group at Aker Solutions.

The master thesis is a continuation of a preliminary study carried out in the autumn semester 2012 in the course *Concept and product realization* (Tip300). The objective of the preliminary study was to generate a new concept proposal for a temporary subsea installable pressure cap. The result was a concept that had the potential of solving challenges related to Aker Solutions horizontal connection system. The main objective of the master thesis was to provide data of whether this cap would function as intended and tolerate the applied load. This relates to the connection principle itself and the locking mechanism. Mathematical computations and finite element analysis were used to provide data. The thesis begins with an introduction of the mission statement. Then the results from the preliminary project are presented and analyzed, followed by a presentation and an evaluation of a modified design.

When the preliminary design was analyzed, the result indicated that the construction did not tolerate the loads. The preliminary design was therefore rejected and a new design proposal was made.
To verify the new proposal, it was assessed in the same way as the preliminary design. Different components were evaluated and optimized. The goal was to end up with a more robust and functional design than in the preliminary study. However, it is still required to modify the design further in order to achieve a design where all the components withstand the operational loads. More developmental work is also needed to find a solution for the guiding and alignment of the cap.

The master thesis contains a description of the design process for a pressure cap and gives an introduction of the assessment of a mechanism consisting of an angle lever and a linkage arm. A step by step approach of dimensioning against static loads for pin bolts, linkages and power screws is described in detail. It also contains a description of how to set up a simulation model of a pressure contained connection. Additionally, this thesis provides a brief understanding of the complexity and challenges that can be encountered when working with subsea connection systems.

First I would like to thank my industrial supervisor Senior Engineer Dag Emanuelson, product manager for caps at Aker Solutions for his useful advices in this project with design and general information about subsea equipment. I would also like to thank Lars Haga, manager for the Tie-In product group for giving me the opportunity to perform this project through Aker Solutions and for giving motivating feedback. A thank you goes to Lead Engineer Kristoffer Holmström that has a broad knowledge when it comes to Finite analysis and has given me helpful advices regarding setting up a reasonable simulation model. A thank you also goes out to the rest of the people at Aker Solutions Tie-In department that has contributed with their knowledge and their expertise during this project.
I would also especially like to thank my academic supervisor, Associate Professor Geir Terjesen and First Chief Engineer at Aker Solutions Knut Møgedal for advice and instruction regarding calculations, your contribution to this project has been highly valuable. Least but not last, I would like to thank my girlfriend Tonje Danielsen Rongved for her support throughout this project.

Ås 15.05.2013

_____
Lars Rimmereid

ABSTRACT

The development of subsea equipment is important in the oil and gas industry because it would be beneficial if the subsea operations could be even more efficient and cost effective. Aker Solutions is one of the leading companies in this industry and they have recently launched a new horizontal connection system. Equipment to this system is under a constant development and one of the products that are not even introduced yet is the twelve inch temporary subsea installable pressure cap. In the preliminary study performed in the autumn semester of 2012, a concept proposal for this type of cap was generated. The main purpose of this master thesis was to investigate the preliminary concept and generate a new design proposal if needed. The assessment of the designs was performed with the aid of hand calculations and finite element analysis.

The project was initiated with a literature study in order to find suitable formulas and methods that were needed when dimensioning the design. Useful books were *"Design of machine elements"* by Bhandari V.B and *"Theory of machines and mechanisms lll"* by Phakatkar H.G. The former provided a practical approach on how to assess the frictional loss in linkages with pin joints, while the second one provided methods for dimensioning pin bolts and power screws. The standard *"ASME 8 div. 2, rules for construction of pressure vessel (section about: design rules for clamped connections)"* provided useful data when investigating what kind of clamp force that was needed.

The computer aided design software SolidWorks was used for making a three dimensional model of the design. SolidWorks Simulation was used to perform a simple simulation and it can acquire relatively quick indication of the stress behavior of a design with simple geometry. Ansys Classic also provides a quick method to make a simple model with a fast computation time. The Ansys Classic software has the advantages of changing input variables and parameters quickly. This was performed by changing the source code of the input file when the geometry, loading and boundary conditions were altered. Abaqus software was used to achieve data for the more advanced geometries and loading scenarios and was an important tool to use when conducting results regarding the separation that occurs between the connected components. It was advantageous to use Abaqus because of the possibility of getting assistance from competent personnel within the Aker Solutions organization.

The preliminary design was rejected because it did not withstand the applied load and a new design proposal was therefore generated. Several components were assessed and modified so that the design could be more robust. The calculations and analysis carried out in this project indicates that the design can tolerate the internal pressure it is exposed for. The peak separation obtained from the simulations resulted in a separation at the sealing area of 0.31mm. It was also found that most of the effective contact area of the cap is located at the top and bottom of the connection. Several components of the locking mechanism were designed against static loads, which resulted in positive values. The total force required to be applied by the power screw was reduced from 1643kN in the preliminary design to only 286kN in the final design. The linkages have been controlled against crushing and buckling failure, which gave a safety factor of 2.6 and 6.4. The pin has been controlled for bending moment and shearing failure, which satisfy the Eurocode 3 requirement. The power screw has been controlled against shearing, buckling and crushing failure and resulted in a safety factor of 2.5, 7.9 and 5.3.

Some components need more investigation before it is a fully finished design. Also, more time is needed on the analysis to perform a convergence study and optimize the design in order to lower the stress concentrations. This is considered to be a manageable task to perform at a later stage. Another aspect that needs to be solved is the necessity of a developed guiding and alignment solution for the cap. This task has a higher degree of uncertainties, because a promising solution does not exist at the moment.

SAMMENDRAG

I olje- og gass industrien er det viktig med en kontinuerlig utvikling av undervannsutstyr fordi det vil være nyttig å gjøre operasjonene på havbunnen enda mer effektive og kostnadsbesparende. Aker Solutions er en av de ledende leverandørene i denne industrien og de har relativt nylig introdusert et horisontalt tilkoblingssystem. Utstyr til dette systemet er under en stadig utvikling og et av produktene som enda ikke er introdusert på markedet er et tolv tommer temporært undervanns installerbart trykklokk. Et konseptforslag for et slikt lokk ble utviklet under forprosjektet i høstsemesteret 2012. Hovedmålet med denne masteroppgaven var å undersøke konseptet fra forprosjektets og eventuelt lage et nytt designforslag om nødvendig. Designet ble undersøkt ved hjelp av håndberegninger og spenningsanalyser.

Prosjektet ble initiert med en litteratur studie for å finne formler og metoder som kunne brukes til å dimensjonere designet. Nyttige bøker var "*Design of machine elements*" av Bhandari V.B og "*Theory of machines and mechanisms lll*" av Phakatkar H.G. Førstnevnte gir en praktisk metode for å beregne friksjonstapet i mekanismer med leddforbindelser, mens den andre ga gode beskrivelser av metoder for å dimensjonere leddbolter og løfteskruer. Standarden "*ASME 8 div. 2, rules for construction of pressure vessel (section about: design rules for clamped connections)*" ble brukt for å finne nyttige data om hvilken forspenningskraft som var nødvendig i tilkoblingen.

Modellerings programvaren SolidWorks ble benyttet for å lage en tre-dimensjonal modell. SolidWorks Simulation ble brukt for å kjøre en forenklet styrkeanalyse av den ukompliserte geometrien og programmet ga raske indikasjoner på spenningene som oppstår i et design med enkel geometri og lastscenario. Ansys Classic er også et effektivt program som ble brukt for å sette opp en forenklet simuleringsmodell. Fordelen med denne programvaren er at den gjorde det enkelt å endre inndata til geometri, laststørrelse og fastlåsningsvilkår. Dette ble gjort ved å endre kildekoden til inndatafilen. Programvaren Abaqus ble benyttet for å analysere den mer komplekse geometrien og lastscenarioet. Dette var et nyttig verktøy for å innhente data om seperasjonen som oppstår ved tetningsområdet for tilkoblingen. En annen fordel med Abaqus er at det var mulig med veiledning hos Aker Solutions organisasjonen.

Designet fra forprosjektet ble forkastet fordi det ikke var i stand til å håndtere de gitte belastningene. Et nytt designforslag ble generert og flere av komponentene ble vurdert og modifisert for å oppnå et mer robust design. Kalkulasjonene og analysene i denne masteroppgaven gir indikasjoner på at det nye designet kan tolerere de belastninger som den blir utsatt for. Analysen resulterte i en maksimal seperasjon i tetningsområdet på 0.31mm med design trykket. Det ble også vist at tilkoblingen hadde mesteparten av den effektive kontaktflaten i topp og bunn av lokktilkoblingen. Flere av komponentene i lukkemekanismen ble designet mot statisk belastning og resulterte i et akseptabelt resultat. Den totale kraften som er nødvendig å bli påført av løfteskruen ble redusert fra 1643kN i designet fra forprosjektet til bare 286kN i det endelige designet. Lenkearmene ble kontrollert mot hullkanttrykk og knekking som gav en sikkerhetsfaktor på 2.6 og 6.4. Leddboltene ble kontrollert mot bøyemoment og avskjæring og resultatet er i henhold til Eurokode 3 standarden. Løfteskruen har blitt dimensjonert mot avskjæring, knekking og lagertrykk og ga en sikkerhetsfaktor på 2.5, 7.9 og 5.3.

Flere av komponentene trenger videre undersøkelser før man kan anse designet som ferdig dimensjonert. Det må brukes mer tid på analysen av lokket og det må utføres en konvergensstudie. Stresskonsentrasjonene må reduseres ved å optimalisere geometrien. Disse oppgavene anses som relativt enkle å utføre senere. En utfordring er å utvikle en løsning for styring og innretting av lokket i forbindelse med installasjon og fjerning. Denne oppgaven har en større grad av usikkerhet fordi en løsning på dette ikke eksisterer per dags dato.

TABLE OF CONTENTS

SUBSEA TERMS

Flowlines   Subsea flowlines are the subsea pipelines that are used to connect a subsea facility to another, for example a manifold to a wellhead. Flowlines can transport oil and gas products, lift gas, injection water and chemicals.

Hot stab   A hot stab is a device that is used to move fluid subsea (often hydraulic fluid) from one device to another by a ROV.

Hydrocarbons   Hydrocarbons in a liquid form are referred to as petroleum or mineral oil, whereas hydrocarbons in a gaseous form are referred to as natural gas.

Jumper   A jumper is a pipeline with connectors at both ends and it is used to transport production fluid or injector fluid between two subsea components.

Manifold   A manifold collects the produced fluid from the wells and distributes it further to other facilities.

Manipulator   A manipulator is a ROV arm.

Metrology   Metrology is used subsea to acquire accurate measurements of the vertical and horizontal distance between subsea assets.

Porch   A porch is the connection structure located on the inboard side.

Retrievable   The term retrievable means removing a component or unit subsea.

Riser   A Riser is a conducting pipe, connecting subsea wellheads, templates and pipelines to equipment that is located on a floating production Installation or fixed offshore structure.

Satellite   A satellite well is an individual subsea well that have the ability to produce oil and gas directly to a surface facility.

Stroke tool   A stroke tool is a hydraulic standard subsea tool operated by a ROV and are typically used for stroking a termination towards a porch.

Termination   A termination is the connection structure located on the outboard side.

Tie-in   Tie-in is a connection system that connects subsea units to each other and make sure that there are securely tied in connections to subsea wells, manifolds and other subsea units.

Torque tool   A torque tool is a hydraulic standard subsea tool operated by a ROV and can provide a torque up to 17 kNm.

Top-site   Top-site is the vessel, rig or onshore location.

Umbilicals   Umbilicals are cables containing electrical wires, hydraulic lines and inhibitors.

ABBREVIATIONS

AKS   Aker Solutions.

BST   Back seal testing (performed after a connection to test the sealing for leakage).

HCS   Horizontal connection system.

IB   Inboard side (connection side located on the subsea unit).

LP   Low pressure.

MEG   Monoethylene glycol (chemical with low freezing point that protect against corrosion, commonly known as antifreeze fluid).

OB   Outboard side (the connection side located at the end of a pipeline, umbilical etc).

ROV   Remotely underwater operated vehicle.

VCS   Vertical connection system.

XMT   Christmas tree (a unit that regulates the flow and the pressure out of a well).

TT   Torque tool.

SIT   System Integration Test (generally refers to an extensive series of tests performed on all of the related subsea equipment. SIT is usually intended to pick up where Factory Acceptance Test (FAT) ended).

ST   Stroke tool.

CAD   Computer aided design.

EC3   The Eurocode 3 standard.

SYMBOLS

Si symbol	Si unit	Description
A	mm^2	Cross section area.
A_c	mm^2	Elongated area of the clamp segments.
A_h	mm	Hub face to cap disc contact area.
b	mm	Breadth of cross section.
D	mm	Effective bore diameter.
D_c	mm	Cross section distance at clamp segment.
D_i	mm	Inner diameter of collar.
D_o	mm	Outer diameter of collar.
D_1	mm	Vertical distance between the two pin joints for the linkage.
D_2	mm	Horizontal distance between the two pin joints of the linkage.
D_3	mm	Vertical distance between the lower linkage joint and clamp hinge.
D_4	mm	Horizontal distance between the lower linkage joint and clamp hinge.
D_5	mm	Vertical distance from the point where the required clamp force is applied and the clamp hinge.
D_6	mm	Vertical distance from the point where the required clamp force is applied and the clamp segment hinge.
D_7	mm	Lever arm length.
D_8	mm	Linkage length.
D_9	mm	Normal distance from pin joint A and clamp segment hinge.
D_{10}	mm	Distance from pin joint B to clamp segment hinge parallel to the linkage.
D_{11}	mm	Normal distance from pin joint B to clamp segment hinge.
D_{12}	mm	Partial length of the linkage.
d	mm	Diameter.
d_c	mm	Core diameter of threads.
d_m	mm	Median diameter of threads.
d_n	mm	Nominal diameter.
E	GPa	Modulus of elasticity for the material.
F	kN	Concentrated force.
$F_{Q'}$	kN	Applied load on the linkage when acounting for friction in pin joints.
$F_{1',total}$	kN	Total applied load when accounting for friction.
$F_{N,x}$	kN	x-component of the normal force.
$F_{N,y}$	kN	y-component of the normal force.

F_N	kN	Normal force on clamp segments.
F_Q	kN	Applied load on a linkage when the friction is neglected.
F_a	kN	Additional force.
$F_{b,Rd}$	kN	Resistance dimensioning value against bearing force.
F_c	kN	Clamp force after the internal pressure as been applied.
$F_{f,x}$	kN	x-component of the friction force.
$F_{f,y}$	kN	y-component of the friction force.
F_f	kN	Friction force.
F_k	kN	Maximum langitudial force before buckling (critical load).
F_n	kN	Normal force acting in the linkage.
$F_{ts,total}$	kN	Tension in clamp segments after the internal pressure as been applied.
F_{ts}	kN	Tension in clamp segments.
$F_{v,Rd}$	kN	Resistance dimensioning value against shear force.
F_0	kN	Applied clamp force in radial direction.
$F_{1,total}$	kN	The total force applied by the power screw.
F_1	kN	Applied force from power screw, at one side of the horizontal plate.
$F_{1'}$	kN	Vertical applied force when accounting for friction.
F_2	kN	The horizontal bearing resultant force applied on the clamp segment hinge.
F_3	kN	Required clamp force.
H	kN	Total hydrostatic end force.
h	mm	Height of cross section.
H_p	kN	Total joint contact surface compression load.
I	mm^4	Moment of inertia.
I_0	mm^4	The least moment of inertia.
i	mm	Radius of inertia.
I_x	mm^4	Moment of inertia about x-axis.
I_y	mm^4	Moment of inertia about y-axis.
l	mm	Length of beam.
l_f	mm	Lead of the thread.
l_k	mm	Effective length of a coloumn.
M_{p_1}	kNm	Moment in point p_1.
M_{Rd}	kNm	Resistance dimensioning value against bending moment.
M_b	kNm	Bending moment.
M_t	kNm	Power screw torque to raise a load.
$(M_t)_c$	kNm	Required torque to be applied to overcome collar friction.

$(M_t)_t$	kNm	Total torque applied on screw.
n_b	-	Safety factor against buckling.
n_c	kN	Clamp force safety factor.
n_y	-	Safety factor against yielding.
P	MPa	Design pressure.
R_{eH}	Mpa	Yeild strength.
R_m	MPa	Tensile Strength (ultimate strength).
R_{pj}	mm	Radius of pin.
r_i	mm	Inner radius of the segemnt ring.
r_o	mm	Outer radius of the segment ring.
r_{pj}	mm	Radius of the frictinal circle.
t	mm	Thread thickness.
t_h	mm	Thickness of horizontal plate (nut).
t_l	mm	Thickness of linkage.
W	mm^3	Section modulus.
w	kN	Axial load provided by the power screw.
w_0	kN	Total clamp connection design bolt load for both lugs for the operating condition.
$x^{'}$	mm	Lever arm length when accounting for friction.
y	mm	Distance from surface to nautral axis of a cross section.
z	-	Number of threads engaged with the nut.

Greek letters:

α	° (degrees)	Clamp shoulder angle.
$\alpha^{'}$	° (degrees)	Angle to determine the vertical applied load to the horizontal plate when accounting for friction.
α_p	° (degrees)	Pitch angle.
$\beta^{'}$	° (degrees)	The inclination of the friction axis.
β	° (degrees)	The angle between D_{12} and D_9.
γ_{M0}	-	Material factor from EC3.
γ_{M2}	-	Material factor from EC3.
δ	mm	Elongation.
δ_1	mm	Elongation for the clamp segments.
δ_2	mm	Elongation at the hub/cap disc contact area.
θ	° (degrees)	Thread Angle.
θ_1	° (degrees)	Linkage angle.
λ	-	Slimness ratio.
$\lambda_{transistion}$	-	The transistion slimness ratio.
μ_c	-	Friction coeffecient acting between clamp segments and hub/cap disc.
μ_{co}	-	Friction coeffecient of the collar bearing.
μ_{pj}	mm	Friction coeffecient of the pin.
μ_t	-	Friction coeffecient for screw threads.

σ_b	MPa	Bending stress.
σ_c	MPa	Compression stress.
σ_k	MPa	Buckling strength.
τ_{max}	MPa	Principal shear stress.
τ	MPa	Shear stress.
ϕ_f	° (degrees)	Friction angle.

FORMULAS

Index	Formula	Description	Reference
2.1	$$w_0 = \frac{2}{\pi}\left(H + H_p\right)\tan[\alpha\text{-}\phi_f]$$	Determines the total required bolt force.	[30]
2.2	$$M_b = \frac{Fl}{4}$$	Moment in the middle of a horizontal beam constrained with a fixed joint in both ends and a consentrated force applied at the middle.	[32]
3.1	$$r_{pj} = \mu_{pj}R_{pj}$$	Radius of the friction circle.	[38]
3.2	$$t_l > \sqrt{\frac{F_Q \cdot \gamma_{M0}}{R_{eH}}}$$	Design requirement for eye thickness in a bolted joint connection.	[39]
3.3	$$M_b \leq M_{Rd} = 1{,}5W_b\frac{R_{eH}}{\gamma_{M0}}$$	Design requirement for bending moment in pin joints.	[39]
3.4	$$F_{Q'} \leq F_{v,Rd} = 0{,}5A\frac{R_m}{\gamma_{M2}}$$	Design requirement for shearing failure of pin.	[39]
3.5	$$\left(\frac{F_{Q'}}{F_{Rd}}\right)^2 + \left(\frac{M_b}{M_{Rd}}\right)^2 \leq 1$$	Design requirement for interaction between shearing and bending moment.	[39]
3.6	$$F_{Q'} \leq F_{b,Rd} = 1{,}5t_l d\frac{R_m}{\gamma_{M0}}$$	Design requirement for crushing failure in base material.	[39]
3.7	$$\lambda = \frac{l_k}{i}$$	Slenderness ratio.	[44]
3.8	$$i = \sqrt{\frac{I_0}{A}}$$	The radius of inertia of a cross section is difined as the square root of the moment of inertia divided with the cross section area.	[41]
3.9	$$\sigma_k = 335\text{-}0.62\lambda$$	Buckling strength of st50/st60 material.	[45]
3.10	$$\tan\alpha_p = \frac{l_t}{\pi d_m}$$	Pitch angle.	[48]
3.11	$$M_t = \frac{wd_m}{2}\frac{\left(\frac{\mu_t}{\cos\theta} + \tan\alpha_p\right)}{\left(1\text{-}\frac{\mu_t}{\cos\theta}\tan\alpha_p\right)}$$	Required torque to be applie on the power screw.	[49]
3.12	$$(M_t)_c = \frac{\mu_{co}w}{4}(D_0 + D_i)$$	Torque required to overcome the collar friction.	[49]
3.13	$$\sigma_c = \frac{w}{\left(\frac{\pi}{4}d_c^2\right)}$$	Direct compression in power screw.	[50]
3.14	$$\tau = \frac{16(M_t)_t}{\pi d_c^3}$$	Shear stress in power screw from the applied torque.	[50]
3.15	$$\tau_{max} = \sqrt{\left(\frac{\sigma_c}{2}\right)^2 + (\tau)^2}$$	Maximum principle stress.	[50]
3.16	$$\tau = \frac{w}{\pi d_c tz}$$	Transverse shear stress in screw.	[50]
3.17	$$\tau = \frac{w}{\pi d_n tz}$$	Transvere shear stress in nut.	[50]

3.18	$$s_b = \frac{4w}{\pi z\left(d_n{}^2 - d_c^2\right)}$$	The bearing pressure between the contact surface between the nut and screw.	[51]
3.19	$$\lambda_{transition} = \sqrt{\frac{2\pi^2 E}{R_{eH}}}$$	The Euler-Johnson transistion slimness ratio.	[52]
3.20	$$\sigma_k = R_{eH} - \frac{R_{eH}{}^2}{4\pi^2 E}\left(\frac{l_k}{i}\right)^2$$	Critical buckling stress (johnson equation).	[52]
3.21	$$\delta = \frac{FDc}{EA}$$	Elongation of a cross section.	[53]
3.22	$$F_a = \frac{H}{1 + \frac{\delta_1}{\delta_2}}$$	Additional force.	[54]

1   INTRODUCTION

In the beginning of the 1970's, Norway started establishing offshore oil industry on the continental shelf. Today this is the major contributor to governmental income, the industry generates jobs for thousands of people and it has played a major role for developing the Norwegian welfare system. Associated with this, development of new subsea technology is an important priority area on the Norwegian continental shelf and internationally. This is important because development and improvement of subsea systems make it possible to recover more oil and gas from the reservoirs in a more efficient way. It also makes it possible to extend the operating life of existing platforms and infrastructure and operate in very deep waters. The subsea segment is been a field of business where Norwegian contractors have a leading technology [02]. One of those contractors is Aker Solutions and they deliver engineering and technology for the oil and gas industry. The company has approximately 25 000 employees in more than 30 countries [03].
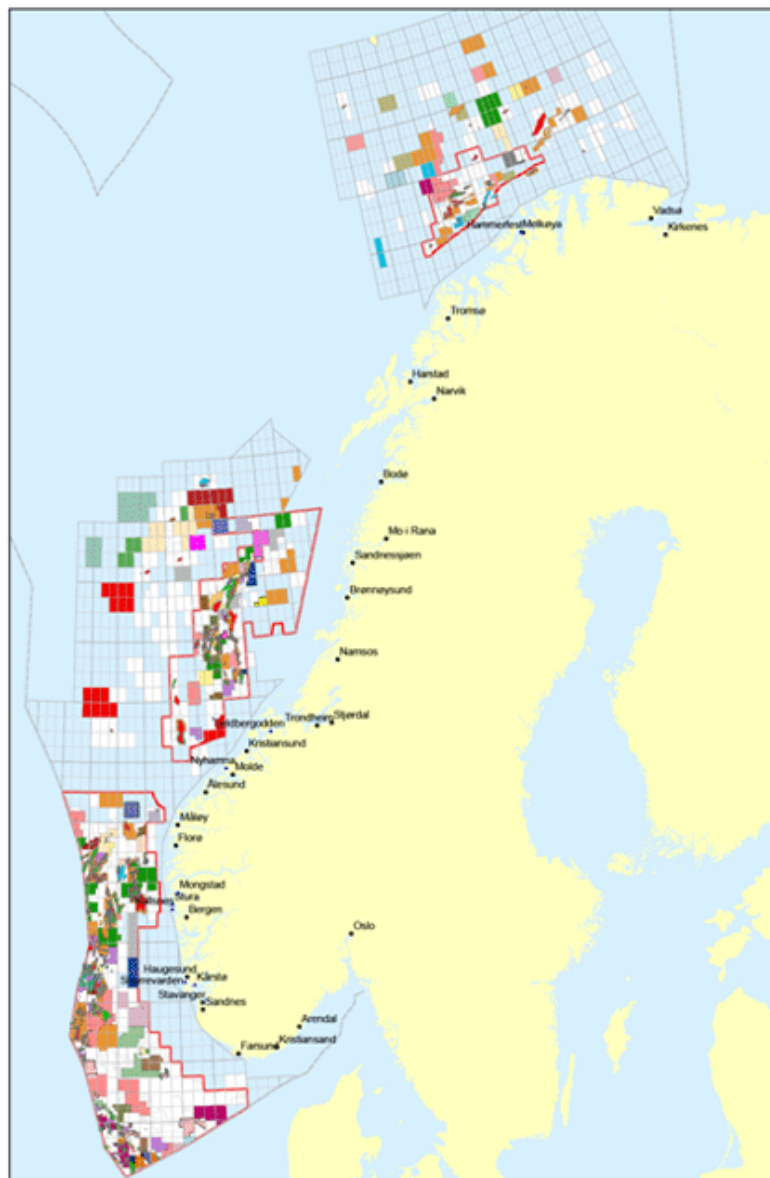
Fig 1.1 An overview of the Norwegian continental shelf with all the oil and gas fields [01].

Subsea systems have advanced from shallow-water, manually operated systems into systems capable of operating via remote control at water depths down to 3 000 meters and in harsher environmental conditions. The subsea technology that is used for oil and gas production is a highly

specialized field of application that place particular demands on engineering. This is mainly because of the inaccessibility of the subsea installations and therefore a remotely controlled installation and operation of the subsea equipment is required. For succeeding in developing new subsea equipment and technology, it is required to strive towards the most reliable, safe and cost-effective solutions. The hiring costs related to vessel, installation equipment and crew is a significant portion of the total costs of subsea equipment. A reduced installation time, fewer personnel or less and simple equipment needed for the installation would have a large impact on the total amount of costs [04].

Subsea tie-backs are becoming popular in the development of new oil and gas reserves. With larger oil and gas discoveries becoming less common, attention has turned to previously untapped, less economically viable discoveries. Tie-back development is the use of old existing facilities and infrastructure which is connected and utilized in a new oil field. This saves time and cost which makes smaller discoveries that in the first place was nearly unprofitable, could now be possible with economic benefits.

The industry maintains strictly safety requirements and well-known and proven technology is often preferred instead of non-proven technology, even if the latter provides significant operational improvement or cost-efficiency. For that reason, comprehensive testing and qualification of the new technology is required before new subsea equipment is introduced.

1.1　SUBSEA EQUIPMENT

To give an understanding of what kind of concept that was developed in this master thesis, a brief explanation of the associated components related to the temporary pressure inboard cap will be given below. The deployment of subsea equipment requires specialized and expensive vessels, which need to be equipped with diving equipment for relatively shallow equipment work, and robotic equipment for deeper water depths [05]. Today, the use of almost all diver based installations has been replaced with ROV operated systems. This trend reflects the constant development towards being able to handle greater depths, and there is a better focus on the safety for offshore employees.

1.1.1　*CHRISTMAS TREE*

To conduct hydrocarbons from the reservoir below the seabed to an offshore or onshore receiving unit, the well need to be connected to a XMT. The XMT is equipped with a various set of valves and a choke. It has the purpose to control the flow of hydrocarbons to the receiving unit, and it also contains safety equipment. To obtain even greater recovery of hydrocarbons, some reservoirs are equipped with a well and XMT to inject water or gas into the reservoir, which enables more hydrocarbons to be recovered.
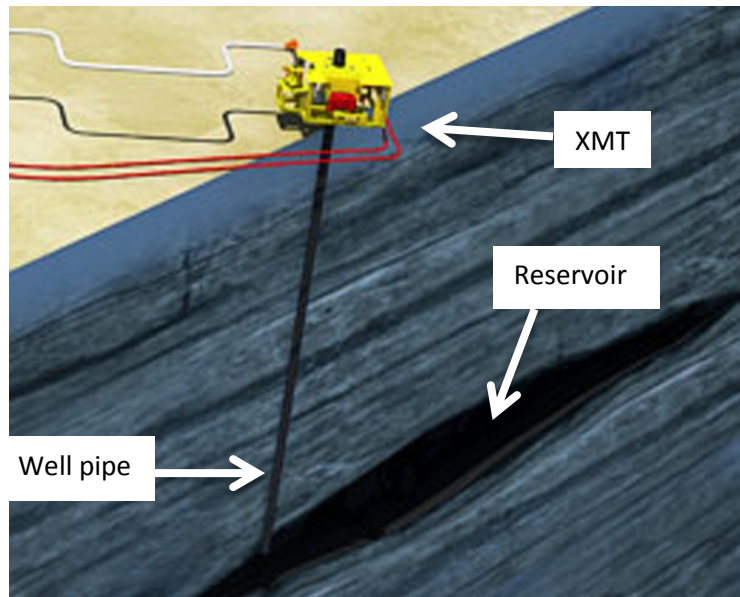
Fig 1.2 A typical XMT which is installed on the top of a wellhead. The well is connected to the reservoir, where hydrocarbons can be recovered [06].

1.1.2   *MANIFOLDS*

The manifold collect produced fluid from the wells and distribute it further to other facilities. The purpose is to minimize the use of subsea flowlines and risers and to optimize the flow of fluid in the system. It also distributes and optimizes the injector fluids. There are many methods for transporting the production fluid from a well to a top-site facility and it relays on the complexity of the specific field. The simplest way is to have a satellite connected to a surface facility. If more than one well needs to be connected, a template with integrated wells can be used, or as showed in figure 1.3, a manifold can be located in an array from the trees that transfer production fluid to the manifold. Then the manifold distributes the production fluid further to a fixed or floating facility or directly to an onshore facility.
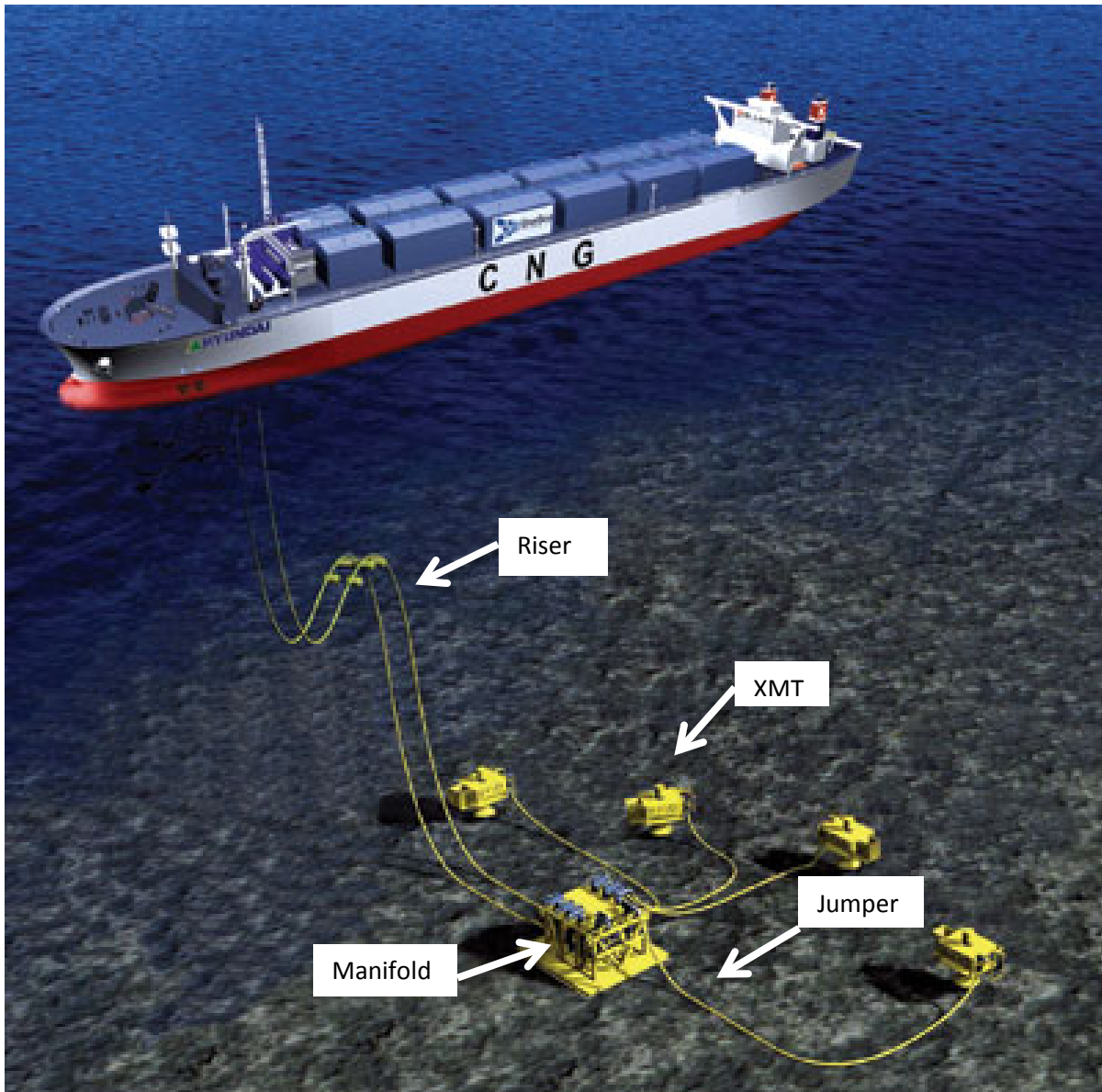
Fig 1.3 *Four XMT's and one manifold connected to a surface facility (receiver of oil and gas). The manifold is located in an array of the XMT's to reduce the total piping, umbilicals and flow lines used [07].*

1.1.3   *CONNECTION SYSTEM*

A connection system is needed to connect a range of flowlines and pipework such as flow lines, jumpers and umbilicals to different facilities remotely subsea. The connection system may also be called a "tie-in" system because it makes sure for securely tied in connections to subsea wells, manifolds and other subsea equipment. This is principally done with either vertical oriented connectors or horizontally oriented connectors [09]. In this master thesis the main focus will be on the horizontal oriented connection system.
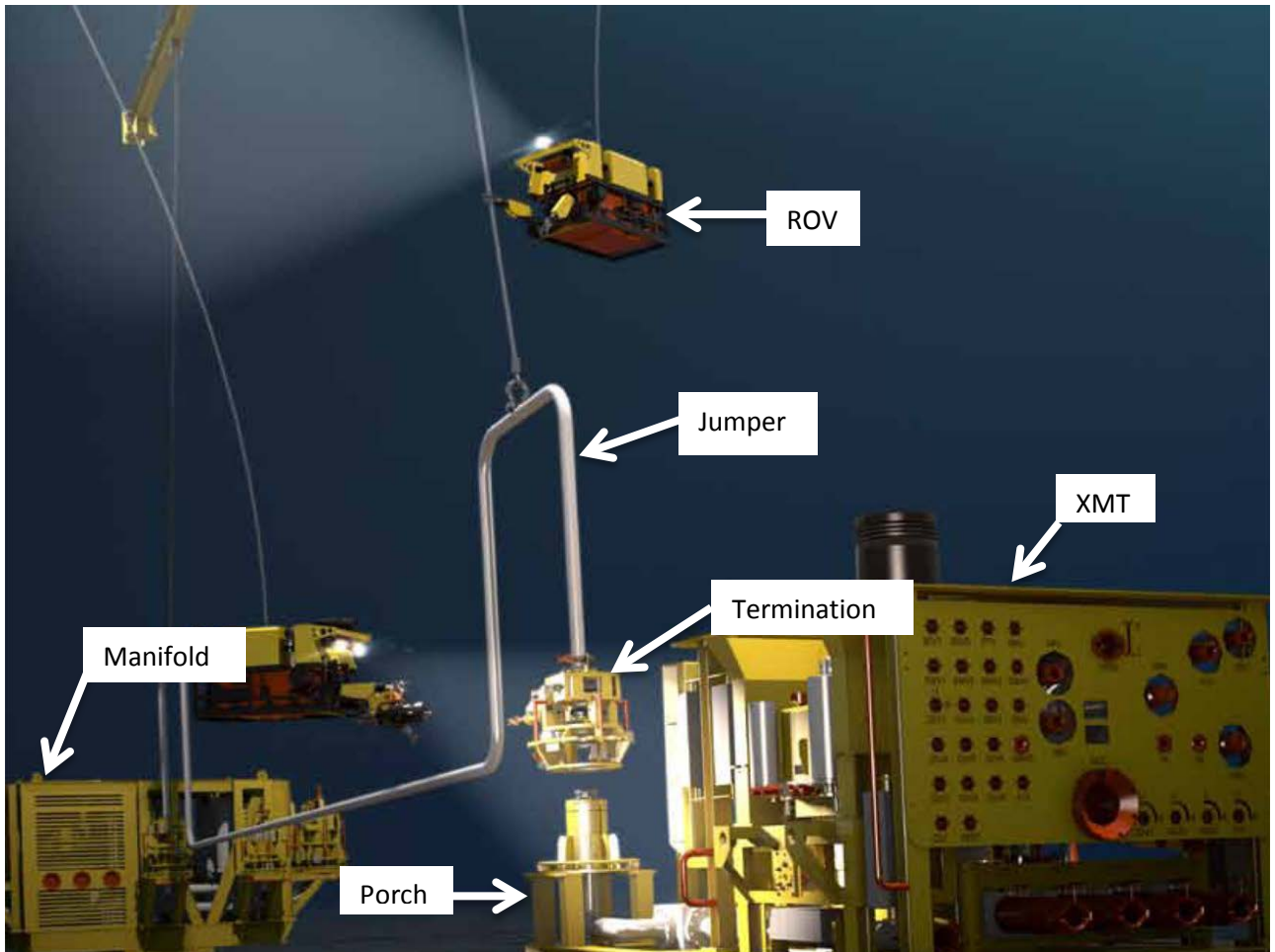
Fig 1.4 AKS vertical connection system [08].
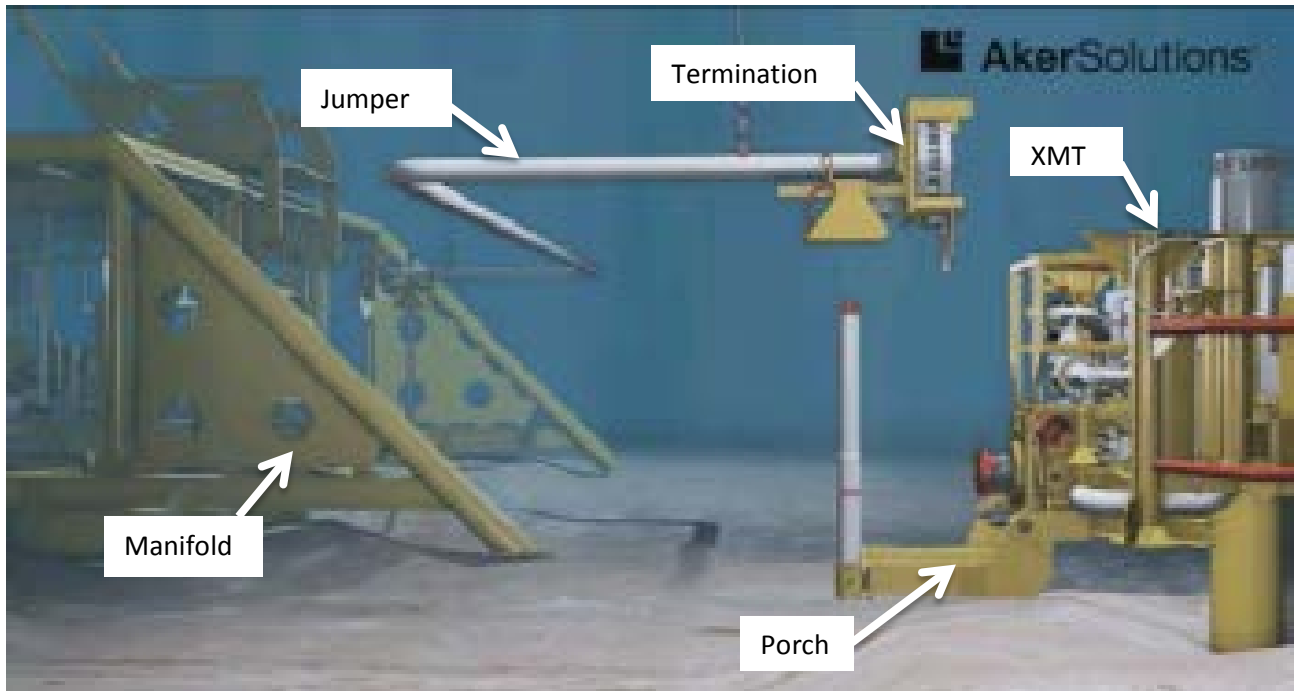
Fig 1.5 AKS horizontal connection system [10].

As mentioned before, subsea engineering has undergone a fundamental change. It has gone from being a diver-dominated activity with a wide use of flange bolts, and instead the use of remote systems for the construction of deep water field developments have become dominating. Therefore a more sophisticated connection system is required [11].

Horizontal connections have both advantages and disadvantages and they are typically used in the following situations:

- When flow lines are pre-installed on the seabed and therefore are oriented horizontally.
- When the equipment on the seabed needs to obtain a low vertical profile in order to not interrupt with fishing activity (trawling).
- When the minimum bend radius on the umbilical or flexible pipeline does not make it possible to connect it vertically.
- When a subsea tree or manifold is to be retrieved back to the surface without also retrieving the jumper.
- When it is an increased necessity for a controlled landing of termination and controlled makeup of the connection.
- When the required deck space should be at a minimum.
- When only light-weight ROV tools is to be used.

A horizontal tie-in system may be made up by clamp connectors operated from a tie-in tool, by integrated hydraulic connectors operated with a ROV, or by nonhydraulic collet connectors with assistance from an installation tool or ROV. AKS uses the former solution.

There are basically two types of the HCS –rigid and flexible. The rigid HCS is designed for rigid pipes, in other words welded stiff pipes. The flexible HCS are designed for flexible piping or umbilicals, which are flexible and allow for more movement. The flexible system requires additional installation

yokes for performing an installation and therefore the installation procedure differs from the rigid. Also the design of connection systems itself has some minor differences because of this.

Rigid and flexible HCS both consist of a termination and porch. The porch can be described as the receiving unit on the seabed that is to be connected to the termination located at both ends of the pipework (Fig 1.7).

AKS HCS is a fairly new system in context of field experience. The first installation of the HCS was performed in August-October 2012, respectively within the Atla and Skuld projects [12]. The system has recently been developed and several products within the HCS are currently being tested and improved.

HCS FOR RIGID PIPELINE
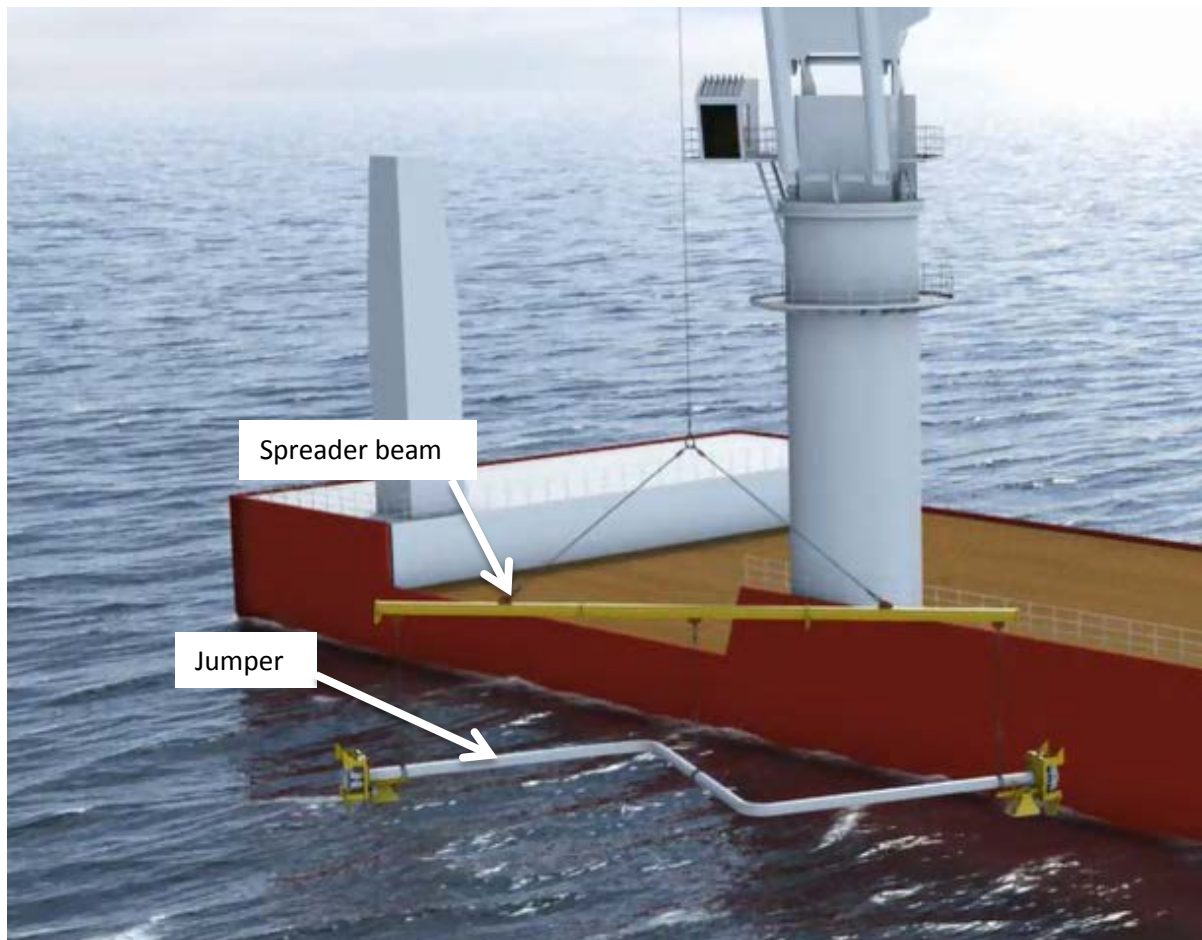
Fig 1.6 *Lowering the jumper with a spreader beam from a vessel* [13].

Installation of a jumper typically starts with a crane on a vessel that lower the jumper in to the sea. A spreader beam is used to support the jumper. This can be done in two ways, with or without guide wires. The guide wires are used in harsh weather conditions or in shallow water, where the sea currents are high and the influence of the waves have a larger impact for the stability of the equipment that need to be lowered in to the sea. For wireless installation, expansion guideposts with different length are needed to be installed at each porch on the seabed. The installation procedure described further in this chapter is for an installation without guide wires.

The jumper have guide funnels at each termination which makes it possible to align with the preinstalled guide posts located at each porch on the subsea unit. The first guide post is entered in to the guide funnel (Fig 1.7). This side has the tallest guide post since it will be entered first. Then the jumper is lowered further down to enter the second guidepost which is shorter.
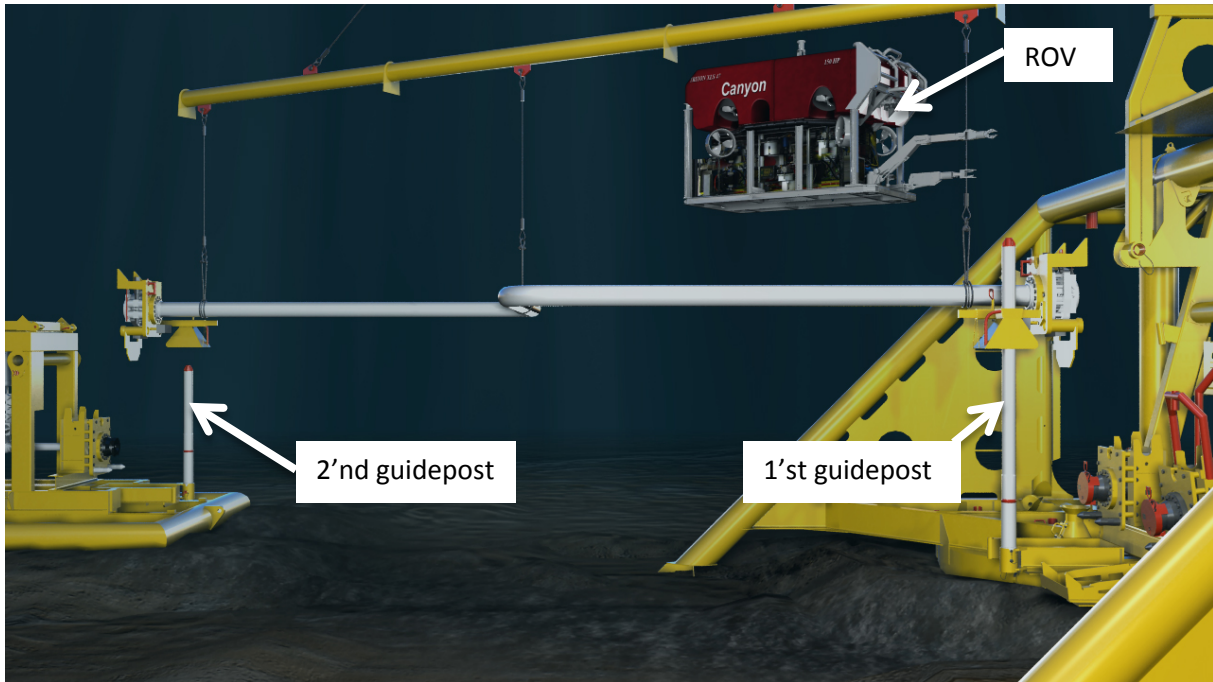
Fig 1.7 The jumper becomes closer to the first guidepost and the ROV helps adjusting the jumper in order to land it in the right position [13].
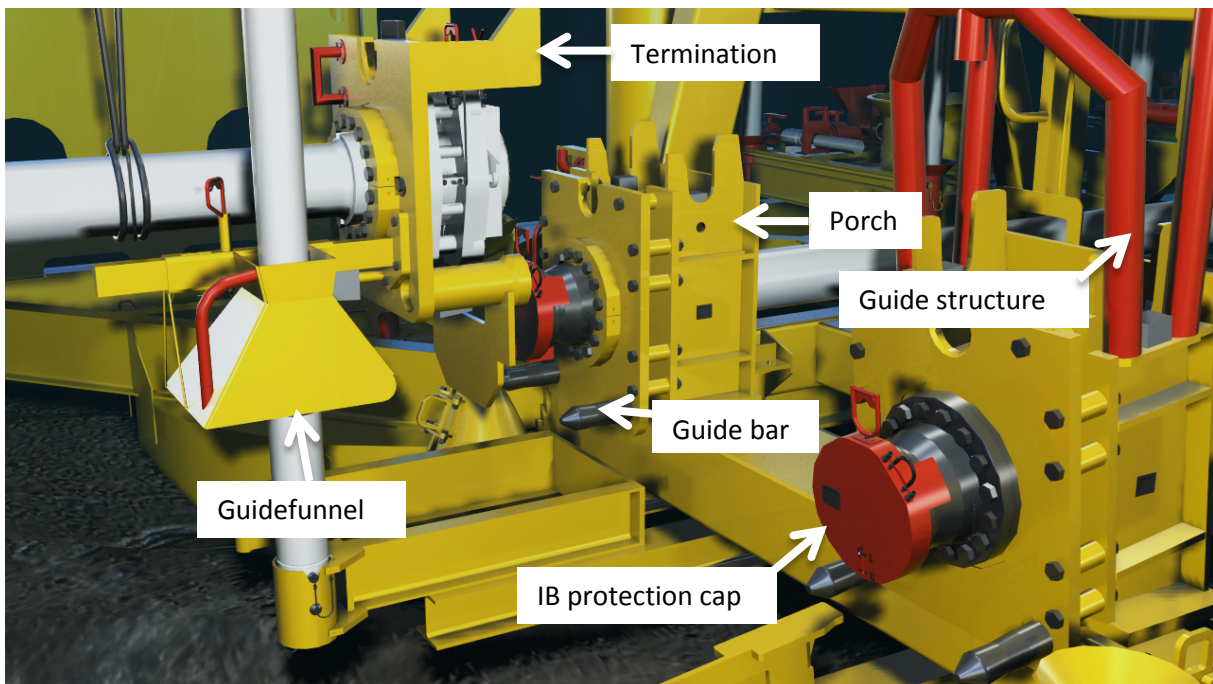

Fig 1.8 The termination is being landed on the porch [13].

Once the jumper has landed properly, the spreader beam can be lifted back to the surface.
After landing, the inboard and outboard cap is removed before the termination is stroked towards the porch with a stroking tool (Fig 1.9). For obtaining proper alignment, the termination is guided in place with the aid of two guide bars. When it has been stroked in to final position, the clamp connector can be tightened with a torque tool, before a pressure test for the seal can be performed to make sure the connection does not leak.
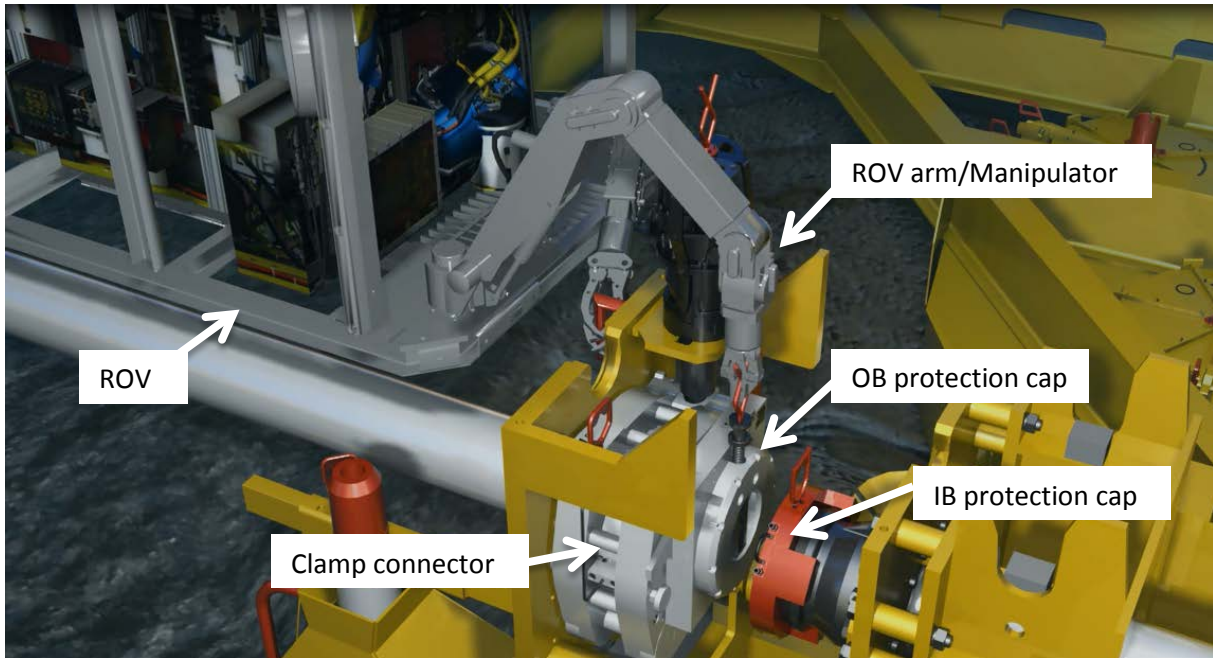
Fig 1.9 Retrieving the OB protection cap [13].

HCS FOR FLEXIBLE PIPELINE

As mentioned, the installation procedure for flexible HCS differs from the rigid, because it use an installation yoke attached to the termination when lowered down from the vessel. The two installation yokes are not similar, the second end are designed to withstand greater forces. This is related to a heavier load that implies to the umbilical or pipeline when it is orienteded along the seabed compered to the first end that have the umbilical or pipeline orientated towards the water surface (Fig 1.11).
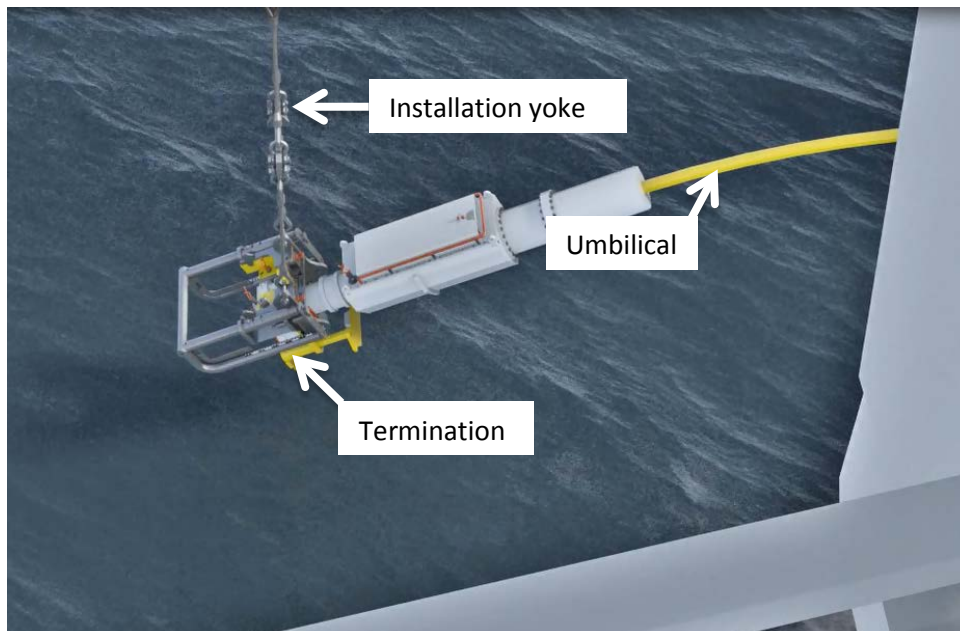
Fig 1.10 An UTH (umbilical termination head) is lowered into the sea with an installation yoke, shackles and a wire [14].
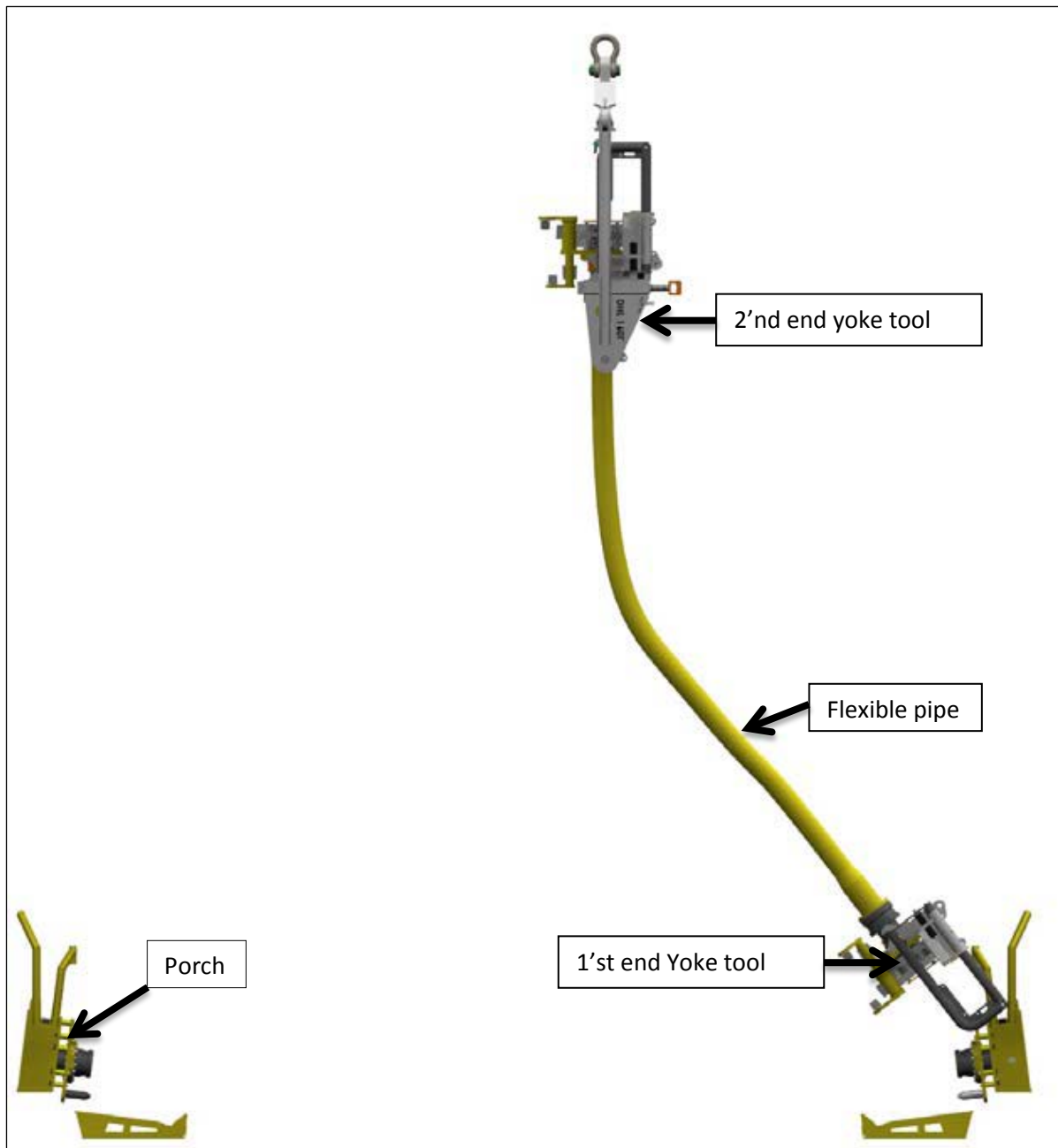
Fig 1.11 A simplified illustration of the flexible HCS that require to use a yoke tool at both ends of the pipeline when installed. The second yoke have a more heavy design to cope with greater forces that come from the bending of the pipe/umbilical when it is orientated horizontally on the seabed [15].

As for rigid connection, the termination is also landed on the porch. After the installation yoke has been retrieved, the same procedure as for rigid connection applies for the flexible connection which involves stroking the termination towards the porch, tightening the clamp connector with a torque tool and finally, perform a BST.
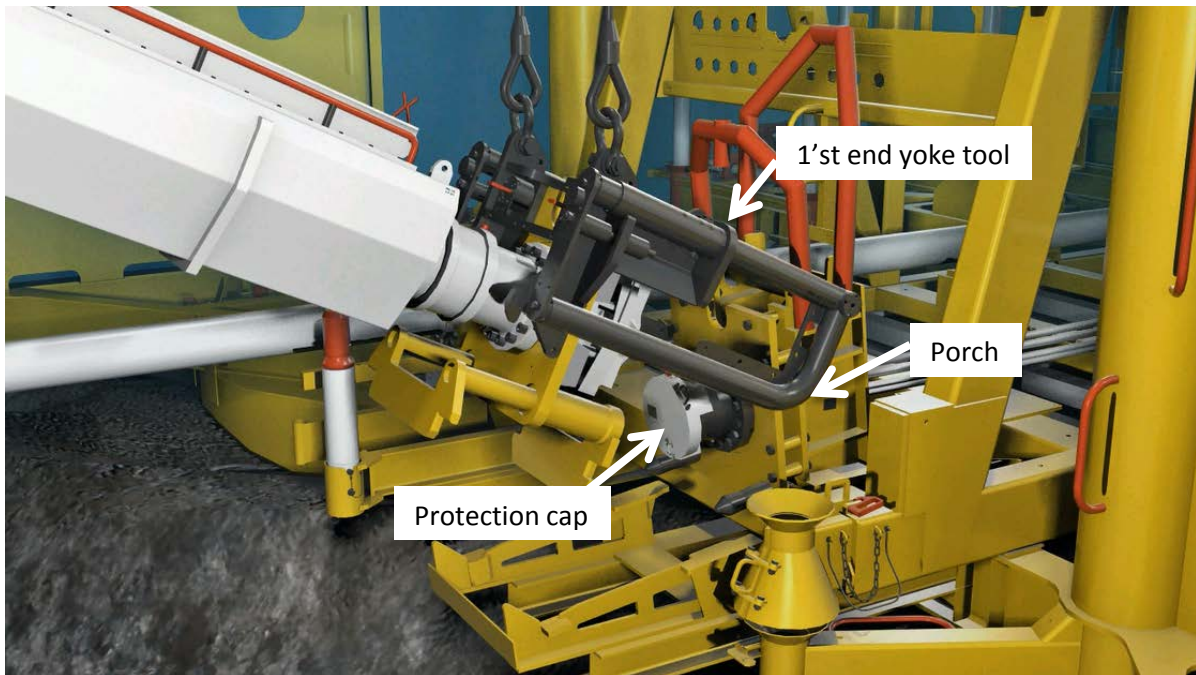
Fig 1.12 Landing the installation yoke on the porch [14].

1.1.4   SUBSEA CAPS

Caps are a critical component within the subsea oil and gas system. They are used for blinding off hubs (end of pipes) on piping and other subsea components. They provide protection against dirt and mechanical damage, and may be designed to maintain an internal pressure. The pressure caps can also be provided with features for pressure testing, bleeding off internal pressure, flushing or filling of fluids.

Caps protect against possible environmental damage or undesired effects on the hub resulting from corrosion and marine growth. All caps needs to be retrievable subsea, but only some of them are installable subsea. The cap needs to have reliable functions, since a malfunction can result in large undesired events. Such undesired events can be leakage or a function failure of the open and closing mechanism. A malfunction could therefore result in disruption or in worst case leakage of the production and an increased operation time. This is highly related to increased costs and environmental impacts. Important requirements for a subsea cap are therefore no malfunctions and zero maintenance. Pressure caps are usually not exposed to the design pressure it is made for, since it is installed as a safety device and normally only work as a second barrier against the production pressure. This is important for preventing unwanted situations when a valve fails or has been unconsciously opened.

Today AKS has basically two different pressure caps to offer for the HCS, one temporary and one permanent. The design of the temporary cap does not enable subsea installation, it can only be retrieved subsea. Below, the two caps are described more in detail.

PERMANENT IB PRESSURE CAP

This cap is commonly named "permanent cap" because it has a design life of typically 25 to 30 years subsea and it is therefore expensive compared to caps for temporary use. When deployed, the cap is located with the aid of lifting slings before it is landed on the porch. Before the cap is placed in the final position where it can be stroked, it undergoes several guiding steps. It is stroked against the reaction plate with a stroke tool (Fig 1.14). Finally the connection is tightened with the clamp connector which "tightens" around the cap disc (blinded hub) and hub end. The clamp connector itself is tightened with a torque tool. The installation procedure for this kind of cap is similar to the procedure for a termination.
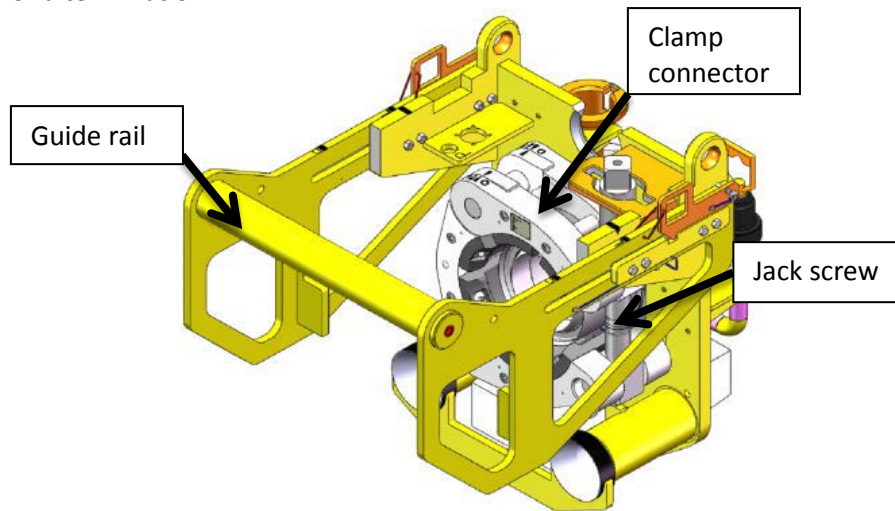
Fig 1.13 **AKS HCS Permanent pressure cap [16].**

The pros and cons for the permanent pressure cap are listed:

Pros:

- It is capable of withstanding a high internal pressure.
- Long lifetime.
- Sufficient space to equip the cap with additional features for flushing, bleeding valves or BST.
- Retrievable and installable subsea.

Cons:

- Require additional tools like a standard torque and stroke tool.
- Require the use of a lifting wire.
- Compared to other caps, it demands more installation time and the installation procedure is more complex. When a jumper needs to be installed, the cap must be retrieved and additionally a temporary protection cap needs to be installed before the jumper can be lowered down to the porch.
- The clamp connector constitutes a fairly large amount of the sale price.
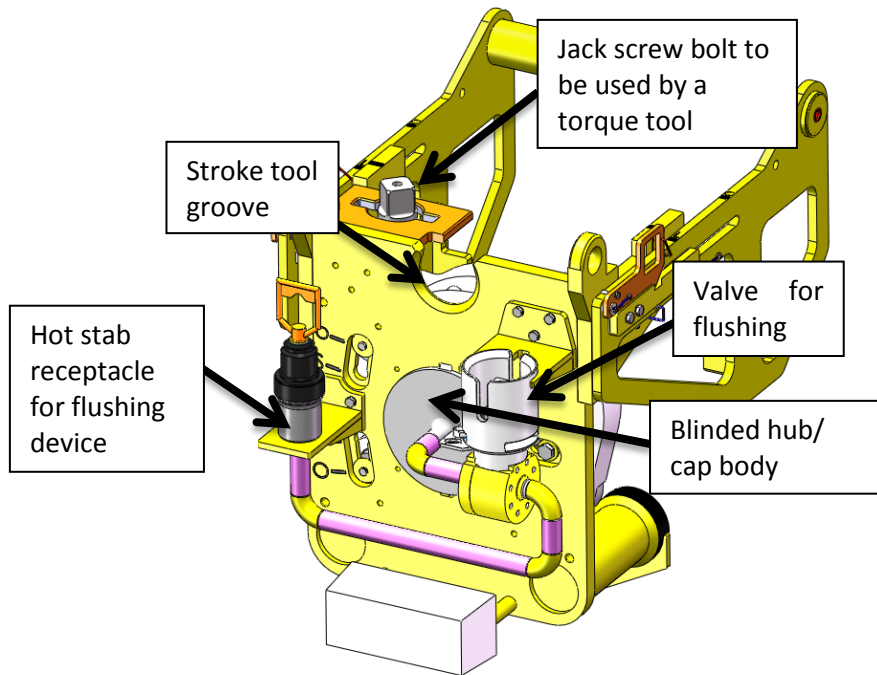
Jack screw bolt to be used by a torque tool

Stroke tool groove

Valve for flushing

Hot stab receptacle for flushing device

Blinded hub/ cap body

Fig 1.14 Backside of the Permanent pressure cap [16].

TEMPORARY PRESSURE CAP

This cap is installed top-site and can only be retrieved subsea. The cap is rated for the full operating pressure. The temporary pressure cap is retrieved by pulling the ROV handle which will open the clamp. It is also provided with a blinded hose which can be punctured if the cap disc is stuck to the hub because of a negative internal pressure. If it is desirable to receive the cap top-site after retrieval, it can be lifted with a crane wire. For protection against corrosion it is provided with anodes.

Release mechanism

Anodes for cathodic protection

Release handle
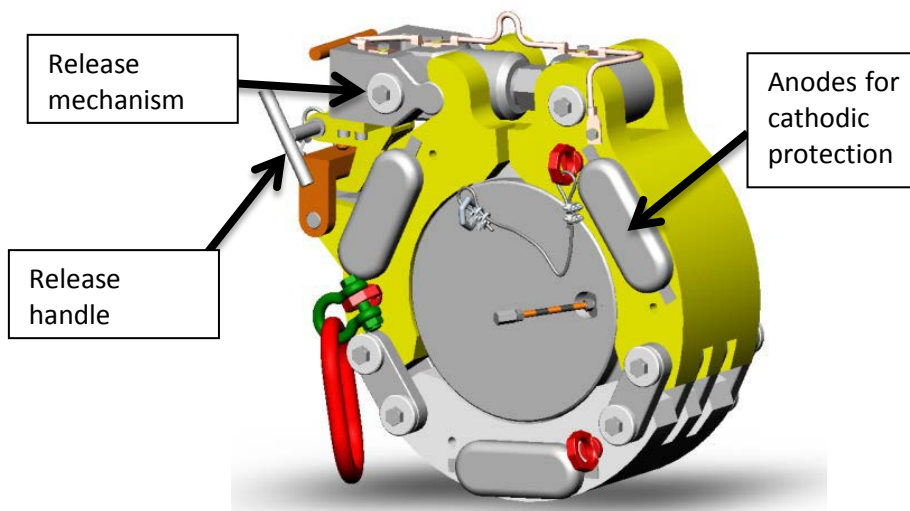
Fig 1.15 IB temporary pressure cap [17].

The pros and cons for the temporary pressure cap are listed:

Pros:

- Designed to withstanding the operational pressure.

- No additional tooling needed, the cap is removed from the hub with only the help of a ROV manipulator (it does need a crane wire to retract it top-site).

- Can be equipped with a double sealing.

- Can be equipped with additional features.

Cons:

- Not installable subsea.

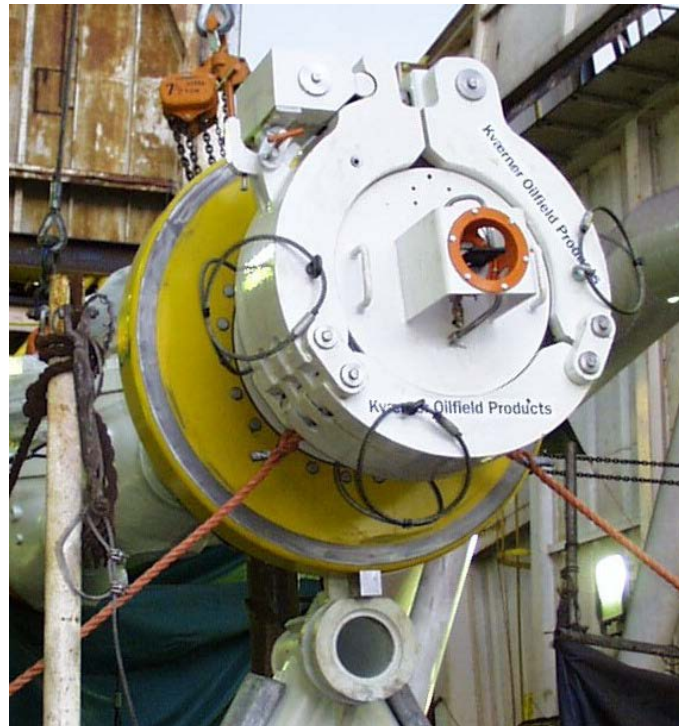- Not possible to land the termination with the cap mounted on IB hub.

Fig 1.16 Temporary pressure ROV clamp connector mounted on hub [18].

1.1.5   *STANDARD ROV TOOLS*

For the HCS it is primarily two types of tools available, the torque tool and the stroke tool. When designing a new product for the HCS it is highly preferable to use these standard tools. This is because of the great advantage of using as few tools as possible when performing subsea operations. The experience with these tools is also very good. The two tools are described briefly below.

TORQUE TOOL

The torque tool is used when it is necessary to produce a rotational movement. It is provided with a digital display that indicates the number of turns and torque level. This is an important feature because it enables a good control of the tool when operating different subsea equipment. It also enables that pressure, number of turns, RPM, oil temperature and torque can be monitored by a surface computer. The TT is based on a hydraulic motor and gear system. The hydraulic oil is received from a hot stab. The TT is an ultra-compact, lightweight and flexible torque tool [19]. The tool typically produces a maximum torque of 17 kNm, but it exists TT which can produce up to 34 kNm.
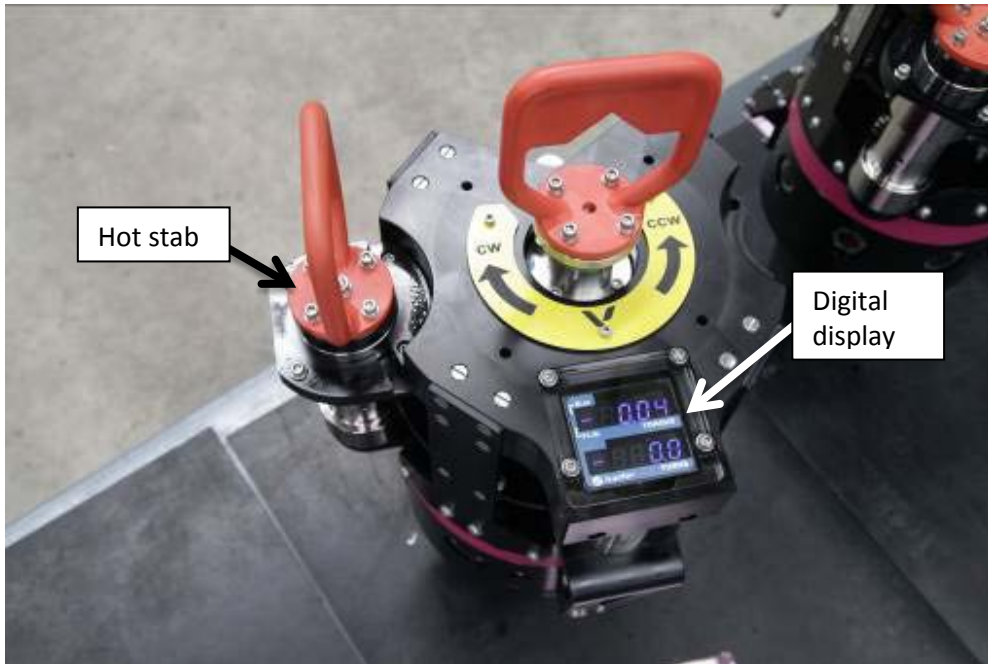
***Fig 1.17** Torque tool with hot stab receptacle and a display which indicates RPM and number of turns [20].*

STROKE TOOL

The Stroke Tool is a double acting hydraulic cylinder, operated by a ROV and designed for connecting and separating AKS HCS. During make-up of the OB and IB hubs, the hubs will be stroked together by the hydraulic ST. When disconnecting the connectors, the ST is used to separate the two hubs. The stroke tool has two grooves: one on the end piece and one on the main body (Fig 1.18). The two grooves will fit the slots on the IB and OB Reaction Plates on AKS connection system. The ST have a weight about 172 kg in air and because of the two buoyancies blocks it has a weight of 58 kg submerged which makes it feasible to be handled by a ROV. Since the tool is designed for connect a whole spool termination, the tool is capable of a stroke force up to 5 000kN [21]. Hydraulic power to the cylinder will be provided by a hot stab connection which is operated by the ROV.
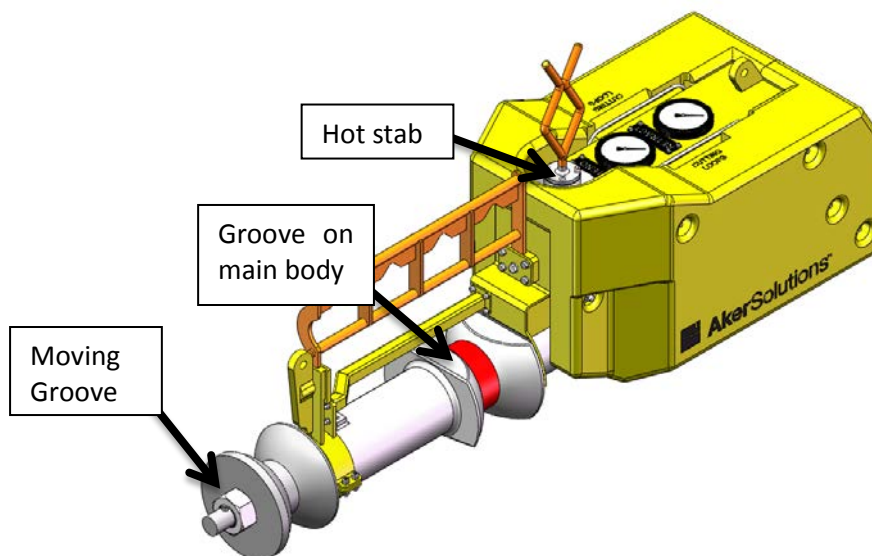

***Fig 1.18** The stroke tool that is equipped with two buoyancy blocks to reduce the submerged weight [21].*
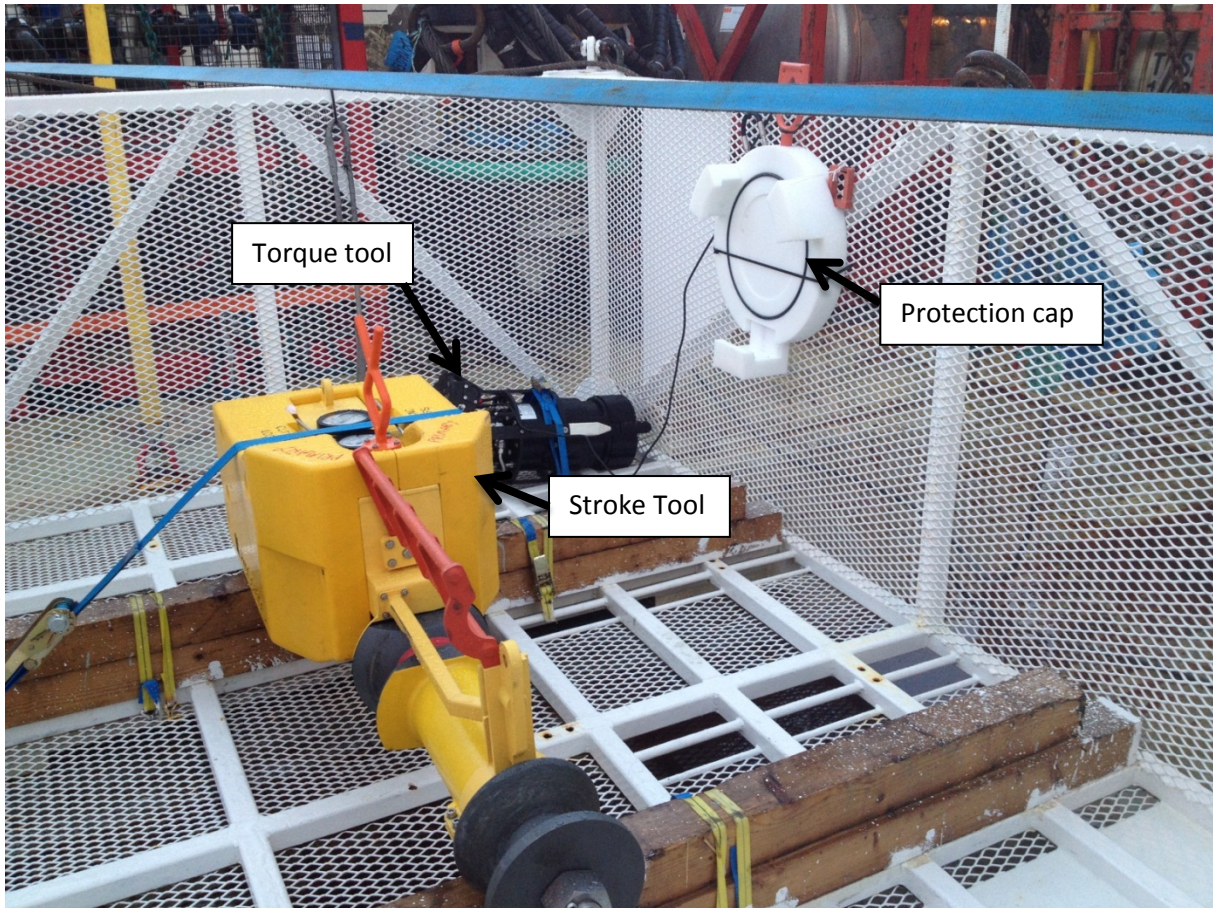
***Fig 1.19** The stroke tool is strapped to the tool carrier basket, the TT can be seen behind the ST. The tool carrier basket is used to transport tools and minor subsea equipment from the vessel down to the seabed close to the operation site [22].*

1.2   MISSION STATEMENT

The main purpose of this master thesis is to optimize and improve the preliminary design and confirm that it will resist the operational loads. This will be done with the aid of hand calculations and verifications through FEA.

1.3   SPECIFIC AIMS

The design process was split into the following specific aims:

- Literature study, finding suitable calculation formulas and methods in order to dimension the design.
- Assess the locking mechanism, make hand calculations, verify with FEA.
- Improve and optimize the locking mechanism design.
- Assess the connection components with hand calculation and verify with FEA.
- Conduct evidence of whether the connection is capable to handle the operational loads.
- Evaluation of the project and components (design review).
- Conclude on the design.

The ideal result will be a description of the work that can give a reasonable indication about the cap design and clarify whether the design is within the specified required limits with an acceptable level of confidence.

1.4   LIMITATIONS

The following limitations are expected in this master thesis:

- Physical tests of the design will not be performed.
- Optimization, improvement and design of a guiding and alignment solution for the cap will not be performed in this master thesis.
- It will not be performed a FEA of the frictional loss that occur in the locking mechanism.
- A solution for attaching the cap disc to the upper clamp segment will not be investigated.
- The ROV bucket support bracket will not be designed against static loads.
- The unlocking scenario for the cap will not be investigated.
- A convergence study of the finite element model will not be performed.
- An economical study will not be performed (Target sale prize, numbers of units sold per year etc.)
- The intellectual property rights (IPR) will not be investigated.
- It will not be investigated whether the design could be scaled to other dimensions.
- The cap will not be completely designed in accordance with prevailing standards.
- It will not be investigated whether the cap is capable to handle both flexible and rigid HCS connections.
- Manufacturing drawings will not be made.

1.5   DESIGN BASIS

The customer needs and the target specifications form the design basis of the cap design. Most of these needs and specifications were established during the preliminary project, but the list has been reviewed and updated after more inputs from AKS Tie-In department during the master thesis. The design basis acts as design instruction and aim the design work to the best result which fulfills as many required specifications as possible.

1.5.1   *CUSTOMER NEEDS*

First of all, it is necessary to identify the customer needs. Customers that purchase pressure caps are AKS clients and are the operators of the field. This is typically companies like Statoil, Total, BP etc. These companies decide on their own which supplier they want to use for delivering their subsea equipment. To find out the demands of the AKS clients, a meeting with the tender group was arranged [23]. The tender group has continuous contact with the clients regarding bidding offers. It is the price, flexibility, simplicity, installation time and reliability that are the main factors for the clients when they are deciding what kind of connection system they want to purchase. Therefore, these factors are important to consider when generating a new cap concept.

The clients purchase the products, but they are not directly involved in the installation and in operating the equipment. It is the installation contractors that are using the equipment in the field and they have useful experience and presumably the best insight on areas of improvement. However, knowledge and experience was mainly collected from people in the AKS tie-in department.

When AKS equipment is installed, an AKS representative is generally present in order to assist in the installation. Hogne Haug and Anders Austad were contacted and a meeting was arranged because they have this kind of experience related to the HCS. Hogne Haug has worked with the installation on the Atla project and Anders Austad on the installation of the Skuld project [12]. Their knowledge and experience were useful when collecting information about customer needs. Advices on critical failures and areas of improvement were also given.

Per Höglund is the former product manager for caps at AKS and an introduction were given from him on important factors when developing a concept for a temporary pressure cap. He also gave an explanation of current issues regarding other cap designs. Snorre Balkøy was contacted because of his knowledge and experience regarding subsea installation, and he has a previous carrier as a ROV pilot. He provided useful feedback regarding the importance of considering a user friendly design for the ROV [24].

A list of customer needs that is based on the information collected through the meetings and conversations with the mentioned people from the tie in department is presented.
The needs are divided into two levels of importance, **required** and **desired**. Required needs are those that are set as absolute requirements to meet, while the desired ones are advantageous but not an absolute requirement.

Table 1.1 The different customer needs that has been collected.

Need	Level of importance	Comment
Protect the hub		
The cap needs to protect the hub from mechanical damage.	**Requirement**	This is one of the main functions and it is essential. Important to avoid making damage to the hub while the cap is operated, especially during landing and installation.
Capable of handle an internal pressure		
The cap needs to be capable of an internal pressure.	**Requirement**	Since it is a pressure cap, it needs to be capable of handling a full operational pressure.
The cap can be equipped with additional features as BST, filling port, bleed and flush valves.	**Desired**	This would be beneficial, and many clients may ask for such features. But this is not one of the main challenges to solve. This could be relevant to implement after establishment of the main design.
The cap needs to have a faultless function for equalizing the internal to the external pressure before retrieval.	**Requirement**	This is critical because a malfunction could make the cap stuck on the hub due to internal vacuum.
The cap needs to have a double set of sealing, that will work as a first and second barrier against the production pressure.	**Desired**	This decreases the risk of leakage, and clients may require such a safety feature. This is not one of the main challenges to solve in this project, and due to the limited space available on the hub surface, this feature may not be possible to realize. A double set of sealing is also beneficial since it can enable BST between the seals.
Flexibility of the cap		
The cap needs to be installable and retrievable subsea.	**Requirement**	This is one of the main functions and is essential for the design.
The cap needs to be used both for the rigid and flexible HCS.	**Desired**	If the cap is made suitable for both flexible and rigid HCS, the market value increases, because a larger amount of the cap can potentially be sold.
The cap needs to be able to function at all applicable water depths.	**Desired**	It is a great advantage if the cap can tolerate the hydrostatic pressure that exists at the deepest oil and gas fields.
The cap needs to allow the termination to be landed and retrieved while the cap is mounted on the IB hub.	**Desired**	This could potentially save installation time and costs in some scenarios. There are uncertainties regarding a technical solution for this specific problem.

Table 1.1 continued.

Need	Level of importance	Comment
The cap needs to be capable of being equipped with metrology equipment.	**Desired**	Not a required, but important to have in mind during the design process.
The cap needs to function for both hydrocarbons and chemicals that are used.	**Requirement**	Hydrocarbons and chemicals are the flowing fluids inside the subsea system. Chemicals that are used are typical MEG.
The cap needs to function with a porch that is equipped with thermal insulation.	**Desired**	It would be beneficial to have a cap design that is capable of being installed on both regular and thermal insulated HCS porch. Some connection systems are equipped with this feature when it is a risk of deposit of hydrate crystals inside the piping. This could potentially lead to flow loss and system blockage. The thermal insulation is present in order to delay the cool down process and prevent heat loss to the surrounding ocean.
The cap needs to be easily operated		
The cap needs to be easily operated by a ROV.	**Requirement**	A user-friendly design for the ROV must be in focus.
The cap needs to have an indication for closed and open position.	**Requirement**	This is important and probably fairly easy to implement after the main design has been established. Must be in mind during the design process.
The cap needs to be installed without the necessity of additional tooling.	**Desired**	Ideally, a cap with no need for additional tooling will reduce installation time and costs. If additional tooling needs to be used, it is a requirement to use existing standard tools.
The cap needs to be installed without the necessity of a crane wire.	**Desired**	Ideally, a cap with no need for a guide wire will reduce installation time and costs. This is difficult to achieve since the weight of the cap most likely will be above the weight that the ROV can handle (the cap is probably made of a steel material to withstand the pressure).
The cap needs to be reliable		
The cap cannot have a malfunction.	**Requirement**	The consequences of a malfunction could be an increased installation time, the production could stop or in the worst case a leakage of the production fluid could appear.

Table 1.1 continued.

Need	Level of importance	Comment
The cap needs to be resistant against corrosion.	**Requirement**	Important aspect to have in mind because the cap is subjected to a corrosive environment. Preventive actions can be the use of anodes, anti-corrosion surface treatment and ground wires.
The cap needs to have a secondary locking.	**Requirement**	A secondary locking in this context means an additional locking to the primary one. This is for safety reasons, to ensure that the connection never will experience to be back-driven or released. Some customers may have this as a requirement.
The cap needs to have a secondary contingency release.	**Requirement**	If the opening mechanism of the cap fails to release the connection, a secondary release solution needs to be available. This is because in a situation where a connection fails to release and no contingency release is present, the associated subsea unit needs to be retracted. This would involve highly unnecessary costs and delay the operation time. The secondary release mechanism can either be an integrated feature or the use of a ROV tool as an angle grinder.
The cap needs to have a minimum of snag points.	**Requirement**	Snag points are sharp or projected obstacles that can potentially harm the ROV wire or where the ROV wire can get stuck. This could happen while the ROV work next to the cap. Snag point needs to be avoided as it can lead to unnecessary situations.
The cap needs to be cost-effective		
The cap needs to be a cheaper alternative compared to the permanent pressure cap.	**Requirement**	It is essential to make the cap less expensive than the already existing permanent pressure cap (chapter 1.1.4).

1.5.2   *TARGET SPECIFICATIONS*

The target specifications are established in order to reflect the customer needs and to transform them in to metric values. The selected design may fail or exceed some of these specifications depending on the final solution. The target specifications will act as a guide in order to reach the best design. Most likely, trade-offs will be made during the design process. Requirements regarding low weight often come in conflict with withstanding high pressure. This means that some requirements need to be sacrificed in advantage of more importance ones .After a design is decided to be brought further in the development process, the final specifications will be established, and the values will be

more precise [25]. The final product should fulfill the requirements in the best possible way by making the most rational trade-offs.

Table 1.2 The different target specifications presented with metric values.

Metric	Ideal Value	Marginal value	Unit	Comment
Design pressure	>345	>345	bar	The standard design pressure for 12" HCS with a 12" bore is 345 bar [26].
Test pressure	>517	>517	bar	The cap needs to be tested for a pressure that is 50% higher than the pressure it will be exposed for as a part of the qualification (FAT). The clients usually perform a pressure test of the whole subsea flow system (commission test). This is done with a 25 % higher pressure than the design pressure, thus 431 bar. The test pressure for the qualification will be 1.5 times greater, which corresponds in 517 bar [27].
Design temperature	-29 - 121	-29 - 121	°C	The lower temperature limit is uncertain.
Axial length from hub edge	90	110	mm	Limited space due to the termination [28].
Upwards length from hub center	600	1020	mm	Limited space due to the installation yoke.
Downwards length from hub center	380	380	mm	Limited space due to the guide bars on the porch.
Sideways length from hub center	370	520	mm	Limited space due to the installation yoke.
Depth from hub edge	260	260	mm	Limited space due to the reaction plate on termination.
Weight submerged	<50	<1800	kg	50 kg is the maximum capacity that the ROV can handle without the use of a crane wire. 1800 kg is the approximate weight of the permanent pressure cap.
Classified according to API 6A (ISO 13628),API 17D (ISO 10423), DnV-RP-A203 and ASME VIII Div2_2011a	pass	pass	Binary	API 6A and API 17D deal with design and testing. DnV-RP-A203 deal with qualifications of new technology. ASME VIII Div2_2011a deals with design rules for constructing pressure containing connections.
Hub interface	12"	12"	Inch	The cap is to be designed for the 12" HCS.

Table 1.2 Continued.

Metric	Ideal Value	Marginal value	Unit	Comment
Target sale price	300 000	300 000	NOK	In a meeting with the tender department the sales price of a temporary pressure cap was set to approximately 300 000 NOK [23]. When considering the AKS VCS as a basis, the temporary pressure cap constitutes half the price compared to the permanent cap that have a price of approximately 700 000 NOK.
Installation time	<60	<240	Min	As a basis, the installation time should be less than 4 hours. The installation time for Atla and Skuld project was 3,5 to 4 hours for one HCS flexible termination [12].
Design life, subsea	>5	>1	Year	The temporary pressure caps that AKS have delivered so far, have a design life of typically 1-2 years. A longer design life would be beneficial.
Water depth	>3000	>1500	m	The target value will be 1500m. This is the deepest water depth that the HCS has been deployed so far [29]. Below this depth, the VCS is generally used. However, it would be beneficial if the cap could manage water depths below 1500m because clients may require the use of HCS at these water depths in the future.

The cap is required to be operated in a top-down approach by the ROV, therefore all ROV interfaces needs to be orientated upwards from the cap (Fig 1.21). The cap has more space to use sideways under an installation or retrieval, but when finally installed on the hub, the above dimensions in table 1.2 require to be obtained sideways.

520 mm

1400 mm

260 mm

110 mm
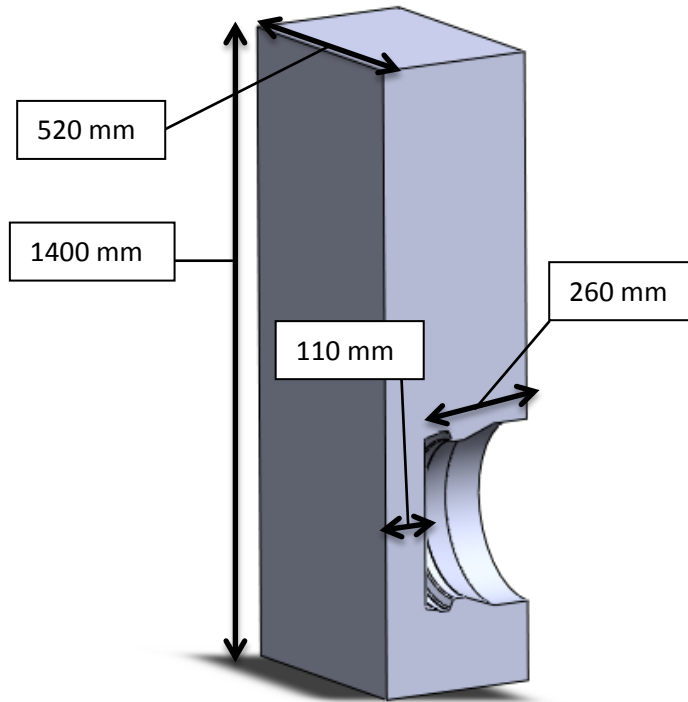
Fig 1.20 The marginal values that can be utilized. The developed design needs to be within these limits.

The purple block illustrates the marginal design values
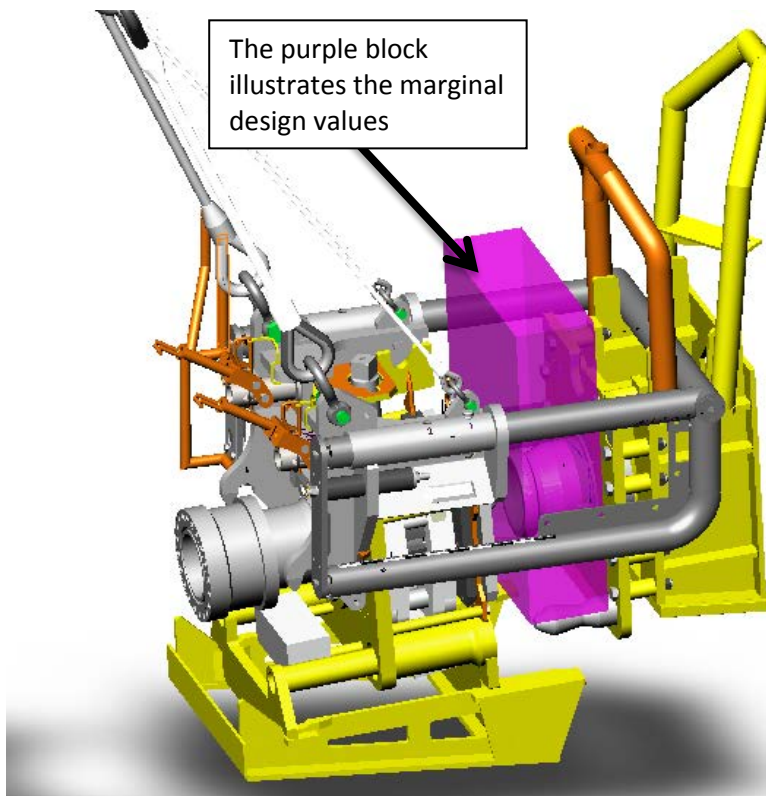
Fig 1.21 A connection assembly with the installation yoke and a purple block that illustrate the limited available space. The installation yoke is retrieved after the termination has landed.

The porch is either bolted or welded to the subsea unit

IB hub

The termination in landed position

OB hub where a flexible pipe or an umbilical is connected

The landing frame is either bolted or welded to the subsea unit
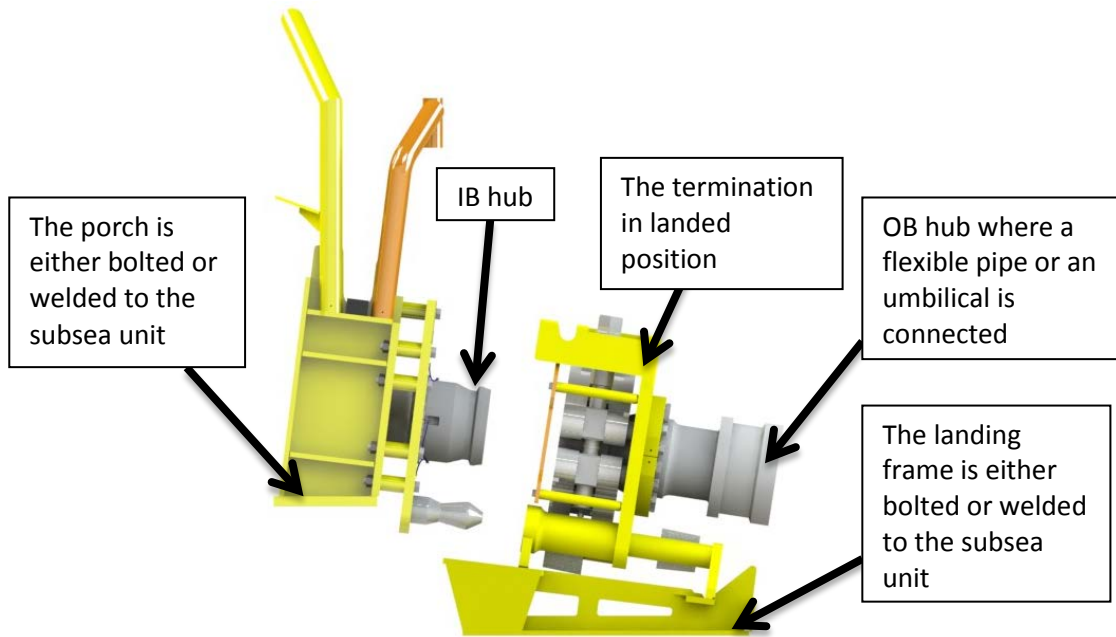
Fig 1.22 *Sideview of the connection assembly with the porch and the termination. The cap needs to be operated with top-down approach by a ROV. It is considered highly beneficial if the temporary pressure cap could be installed and retrieved while the termination is in landed position.*

2   PRELIMINARY DESIGN

A preliminary study was performed in the autumn semester 2012 through the course *"Concept and product realization"* (TIP 300). In this chapter the results from the preliminary study will be described and the design will be investigated.

2.1   PRELIMINARY STUDY

2.1.1   *OBJECTIVES*

The objective for the preliminary project was to generate a concept proposal for a temporary subsea installable pressure cap. The project followed a typical product development process which included the following activities:

- Literature study.
- Assessment of existing AKS caps.
- Carried out a competitor analysis.
- Establish a design basis (product specifications).
- Functional analysis.
- Concept generation.
- Concept screening.
- Concept selection.

2.1.2   *FINDINGS*

The final conceptual design had the potential of solving several issues that exist for the HCS.
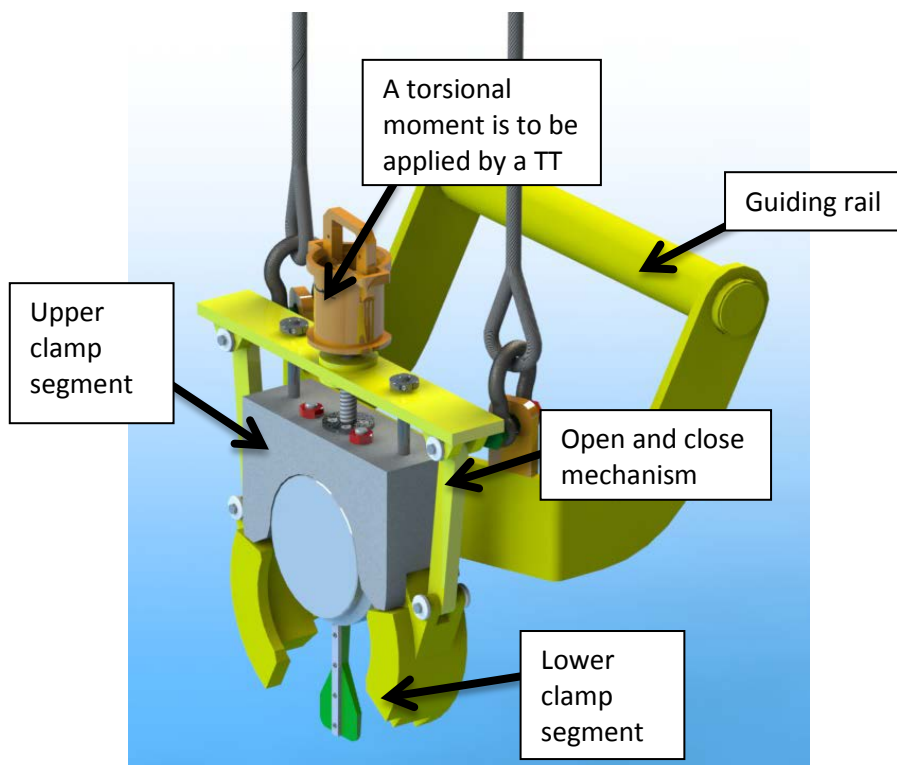
Fig 2.1 The concept from the preliminary study, provided with shackles and lifting wire.

The potential advantages of the developed concept are:

- Only torque tool is needed as additional tooling to perform a retrieval and installation of the cap.
- The cap can potentially be installed or retrieved while the termination is in landed position. If a termination is connected, it is sufficient to stroke the termination back to landed position. Compared to the permanent cap, the termination need to be fully retrieved from the porch.
- Great potential of reducing the cost compared to the permanent cap (simpler design).
- The possibility to be equipped with features for BST and bleeding. The ability of implementing a flushing feature may be difficult if the termination is to be retrieved and installed while the cap is mounted on the IB hub because of limited space.
- Potential of reducing the weight compared to the permanent cap.
- The possibility of implementing a feature for equalizing the internal to the external pressure.
- The cap enables a fast make up time.

2.1.3 NECESSARY IMPROVEMENTS AND FURTHER WORK

Because of limited time of the preliminary project, comprehensive stress and load assessments of the design where not performed. Therefore the following tasks were considered as further work:

- Perform a comprehensive FEA on the connection principle with particular focus on the sealing area.
- Investigate if the open and close mechanism works as predicted and withstand the applied load.
- Perform an optimization of the clamp segments in order to get a design that is capable of aligning and tightening correctly around the hub.
- Make improvements and a design proposal of a guiding and aligning solution which is required for installing and retrieving the cap.
- Investigate how the sealing behaves through a landing and installation.
- Investigate the feasibility to use the cap on both flexible and rigid porches.
- Investigate how the plastic slider behaves through an installation.
- Perform a ROV study to get a ROV friendly design.
- Investigate the design according to prevailing standards.
- Investigate the submerged design life of the cap.
- Investigate the design temperature that the cap can handle.
- Investigate what kind of sealing that is required on the cap disc.
- Investigate the materials for the different components.
- Investigate the surface treatment of the different components.
- Improve the design of the guiding structure for the cap and make it retrievable, so that the guiding structure can be removed after the cap has been installed. This could make it possible to perform a landing of a flexible termination were an installation yoke require the use of the guide structure to the porch (were the guide structure of the porch are occupied with the guide rails to the cap, if not removed).

2.2 CALCULATIONS AND ANALYSIS OF THE PRELIMINARY DESIGN

Due to the time limit in the preliminary study, investigation of the design in a mathematically and analytically way was not prioritized. Therefore, it was necessary in this master thesis to find evidence

that could prove that the developed cap concept could handle the operational loads. This work was initiated by investigating how much clamp force that is required to handle the internal pressure and maintain a tight and stable connection. Further, the locking mechanism was assessed to find out if it could generate enough force and have sufficient strength properties. This had a first priority in the master thesis, because it was not relevant to continue further with the design if the cap was not capable of generating enough clamp force.

The preliminary design was based on a clamp connector which tightens around the hub and locks the cap disc against the hub face. The cap is provided with an elastomer seal that is inserted in a circumferential groove and will seal against the hub face. When the connection is closed, the clamp segment tightens on the tapered hub and cap disc profile. The clamping device preloads the hub and cap disc as the device is tightened. The intension is to get a cap design with a relatively simple construction that has a fast make up time.
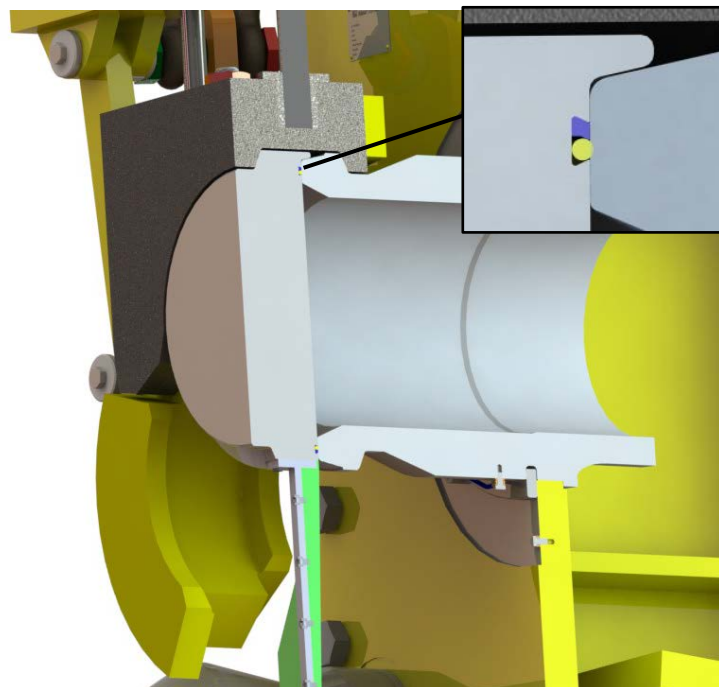
***Fig. 2.2** Section view of the cap in landed position where the clamp and cap disc/hub profile will have a wedge effect. The location of the sealing can be seen in the magnified square.*

Closing of the connection is done by a mechanism consisting of a ROV bucket which enables the torque tool to rotate a power screw that further moves a horizontal plate and two linkages.
The linkages are attached to the lower clamp segments and enable the connection to be tightened. Generally, linkages can be used to change the direction of a force and is therefore an attractive part to implement in the locking mechanism. The linkages have a pin bolt in both ends which can move freely.
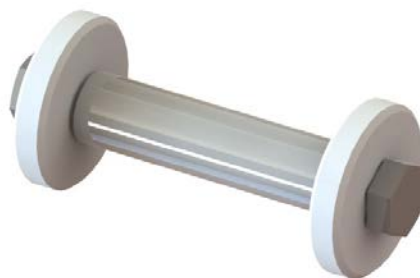
***Fig. 2.3** The linkage pin, provided with washers and bolts.*
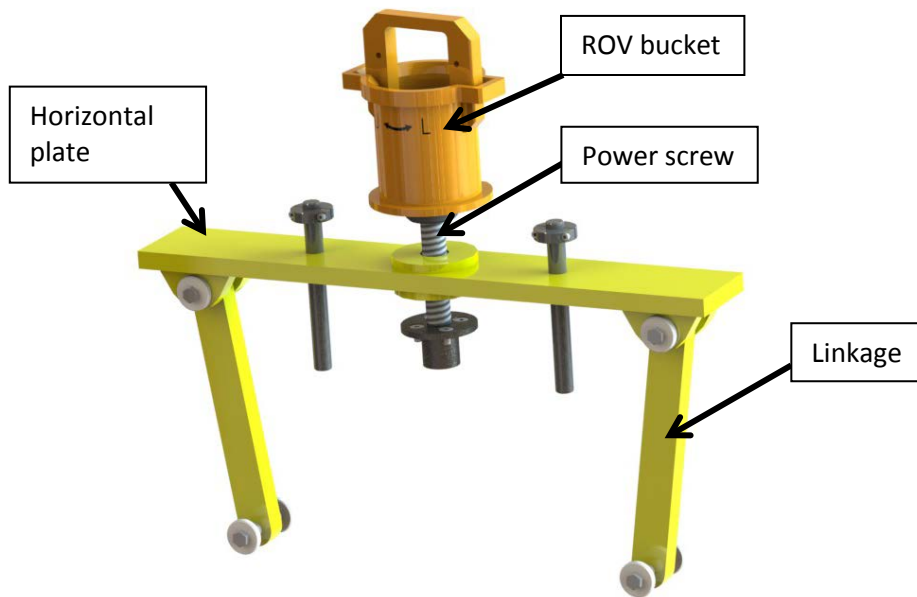
Fig. 2.4 The locking mechanism.

The two lower clamp segments are connected to the linkage by a lug. The upper clamp segment is bolted to the lower clamp segments by a pin bolt which enables the lower clamp to rotate freely.
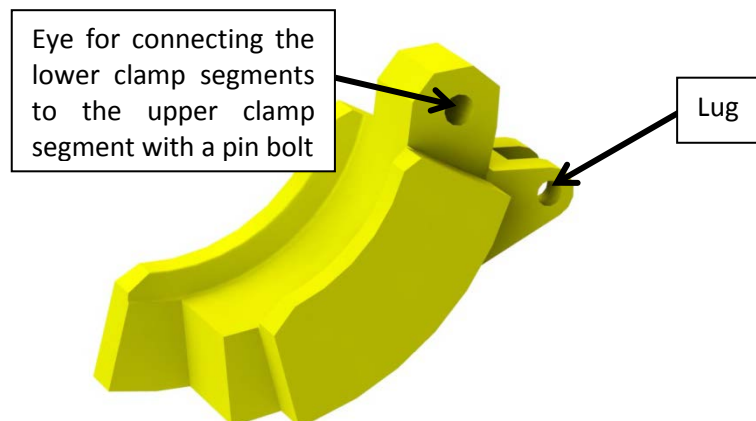
Fig. 2.5 The lower clamp segment.

As torque is added on the power screw, the screw will rotate and the horizontal plate will move downwards. To prevent damage from happening, two guiding bars were implemented (Fig 2.6). Without these guiding devices, the linkage joints could be twisted or be prevented from rotating because of an excessive moment exerted from the power screw. The cap disc is attached to the upper clamp segment by two bolts. The bolts do not tighten the disc to the upper clamp segment entirely, but allow the cap disc to some movement radially. This is necessary to provide a correct locking and aligning of the connection when the clamp segments are tightened during a make-up.
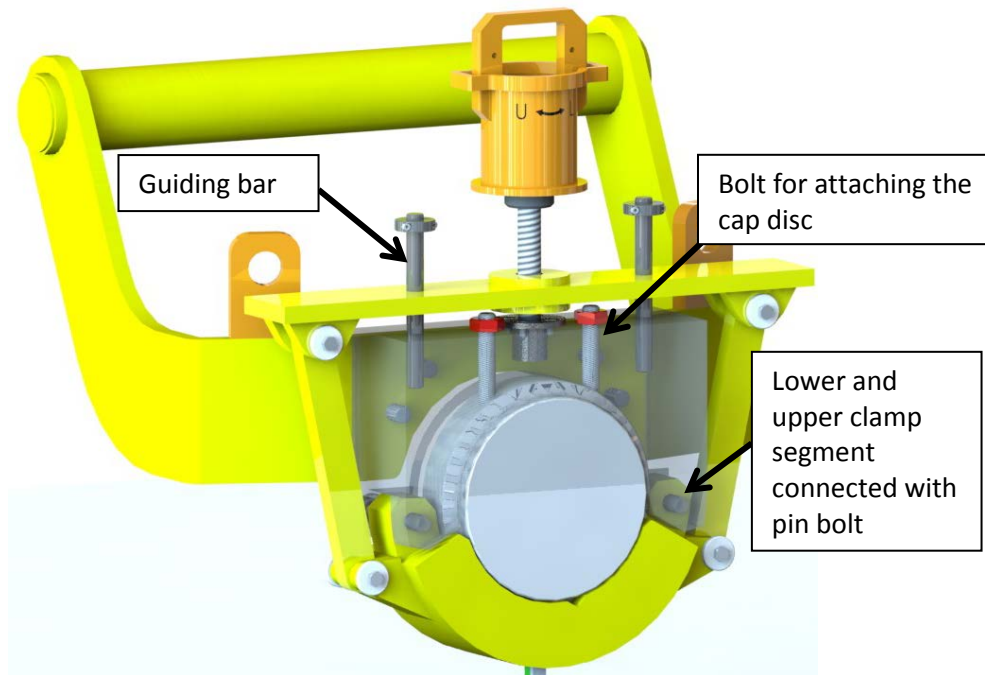
Fig 2.6 Upper clamp segment showed as transparent.

2.2.1   DETERMINATION OF THE CLAMP FORCE

A formula for clamp connectors with two bolts was obtained from the ASME VIII div2 standard and it was used to establish a rational basis for the required clamp force [30]. The formula represents how much total bolt load that is required for a given design pressure, diameter, clamp angle and friction coefficient.
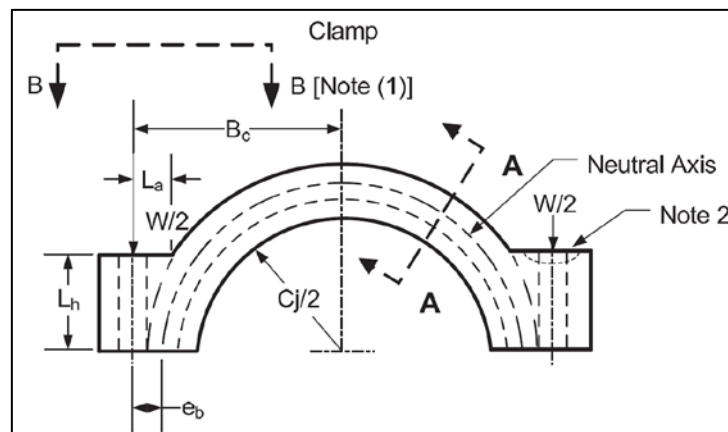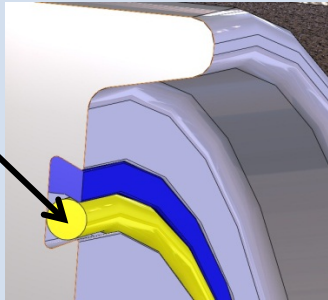
Fig 2.7 "W" represents the total bolt force for a clamp connector provided from the ASME VIII standard [31].

$$w_0 = \frac{2}{\pi}(H + H_p)\tan[\alpha - \phi_f]$$

(2.1)

It is assumed that the cap connection with the clamp segments will have a relatively large amount of the force acting on limited areas (Fig 2.8). The clamp mechanism will produce a vertical force that tightens the connection together. The total vertical force developed from the mechanism should be equal or more compared to the required load from equation 2.1 (total bolt load).
The total bolt load was calculated and the different values are described in table 2.1.

Table 2.1 Inputs for the total required bolt load.

Input	Variable	Value	Unit	Comment
Clamp shoulder angle	α	24	° (degrees)	The clamp segment angle is the same angle as for the ROV clamp connector (chapter 1.1.4) which fits the 12 inch hub interface.
Friction coefficient between hub and clamp	μ_{CC}	0.1	-	The material "ASTM A694 F60" was selected for the cap disc and clamp segments. The friction coefficient between the hub and clamp segment was set to 0.1. This can in reality change from 0.05 up to 0.15 and uncertainties are therefore related to this value. The friction coefficient was set to 0.1 based on engineering experience from AKS.
Friction angle	Φ_f	5.71	° (degrees)	
Effective bore diameter	D	347.8	mm	The effective bore diameter was set to the largest diameter that the pressure can act on the cap disc. The diameter was set to the center of the elastomer sealing.

The maximum diameter that is exposed for pressure

Fig 2.9 Elastomer seal.

Input	Variable	Value	Unit	Comment
Design pressure	P	34.5	MPa	The maximum design pressure for the 12 inch full bore hub is 345 bar [26].
Total hydrostatic end force	H	3277.69	kN	The total hydrostatic end force is the same as the resultant load from the pressure acting on the cap area.
Total Joint contact surface compression load	H_p	0	kN	The requirement for a joint contact surface compression load does not exist. The cap is equipped with an elastomer seal that is a self-energized gasket, meaning that the gasket does not need a certain pre-compression to provide a pressure tight sealing.

Computation of total bolt load required

Input	Variable	Value	Unit	Comment
Total clamp connection design bolt load on both lugs for the operating condition	W_0	690	kN	This is the total bolt load required for operating conditions for a standard clamp connector (Fig 2.7). The new concept should generate at least this amount of loads in vertical directions (Fig 2.8).
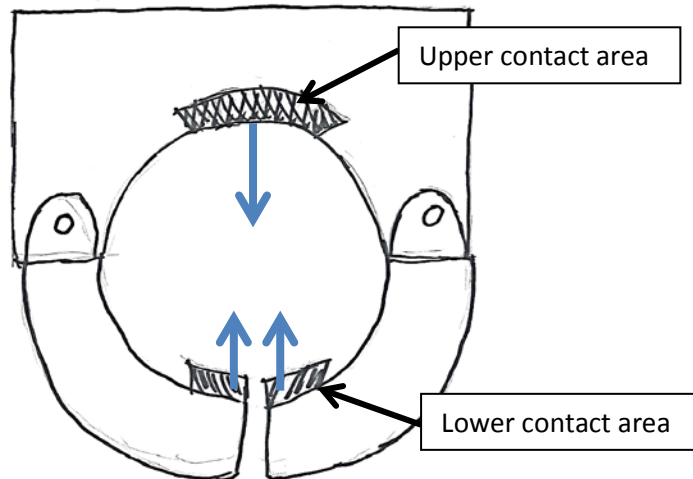
Fig 2.8 To make a reasonable basis for a computation model, the clamp force can be simplified to a contact area. This simplification was done in order to compare to the equation 2.1 with the preliminary cap design.

The total hydrostatic end force is calculated:

$$H = \pi P \left(\frac{D}{2}\right)^2$$

$$H = \pi \cdot 34.5 \text{MPa} \cdot \left(\frac{347.8 \text{mm}}{2}\right)^2 = 3277.69 \text{ kN}$$

The total bolt load is calculated with equation 2.1:

$$w_0 = \frac{2}{\pi}(3277.69 \text{kN} + 0) \tan[24° - 5.71°] = 690 \text{kN}$$

The ASME VIII standard states that the connection needs a bolt load of 690 kN.

2.2.2 DETERMINATION OF THE APPLIED LOAD FOR THE POWER SCREW

To investigate how much force that corresponds in applied force from the power screw, the mechanism was assessed with static equilibrium equations, with the clamp segments in closed position. Since the cap design is symmetric, only one halve of the model was assessed.
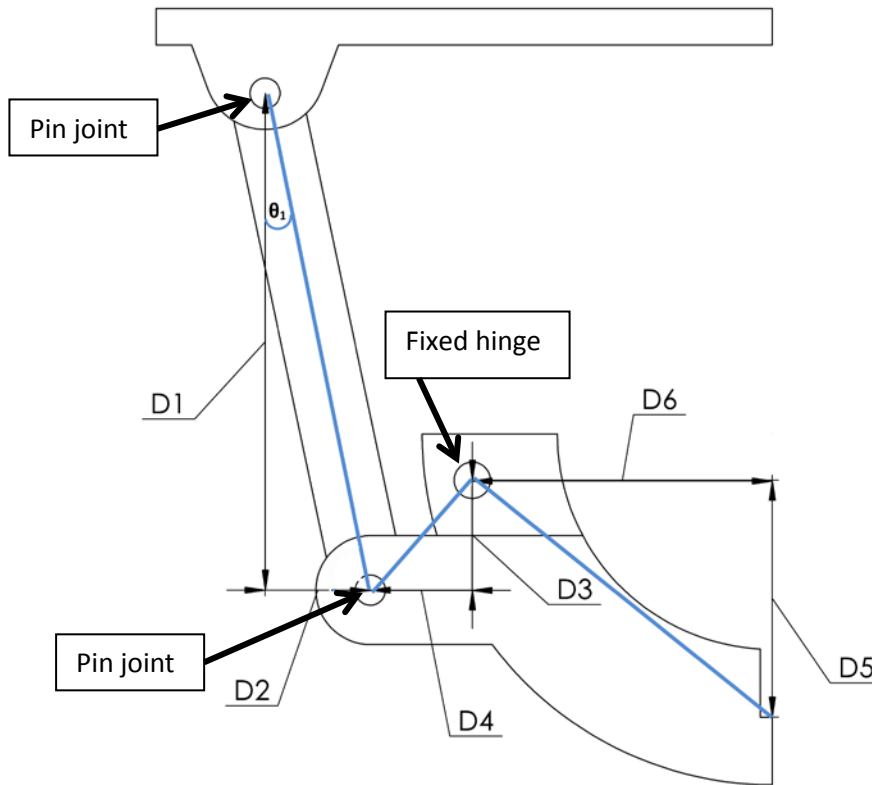
__Fig 2.10__ The mechanism was divided into a linkage and an angle lever in order to get a determination of the required force that needs to be applied. The angle lever is connected to a fixed hinge joint and the linkage has pin joints in both ends.
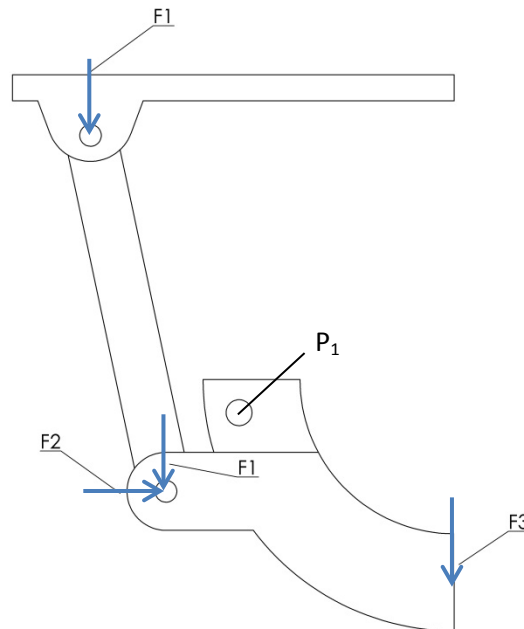
__Fig. 2.11__ F_1 represents the force applied by the power screw, F_2 the bearing load applied to the pin joint in horizontal direction and F_3 the required clamp force from equation 2.1.

To produce the required load F_3, the load F_1 in figure 2.11 illustrates the load that the power screw needs to provide. The positions and lengths of the linkage and angle lever, decides how much force that is required to be generated from the power screw.

Table 2.2 Inputs for determining the applied load. The variables are illustrated in Fig 2.10.

Description	Variable	Value	Unit
Vertical distance between the two pin joints of the linkage	D_1	410.8	mm
Horizontal distance between the two pin joints of the linkage	D_2	87.2	mm
Vertical distance between the lower linkage joint and clamp segment hinge	D_3	90.8	mm
Horizontal distance between the lower linkage joint and clamp segment hinge	D_4	84.4	mm
Vertical distance from the point where the required clamp force is applied and the clamp segment hinge.	D_5	234	mm
Horizontal distance from the point where the required clamp force is applied and the clamp segment hinge	D_6	248.4	mm
Linkage angle	θ_1	12.35	°(degrees)

The mechanism has two linkages which are attached to a clamp segment at both sides, and the bolt load is therefore divided by two:

$$F_3 = \frac{w_0}{2} \rightarrow \frac{689.663\text{kN}}{2} = 344.832\text{kN}$$

To determine the force F_1 and F_2, a moment equilibrium equation was established at point P_1 (Fig 2.11). The sum of all moments is zero in this point, and the two unknown forces can be determined. The normal force F_n for the linkages is used to determine the two forces.

$$\sum M_{P_1=0}$$

$$0 = -F_n \cdot \sin\theta_1 \cdot D_3 - F_n \cdot \cos\theta_1 \cdot D_4 + F_3 \cdot D_6$$

$$0 = -F_n \cdot \sin 12.35° \cdot 90.8\text{mm} - F_n \cdot \cos 12.35° \cdot 84.4mm + 344.832kN \cdot 248.4mm$$

The force F_n is the load applied normal to the linkage:

$$F_n = 840.878kN$$

The applied load from the power screw is calculated:

$$F_1 = F_n \cdot \cos\theta_1 = 821.425kN$$

The horizontal resultant force applied on the clamp hinge is calculated:

$$F_2 = F_n \cdot \sin\theta_1 = 179.823kN$$

Since the mechanism was split in half, the total applied load needs to be multiplied with 2:

$$F_{1,total} = 1642.9kN$$

The calculations resulted in a force of 1642.9 kN that is required to be applied by the power screw. This is not a completely realistic value since the calculations does not account for frictional loss. Friction can be found in the linkage pin joints, the clamp hinge and between components that come in contact with each other. It should be investigated how much this frictional loss possibly can be. This is to assure that the force applied is sufficient. If the frictional force is small, it needs to be assured that the applied force is not too high so it could overload any component.

2.2.3   *FEA COMPARISON OF THE APPLIED LOAD*

To verify that the calculated result was reasonable, a simplified model was created to perform a static analysis of the locking mechanism. The simplified model consisted of a horizontal plate, linkages and the lower clamp segments. It was constrained in appropriate directions and a force was applied at the middle of the horizontal plate (Fig. 2.12).
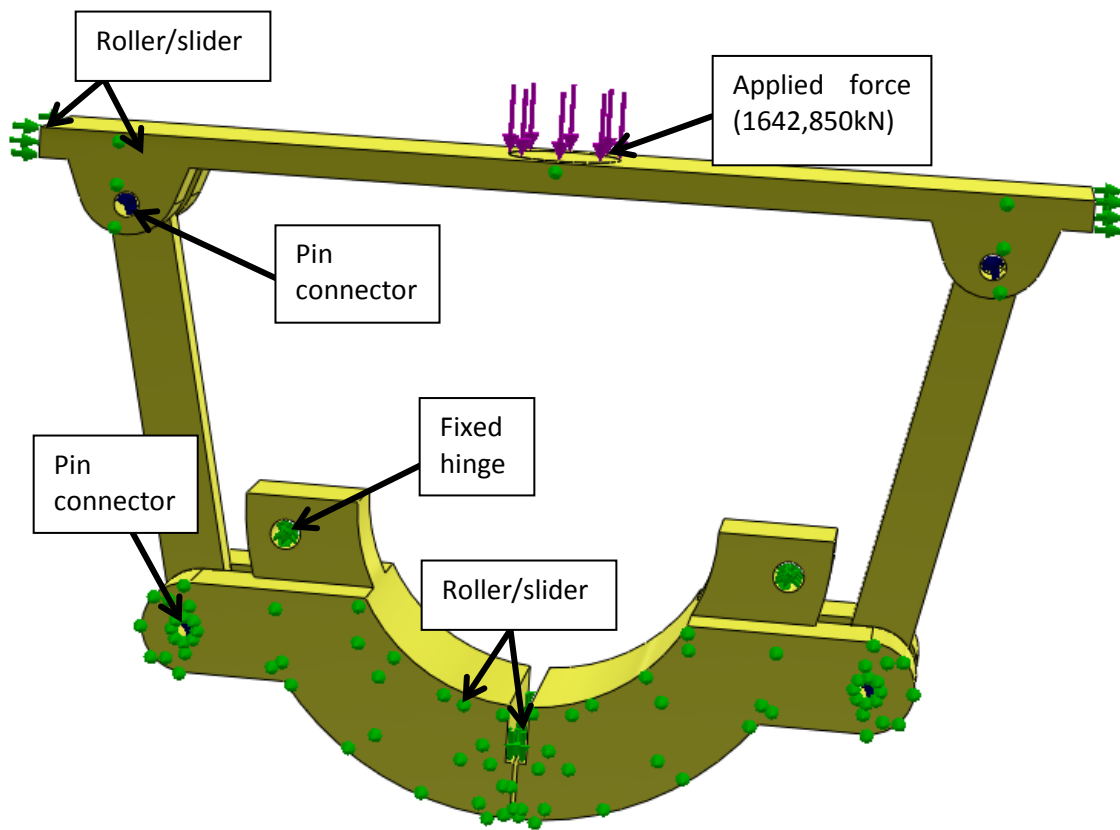
Fig 2.12 The loads, fixtures and connector conditions applied on the FEA model.

SolidWorks Simulation is a user friendly add-in to the CAD software SolidWorks. Although it gives the user an easy way to carry through a static analysis, it has some limitations. For instance, contact, fixtures and applied loads needs to be placed on surfaces of the geometry, and not directly on nodes or keypoints which is common practice in other analysis programs. It does not provide the user advanced analysis tools and possibilities, but it is a handy software for this case. A curvature based solid mesh was used. The analysis did not account for friction since this was not done in the hand calculations. The analysis established 18510 nodes and 10468 elements.
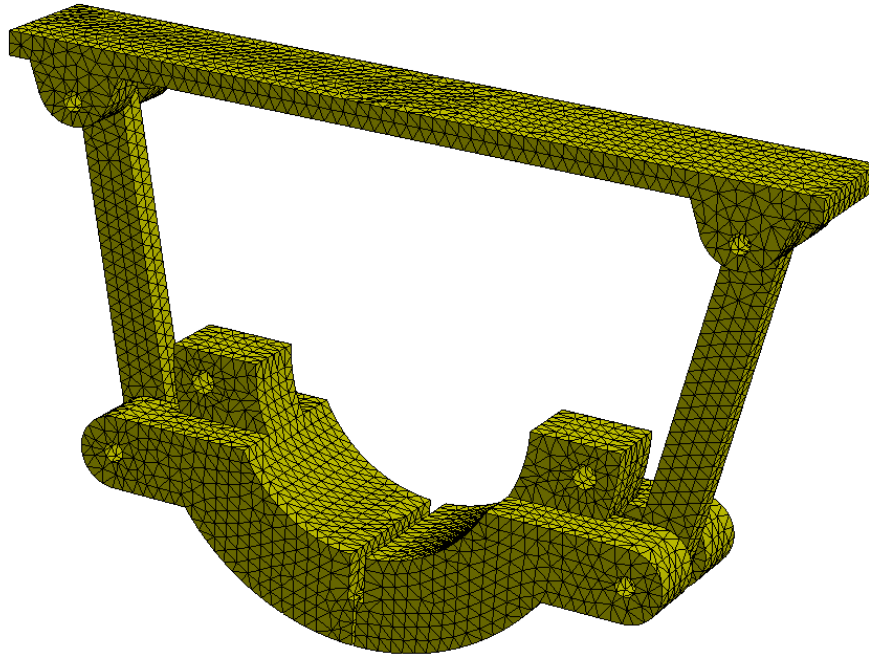
__Fig 2.13__ The mesh of the SolidWorks Simulation model.

A reasonable verification of the simulation was to check the force F_3 in the solved model to ensure a correct use of boundary conditions, applied load and geometry was used. The result was satisfying, the F_3 was 355kN (Fig 2.14) where F_3 from equation 2.1 had a force of 345kN.
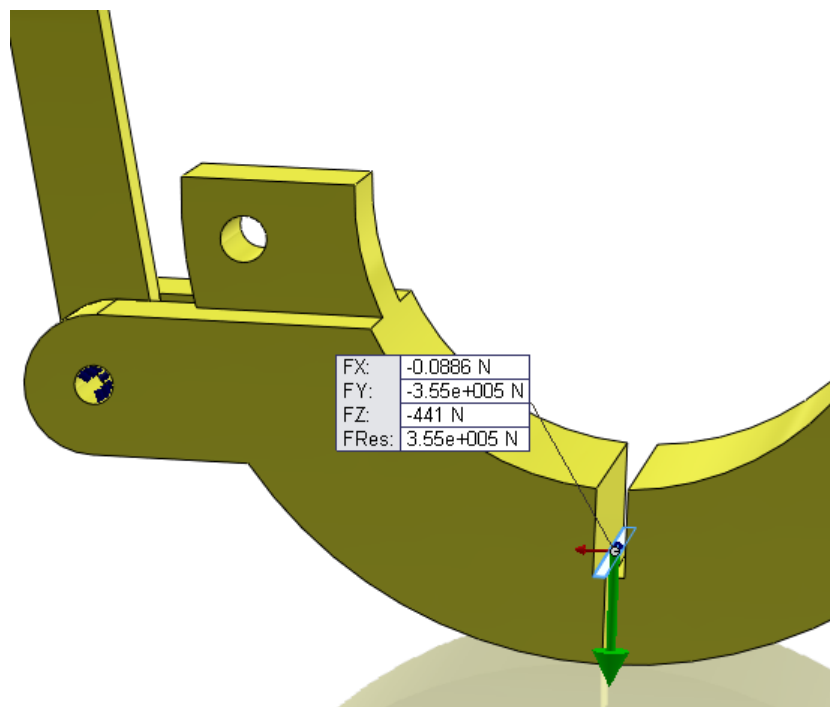
__Fig 2.14__ An edge was created at the end of the clamp segment to constrain it in y-direction, the resultant force acting on the planar face was 355kN which gave a difference of approximately 10kN to the calculated result.

A simplified model of the lower clamp segments and the locking mechanism was also made in Ansys Classic.
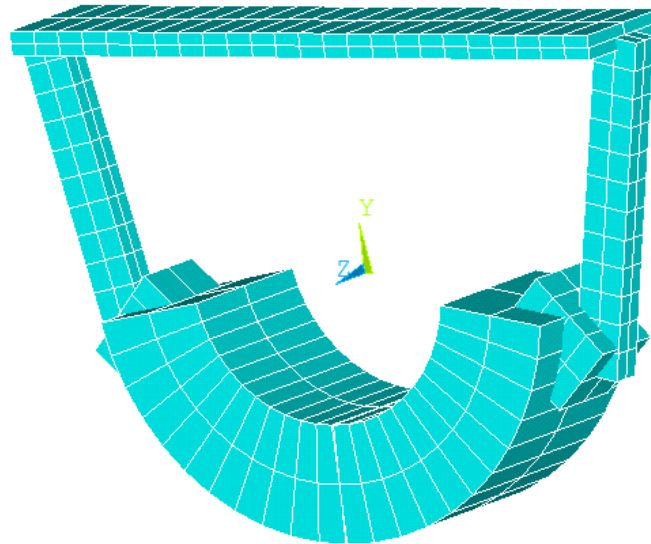
__Fig 2.15__ A simplified model of the cap, the model is divided into 78 elements.

Fourteen keypoints were made, and two keypoints were placed on the same location on both ends of the linkages. This was done to create linkage joints with Ansys "coupled constraint" function. The function enables two components to be connected to each other by a joint which is constrained in all directions except in the z-rotational direction. All of the keypoints where constrained in the z-direction. The two end-keypoints to the horizontal plate was constrained in the x-direction. The clamp segments hinge was constrained in all directions and rotations, except in the z-rotation. At the bottom of the two lower clamp segments, a keypoint was constrained in y-direction to obtain the desired output (Fig 2.16).
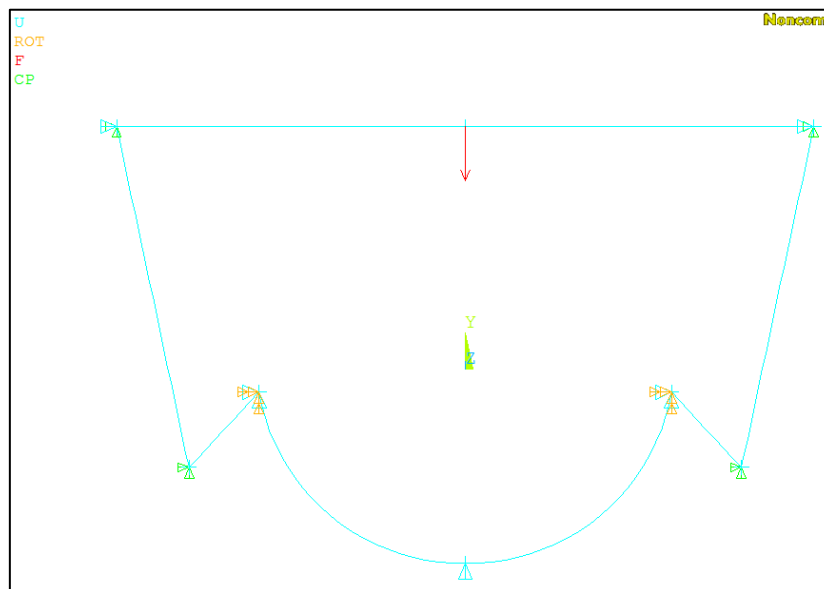
__Fig 2.16__ The model boundary conditions. The red arrow illustrates the applied force, the turquoise triangles shows which direction the model is constrained in. The green triangles show the pin joints and the yellow triangles shows where the model is constrained in the rotational direction.

The meshing was done with Beam189 elements, 78 elements and 161 nodes were created. As a final control to verify that the boundary conditions, applied loads and geometry, the force in y-direction was checked in the elements at the end of the clamp segment. The result was satisfying. A complete source code for the analysis can be found in appendix 1.
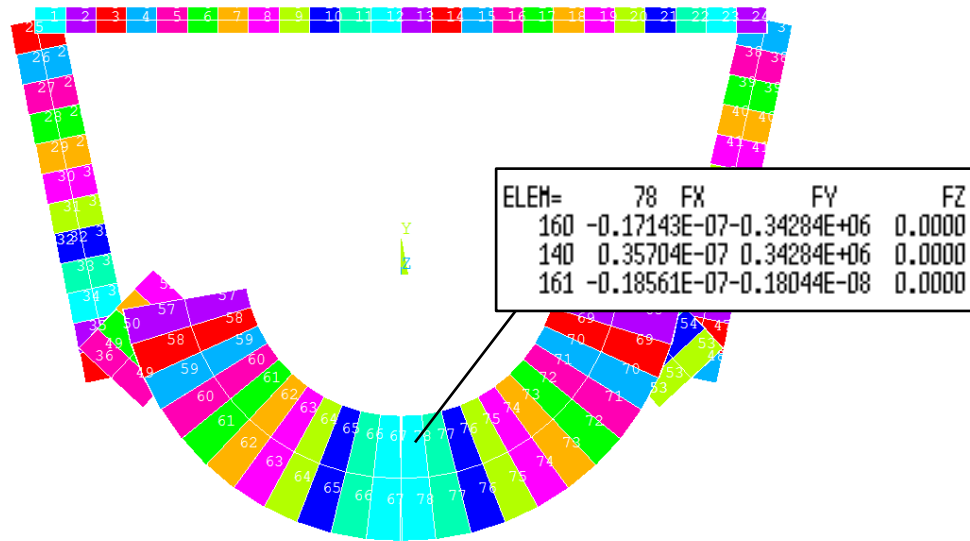
Fig 2.17 The element 67 and 78 have a resultant force in the y-direction of approximately 343kN, which is a satisfying match compared with the hand calculated result.
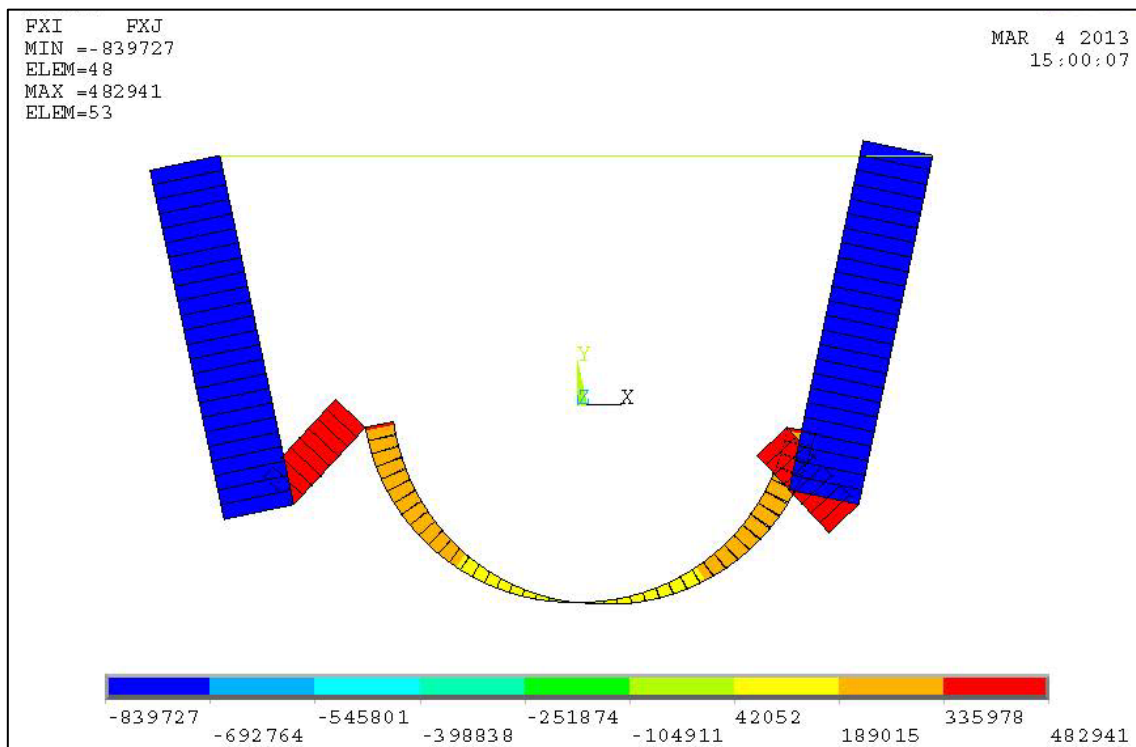
Fig 2.18 The axial force diagram show that the largest axial force is acting on the linkage with a force of 839.7kN. This is in accordance with the hand calculated result of 840.878kN (F_n).

The two linkages cannot pick up any moment (Fig 2.19), but as figure 2.18 shows, the axial force is acting through the linkages and makes a compression stress in the beam. It will therefore be appropriate to verify the linkage beams against buckling.
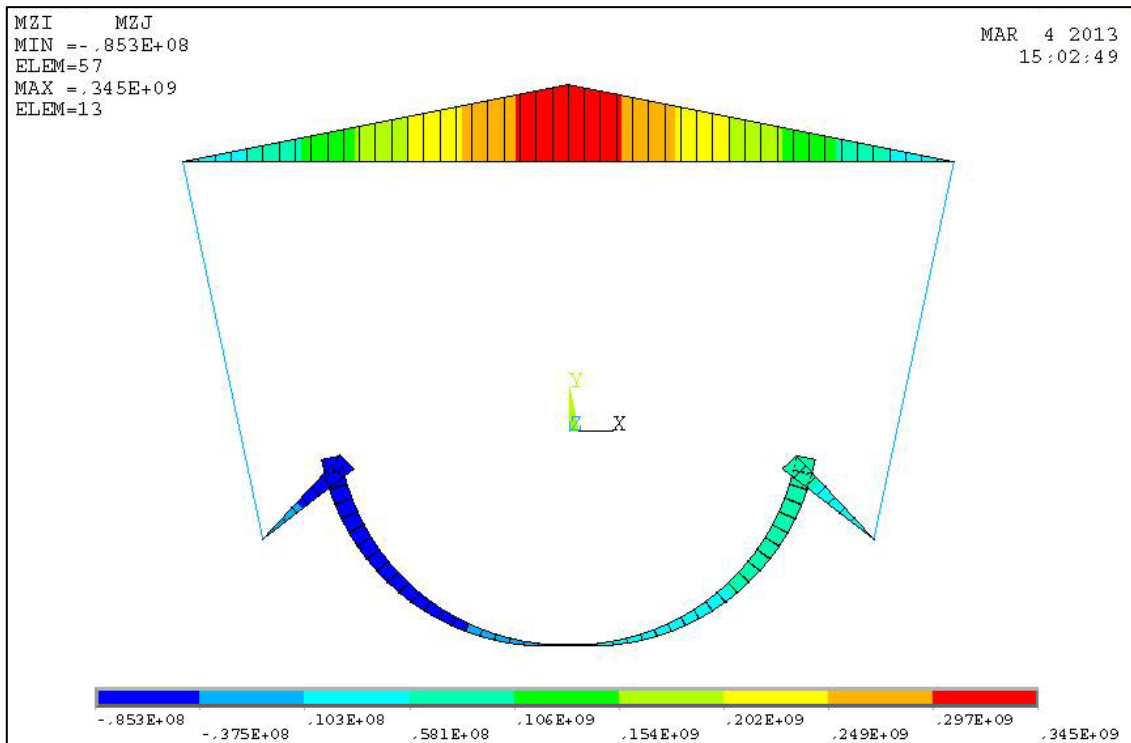
__Fig 2.19__ The largest moment is located at the middle of the horizontal plate where the power screw force is applied. The moment is excessive high giving a bending moment of 345 000kNm.
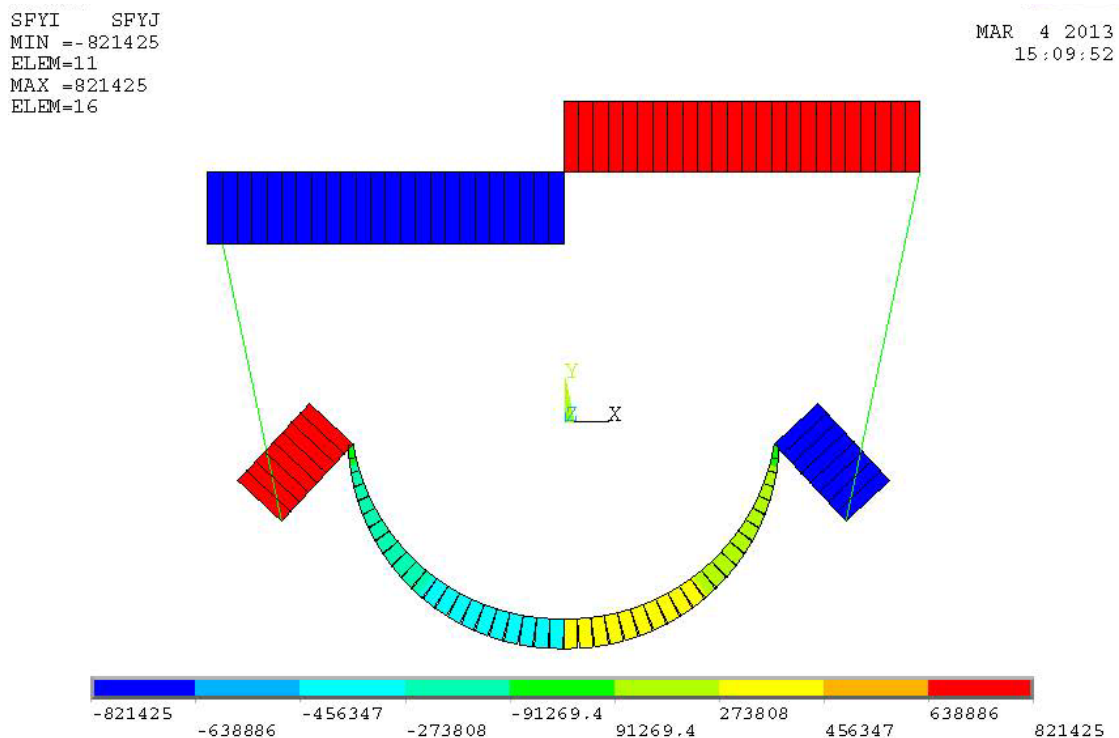
__Fig 2.20__ The shear force showed as the blue and red diagrams. The applied force on the horizontal plate gives an excessive shear force in the middle of the plate of 821.425kN.

Based on the moment diagram and shear force diagram, the mechanism weakest point is the middle of the top plate. This is the area where the construction will yield/break first.

2.2.4   *STRESS DETERMINATION OF THE LOCKING MECHANISM*

The previous hand calculation indicated the magnitude of the force that was necessary to be applied by the power screw mechanism. The next step will be to determine what kind of stress the applied force causes in the horizontal plate and the linkages.
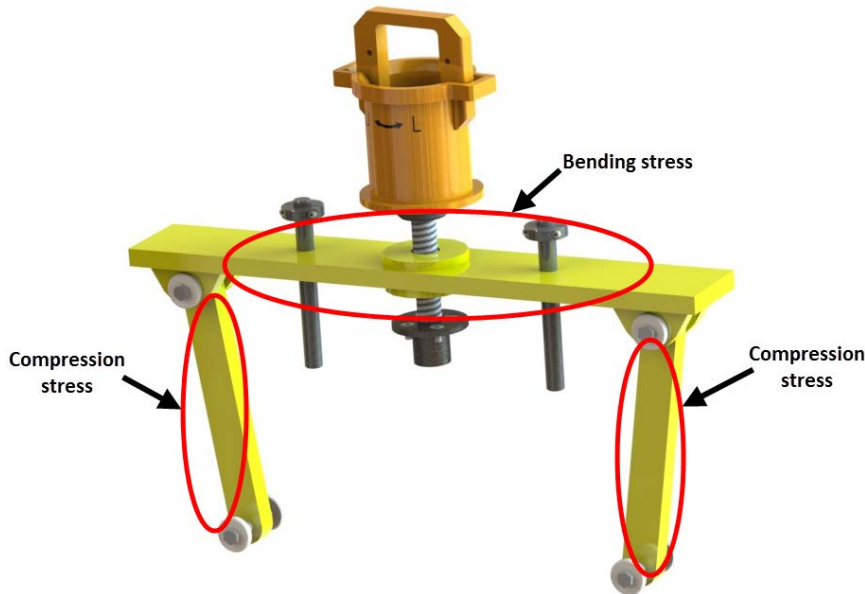
***Fig 2.21** The location of the bending stress and the compression stress that occur in the horizontal plate and linkages.*

HORIZONTAL PLATE

The horizontal plate can be assessed as a simple horizontal beam supported with two fixed joints in both ends and a force applied in the middle.
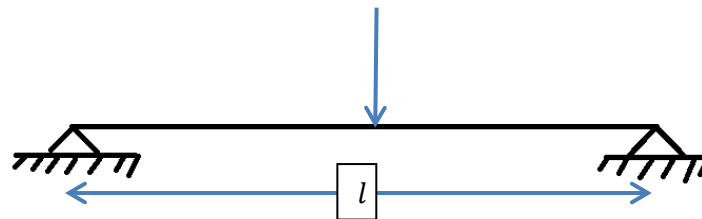
***Fig 2.22** A simple beam constrained with a fixed joint in both ends.*

The maximum moment occur at the middle of the beam:

$$M_b = \frac{Fl}{4} \tag{2.2}$$

$$M_b = \frac{1642.85kN \cdot 840mm}{4} = 3.45 \cdot 10^5 kNm$$

The calculated bending moment correspond well to the Ansys Classic result (Fig 2.19). To determine the bending stress it is necessary to find the section modulus:

$$W = \frac{1}{6}bh^2$$

$$W = \frac{1}{6} \cdot 150mm \cdot 30^2 mm = 22500mm^3$$

The bending stress can be determined:

$$\sigma_b = \frac{M_b}{W}$$

$$\sigma_b = \frac{3.45 \cdot 10^5 kNm}{22500mm^3} = 15333.3MPa$$

The result can be compared with the Ansys Classic result with a good match (Fig 2.23). The safety factor is calculated:

$$n_y = \frac{325MPa}{15333.3MPa} = 0.02$$

LINKAGES

The linkages will have a stress resulting from the normal force applied on the pin joint. As mentioned before, it is assumed to not be any bending stress in the linkage since the pin joint cannot transfer any moment.

$$\sigma_c = \frac{F_n}{A}$$

$$\sigma_c = \frac{840.878kN}{60mm \cdot 38mm} = 368.8MPa$$

The stress level obtained have a good match with the Ansys Classic result (Fig 2.23).

$$n_y = \frac{325MPa}{368.8MPa} = 0.9$$

The stress levels were compared with the Ansys Classic model and the SolidWorks Simulation model.
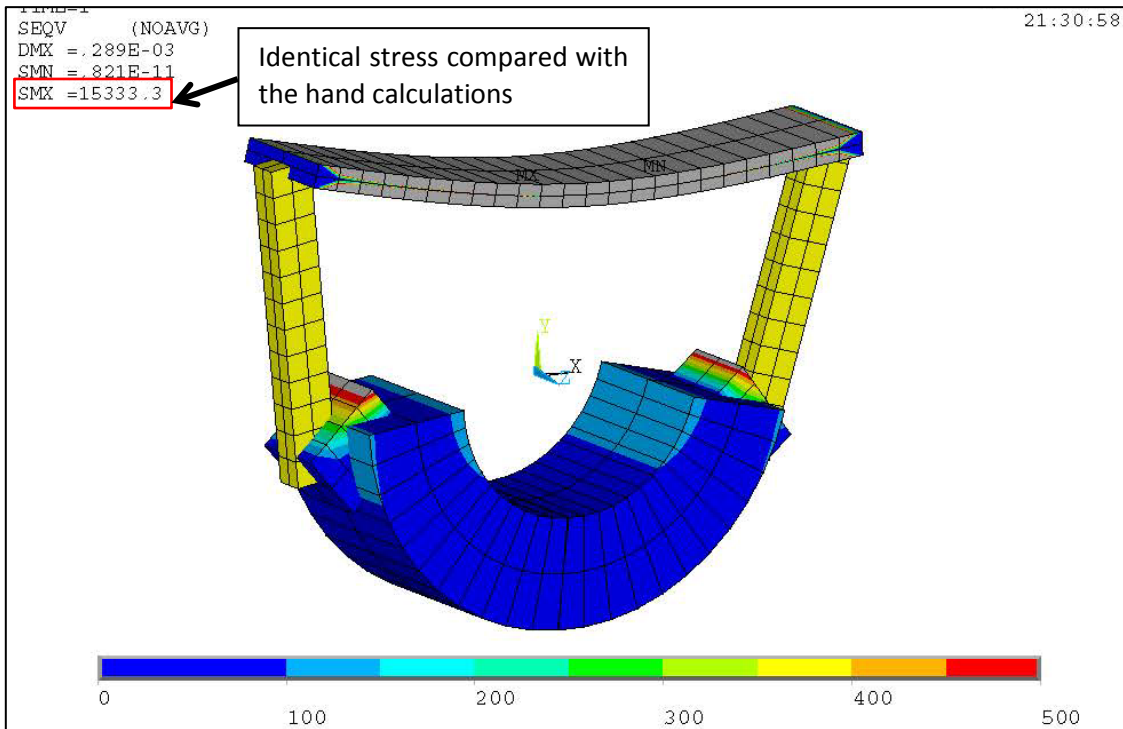
Fig 2.23 *A stress plot of the model. The counter plots is divided into ten different sections and the maximum stress plot is 500MPa. The grey fields indicate stress which is above the maximum value. Almost the whole horizontal plate is grey and the linkage has a stress between 350 and 400MPa which is in accordance with the hand calculated result. The maximum stress obtained is 15 333.3MPa. This comes from the bending moment applied by the power screw.*
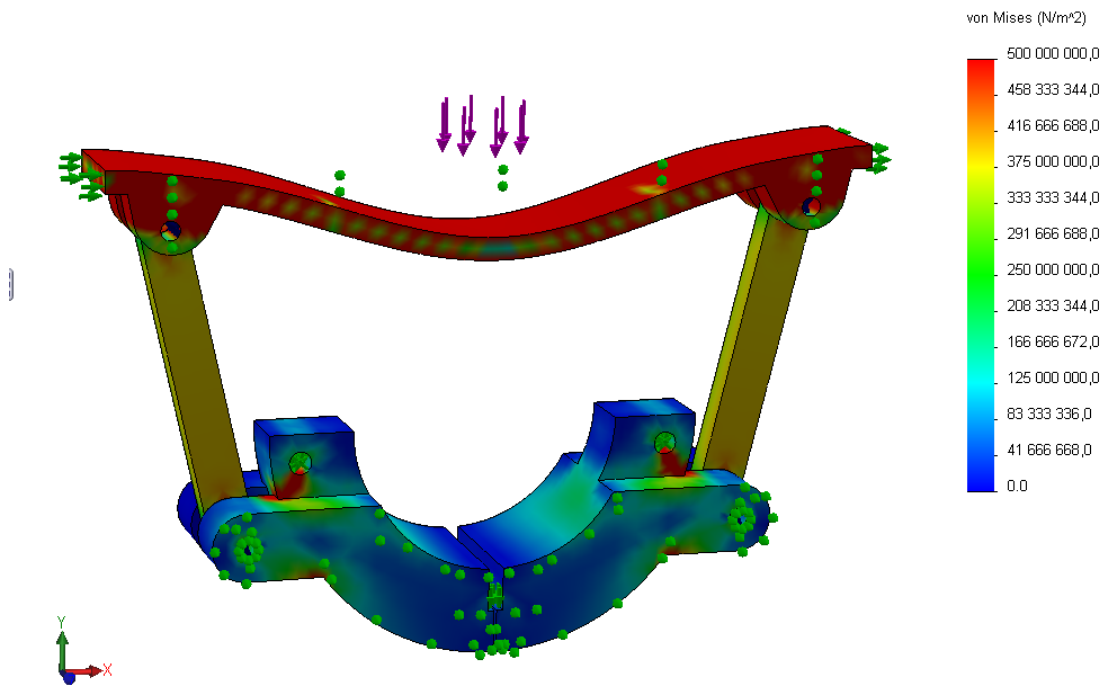

Fig 3.24 *A stress plot of the SolidWorks Simulation model, the maximum value was set to 500MPa and the red fields indicate stress above this value. Almost the whole horizontal plate has an excessive stress level and the linkage has a stress of approximately 375 MPa which is a good match compared to the hand calculations.*

2.2.5 *COMMENTS OF THE RESULT*

The hand calculated vertical reaction force at the end of the clamp segment was compared with Solidworks simulation and Ansys Classic, both with a satisfying result. The stress level that occurs in the horizontal plate and linkages from the applied load seems to match. The stress plot clearly indicates that the construction is weak and it will not withstand the applied load. The stress in the horizontal plate was determined to be 15 333MPa by hand calculations and Ansys classic. This gives a utility factor of 43.2. This is far above an acceptable value and the mechanism needs to be modified and improved to get more promising stress level. The linkages have an excessive stress level of approximately 375MPa.

3   DESIGN OF TEMPORARY SUBSEA INSTALLABLE PRESSURE CAP

3.1   CALCULATIONS AND ANALYSIS OF THE MODIFIED DESIGN

A new design was necessary because of excessive stress levels that occurred in the preliminary design. The goal was to optimize the utilization of the power screw force. This could be done by implementing a longer arm on the lever in such way that a larger moment will be produced. The result will be a less required force to be applied to make the same amount of vertical force at the clamp segments. The horizontal plate is extremely overloaded, therefore it was appropriate to decrease the length of the plate so the bending stress decreased. A new design was established with a long lever arm and two linkages at the two sides instead of one (Fig 3.1).
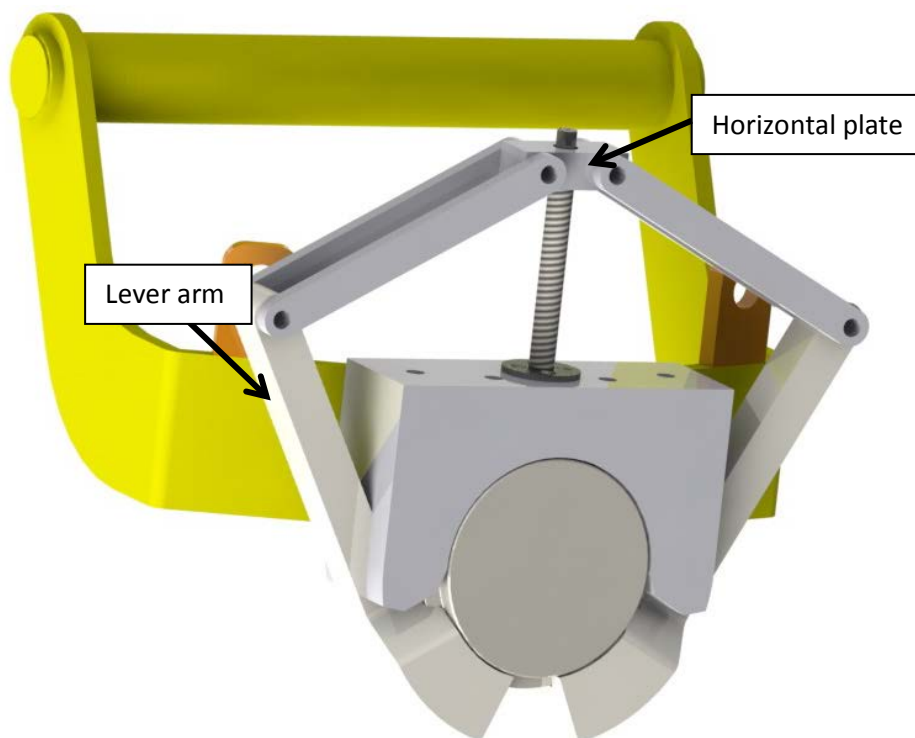
Fig 3.1 The first new design proposal. The lever arm length was increased so that a larger moment is generated with a less applied force. The length of the horizontal plate has been decreased to get lower bending stress values.

The modification would decrease the stress level in the mechanism, but on the other hand the lever arm is too large. This leads to a fairly large distance required to be travelled by the horizontal plate to open and close the segments, and the mechanism would use an excessive space upwards. The lever arm was also crashing into the upper clamp segment geometry.

When the locking mechanism is to be designed, the best balance between the smallest travelled distance by the horizontal plate and the maximum lever arm length needs to be considered. With a short lever arm, the required travelled distance for the horizontal plate is short since little movement of the horizontal plate gives a larger rotation of the clamp segments. On the other hand, the force required to be applied by the linkage need to be large because of a short moment arm.

The objective is to find an ultimate solution that gives:

- A minimum required travelled distance by the horizontal plate (leads to a minimum use of space upwards).

- A lever arm length long enough to provide a sufficient moment (a long lever arm enables a smaller force to be applied by the power screw).

- A mechanism that will open the clamp segment enough to enable it to be landed on the IB hub (needs to have sufficient clearance between clamp segment and hub when landed).

- A mechanism that do not interfere with other components while it opens or locks.

- All components need to have acceptable stress values (in accordance with prevailing safety factors).

A new design was generated with improvements. The horizontal plate was made thicker to reduce the bending stress and it was made openings for guide bars (Fig 3.2) which aid the guiding of the horizontal plate while it moves up and down. It also helps prevent the torsional moment applied on the plate by the power screw to not destroy or twist any pin joints or components in the mechanism. The upper clamp segment was also modified and excessive materials were trimmed away.
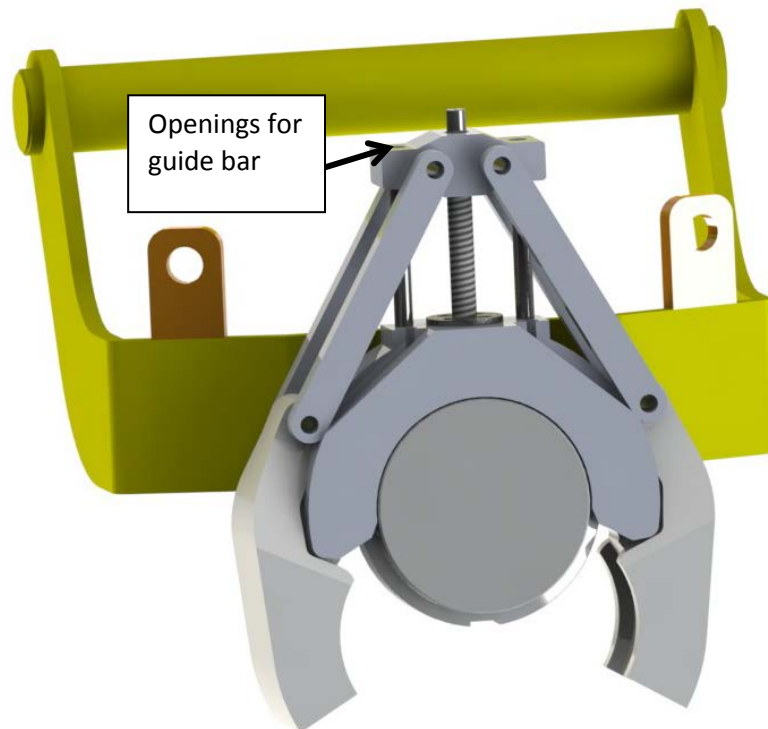
Fig 3.2 The cap in open position, instead of one linkage arm, two linkage arms were implemented to make a stronger mechanism.

The geometry and dimension of the clamp segment lever and the length of the connection part of the clamp segment was assessed to find the best solution. The objective was to establish a larger lever arm than the distance from the clamp hinge to the clamp segment edge. In other words, the mechanism should have a larger moment arm on the lever compared with the moment arm on the connection parts of the clamp segment (Fig 3.3).
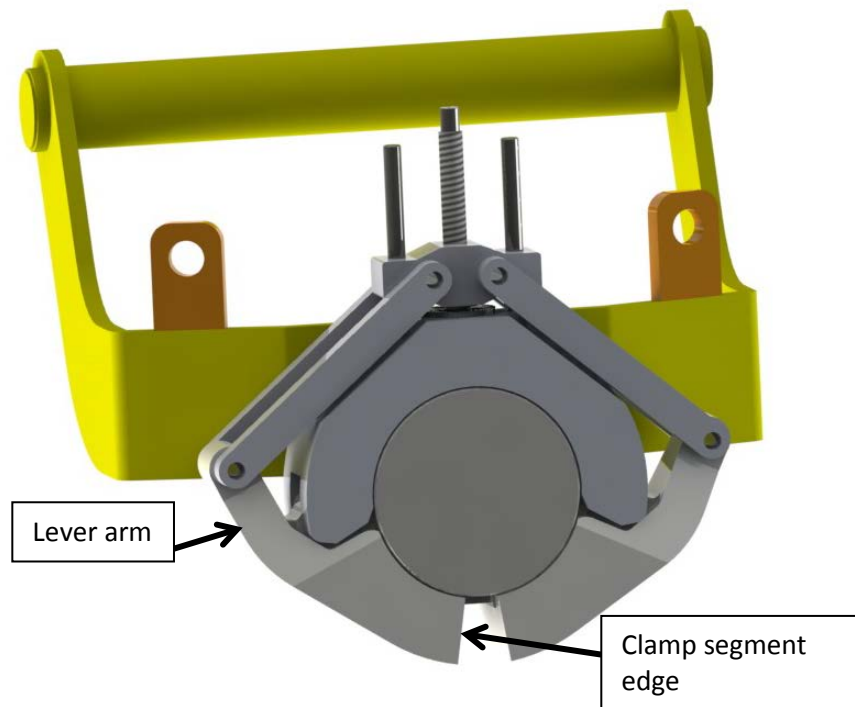
Fig 3.3 The cap in closed position.

3.1.1   *MATERIAL SELECTION*

The material selection is based on common materials that are used for similar components in AKS. For the clamp segments and cap disc, the ASTM A694 F60 material was selected, this because it has a relative high strength. This is a material that commonly is used on pressure contained components as flanges, valves and fittings. The designation "F60" is indicating that the material have a minimal tensile strength of 60 ksi, which corresponds to 414MPa. The locking mechanism uses S355 construction steel. The power screw, pin joints and other fittings is made of inconel 718 since these components can undergo heavy stresses and the components need to be resistant against wear. Inconel 718 has excelent corrosion resistance in seawater.
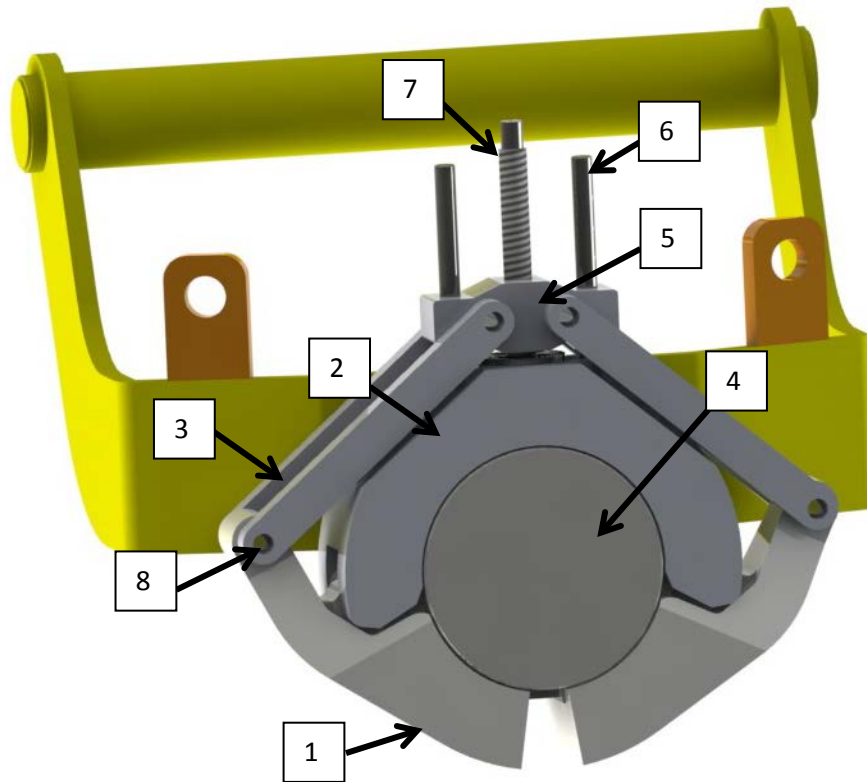
Fig 3.4 The components have different types of materials.

Table 3.1 The material selection of the components and their properties.

No	Component	Material type	Modulus of elsticity	Poision ratio	Yield strength	Ultimate strength
1	Lower clamp segment	ASTM A694 F60	200 GPa	0.3	448 MPa @ 21°C	530MPa
2	Upper clamp segment	ASTM A694 F60	200 GPa	0.3	448 MPa @ 21°C	530MPa
3	Linkage	S355	202.7 GPa	0.31	325 MPa @ 21°C	460MPa
4	Cap dsic	ASTM A694 F60	200 GPa	0.3	448 MPa @ 21°C	530MPa
5	Horizontal plate	S355	202.7 GPa	0.31	325 MPa @ 21°C	460MPa
6	Guide bar	S355	202.7 GPa	0.31	325 MPa @ 21°C	460MPa
7	Power screw	Inconell 718	206.8 GPa	0.29	414 MPa @ 21°C	827MPa
8	Pin joint	Inconell 718	205 GPa	0.294	827 MPa @ 21°C	1034MPa

3.1.2 APPLIED FORCE

The new design proposal needs to be evaluated in the same way as the preliminary design. The applied force and stress in the mechanism was determined.
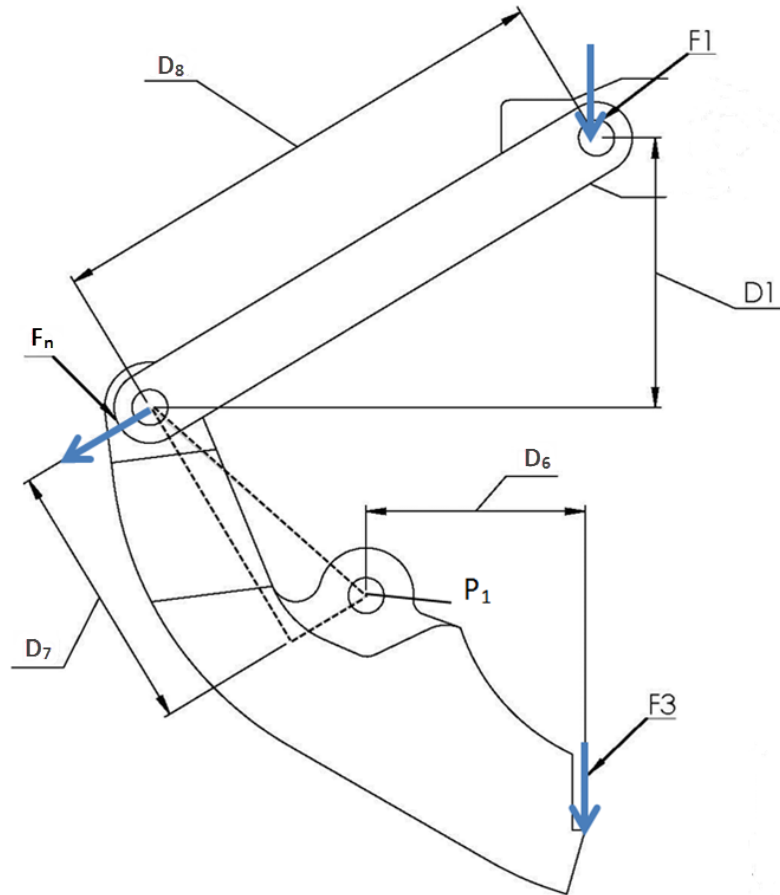
Fig 3.5 *The lever arm lengths and directions of forces to determine the required applied force F_1.*

Table 3.2 *Distances for lever arm and linkage.*

Description	Variable	Value	Unit
Vertical distance between the two pin joints of the linkage	D_1	226.3	mm
Horizontal distance from the point where the required clamp force is applied and the clamp hinge	D_6	183.9	mm
Lever arm length	D_7	229.1	mm
Linkage length	D_8	438	mm

The new lever arm length gives a mechanical advantage of 1.25 (229.1mm/183.9mm), which is a great improvement from the old design that had a mechanical disadvantage of 0.36 (123.4mm/341.3mm). From chapter 2.2.1 the required load for F_3 was determined to be 345kN.

$$\sum M_{P_1=0}$$

To determine F_1 and F_n, a moment equilibrium equation was established at P_1 (Fig 3.5). The sum of all moments is zero, and the two forces can be determined.

$$0 = -F_n D_7 + F_3 D_6$$

The compression load in the linkage can be determined:

$$0 = -F_n \cdot 229.1mm + 344.832kN \cdot 183.9mm$$

$$F_n = 276.799kN$$

The force F_1 can be determined by multiplying the D_1 and D_8 ratio:

$$F_1 = F_n \cdot \frac{D_1}{D_8} \rightarrow 276.799kN \cdot \frac{226.3mm}{438mm} = 143.013kN$$

Since this force needs to be applied on both sides of the horizontal plate F_1 is multiplied with 2:

$$F_{1,total} = 286kN$$

The total force required to be applied by the power screw is reduced from 1642.9kN in the preliminary design to only 286kN. This is a significant reduction and will lead to a major decrease in stress. The main contributor for this is change is the modification to a smaller horizontal plate length and increment of the lever arm length to generate moment for the clamping force.

3.1.3   STRESS DETERMINATION OF THE LOCKING MECHANISM

To compare the stress in the linkage and horizontal plate with the preliminary design, the generated stress in the modified design was determined.
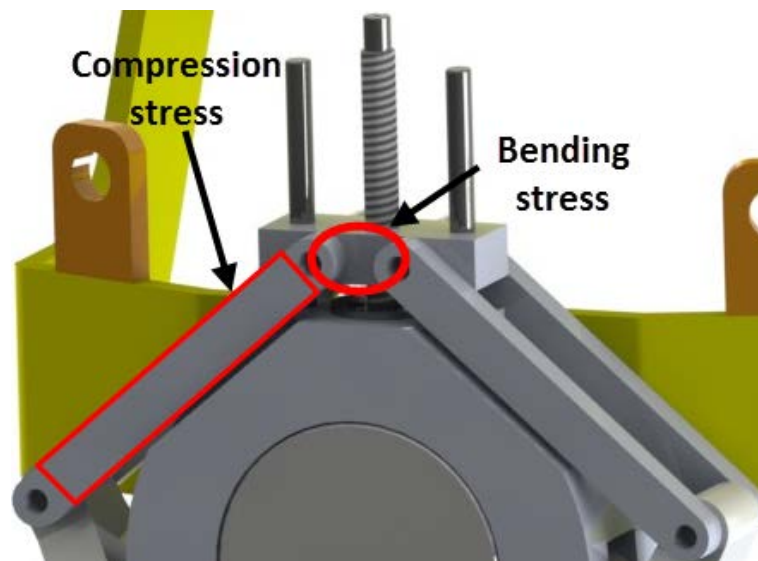
Fig 3.6 The location of the bending stress and the compression stress that occur in the horizontal plate and linkages.

HORIZONTAL PLATE

Most of the stress generated in the horizontal plate is assumed to be bending stress. The bending moment is calculated with equation 2.2:

$$M_b = \frac{pl}{4}$$

$$\frac{286.025 kN \cdot 110 mm}{4} = 7865.69 kNmm$$

The section modulus is calculated:

$$W = \frac{1}{6} bh^2$$

$$W = \frac{1}{6} \cdot 100 \cdot 100^2 = 17 \cdot 10^4 mm^3$$

The bending stress is calculated:

$$\sigma_b = \frac{M_b}{W}$$

$$\sigma_b = \frac{7865.69 kNmm}{17 \cdot 10^4 mm^3} = 46.3 MPa$$

$$n_y = \frac{325 MPa}{46.27 MPa} = 7$$

A bending stress of 46.3MPa is generated in the horizontal plate which corresponds in a factor of safety of 7. This is highly acceptable.

LINKAGES

The linkages will have a stress resulting from the compression force applied on the pin joint. The force F_n is divided by 2 since the design is implemented with two linkages on each side of the horizontal plate.

$$\sigma_c = \frac{F_n/2}{A}$$

$$\sigma_c = \frac{276.799 kN/2}{60mm \cdot 40mm} = 57.7 MPa$$

$$n_y = \frac{325 MPa}{57.67 MPa} = 5.6$$

A bending stress of 57.7MPa is generated in the linkage which corresponds in a factor of safety of 5.6. This is highly acceptable.

3.1.4   FEA RESULTS FOR THE LOCKING MECHANISM

A simplified model was created in Ansys Classic and Solidworks Simulation to verify that the calculations were reasonable. Both models gave satisfying results. It would be possible to have an asymmetric model, but because these models had very few elements and is only used to give an indication of the forces and stresses the whole model was used. However, the models had a fast computation time and it was therefore no reason to perform an additional simplification.
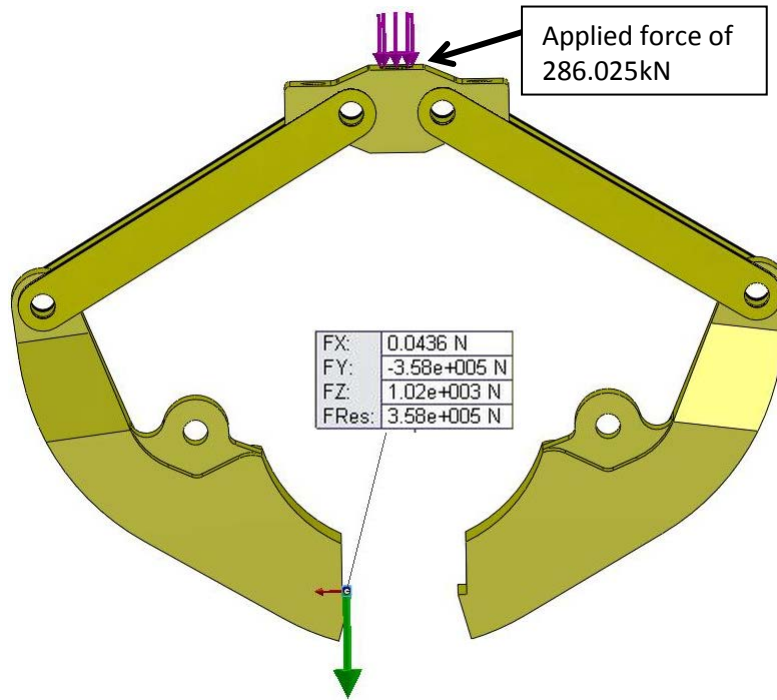
Applied force of 286.025kN

FX:	0.0436 N
FY:	-3.58e+005 N
FZ:	1.02e+003 N
FRes:	3.58e+005 N

__Fig 3.7__ The SolidWorks Simulation gives a vertical reaction force of 358kN, which is satisfying compared to the hand calculations.

Also a simplified model was created in Ansys Classic to judge if the forces and stresses is in accordance with the hand calculations. The source code can be found in appendix 2.
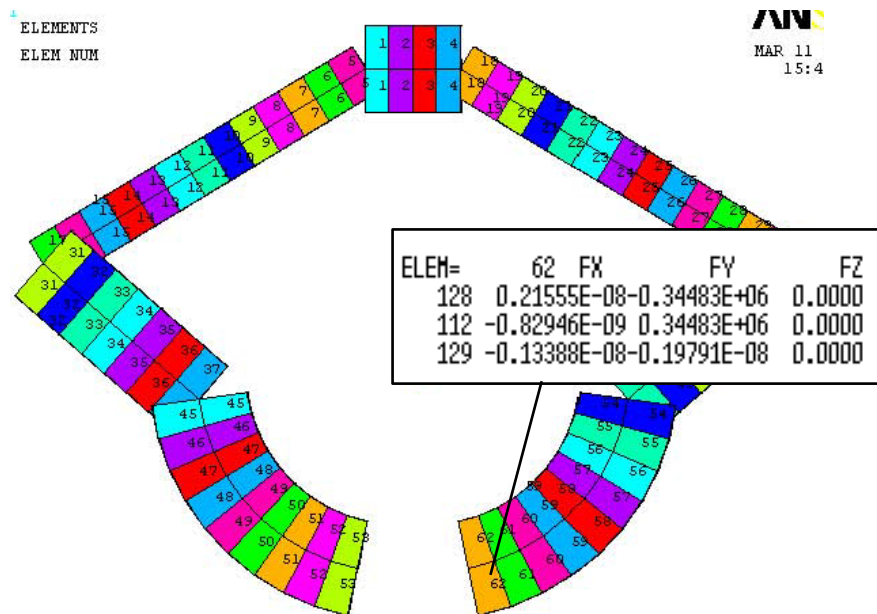

ELEMENTS
ELEM NUM

MAR 11
15:4

ELEM=	62 FX	FY	FZ
128	0.21555E-08	-0.34483E+06	0.0000
112	-0.82946E-09	0.34483E+06	0.0000
129	-0.13388E-08	-0.19791E-08	0.0000

__Fig 3.8__ The Ansys Classic gives a spot on value of the vertical force that is developed from the mechanism.

The axial force diagram show that the compression loads in the linkage is 276.8kN which corresponds well to the calculated value F_n. Axial loads exists in the lower clamp segments and will results in tension stresses (Fig 3.9).

SUB =1
TIME=1
FXJ   FXI
MIN =-276793
ELEM=14
MAX =342108
ELEM=45

APR 16 2013
20:07:45

-276793   -139259   -1725.84   135808   273341
    -208026   -70492.7   67041   204575   342108
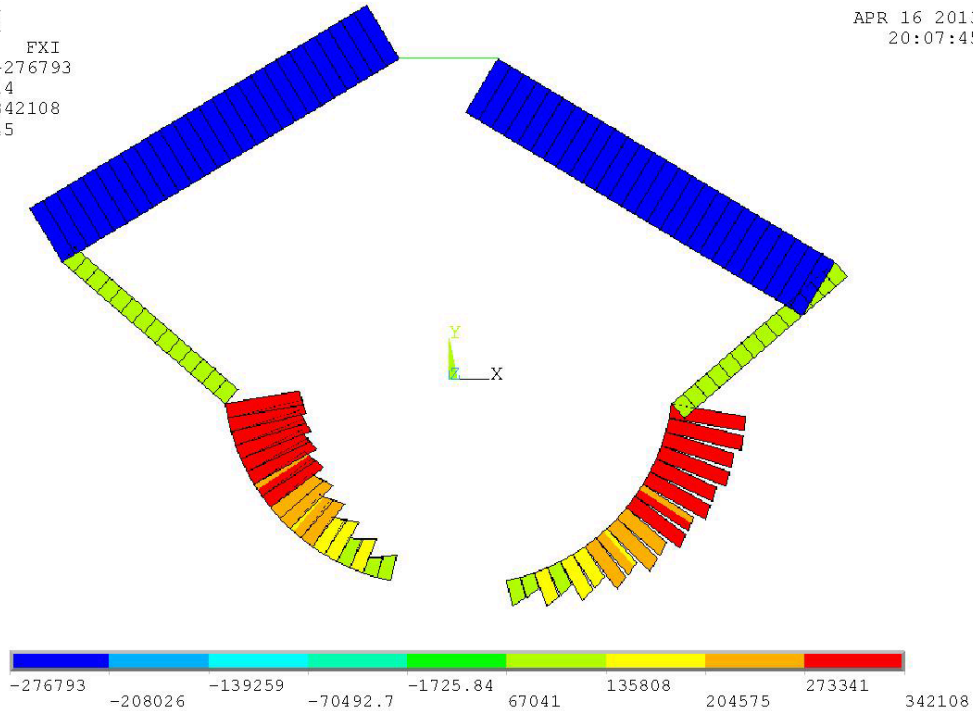
Fig 3.9 **The axial force diagram of the mechanism.**

The shear force diagram show that the horizontal plate will undergo a shear force of 112.7kN and the upper part of the lower clamp segment a shear force of 187.8kN. The end of the lower clamp segment gives a shear force of 338kN, which is most likely an unrealistic value since it is constrained at only one point in the y-direction.

LINE STRESS

STEP=1
SUB =1
TIME=1
SFYI   SFYJ
MIN =-338049
ELEM=53
MAX =338049
ELEM=62

APR 16 2013
20:17:34

-338049   -187805   -37561   112683   262927
    -262927   -112683   37561   187805   338049
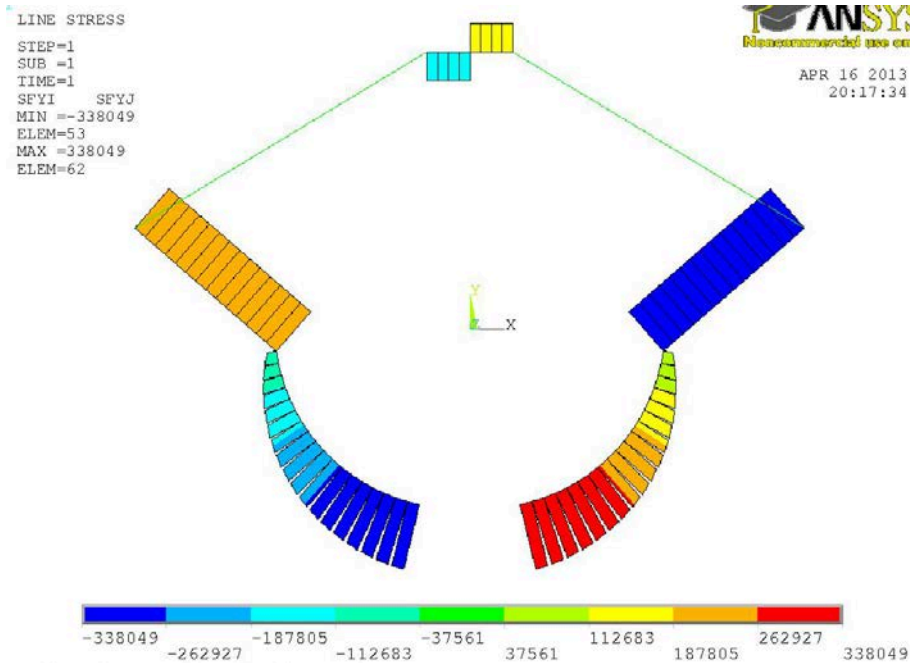
Fig 3.10 **The shear force diagram of the mechanism.**

The bending moment has been greatly reduced in the horizontal plate due to the modifications. The lower clamp segment will have a relative large bending moment. However, the model can indicate wrong indications for the value since it is constrained in the y-direction at the end of the segment and therefore make unrealistic values. It exist a large axial force in the region where the lower clamp

segment is attached to the upper clamp segment and also a shear force and bending moment. This region will be important to investigate further to evaluate if it is subjected to excessive loads and an area of stress concentrations.
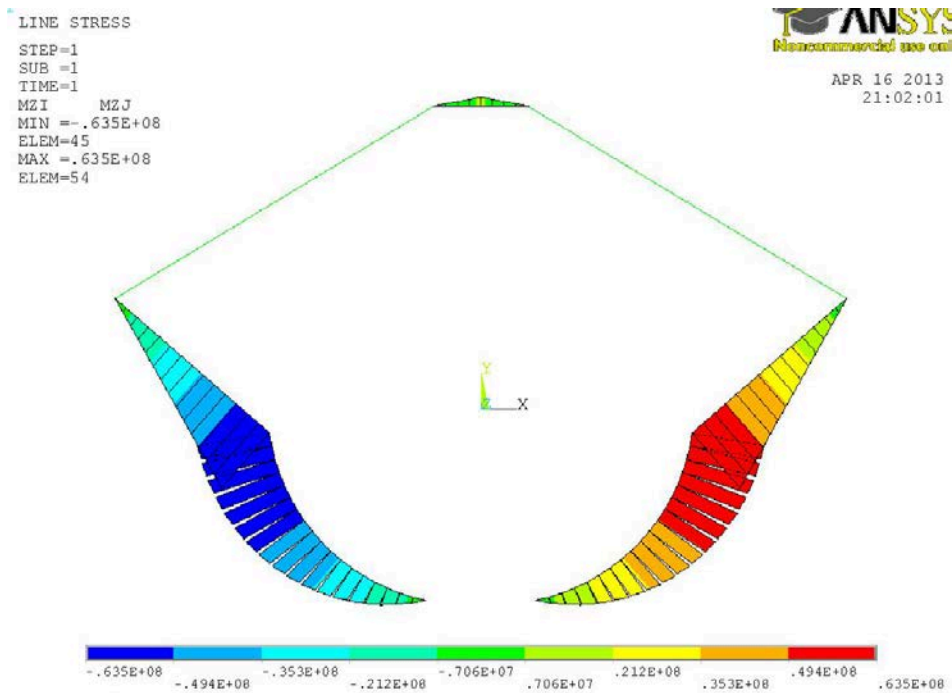
Fig 3.11 The bending moment diagram of the mechanism.

The linkage and horizontal plate have a simple load scenario and geometry. Therefore the indications of the stress gives a promising indication about the strength of the design. However, more assessments are needed in order to provide a complete dimensioning of the design. To provide trustworthy data for the stress in the clamp segment, a more comprehensive analysis should be carried out. This is because of a rather complex geometry that needs to be treated with advanced boundary conditions. It is too early to conclude on this kind of analysis and to justify whether the mechanism will withstand the applied load.

STEP=1
SUB =1
TIME=1
SEQV   (NOAVG)
DMX =.213E-05
SMN =.605E-14
SMX =259.32

APR 16 2013
19:58:42

.605E-14   57.6266   115.253   172.88   230.507
      28.8133   86.44   144.067   201.693   259.32
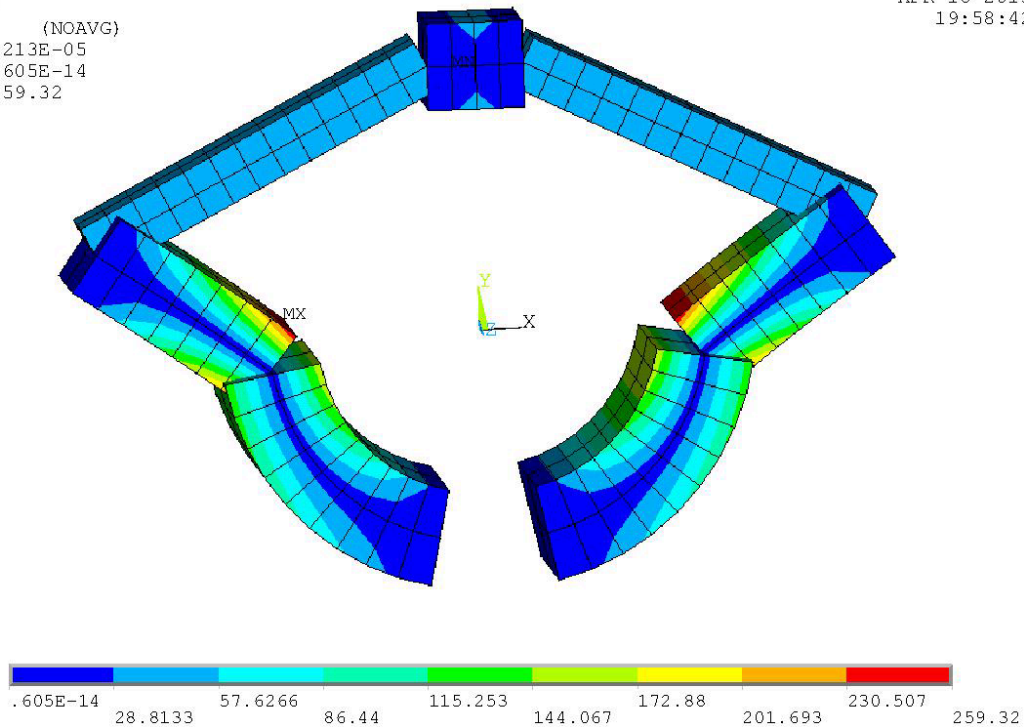
Fig 3.12 The simplified Ansys Classic model gives a maximum stress value of 259.3MPa

von Mises (N/m^2)

325 000 000,0
297 916 672,0
270 833 344,0
243 750 000,0
216 666 672,0
189 583 344,0
162 500 000,0
135 416 672,0
108 333 336,0
81 250 000,0
54 166 668,0
27 083 334,0
0.0

Weak point
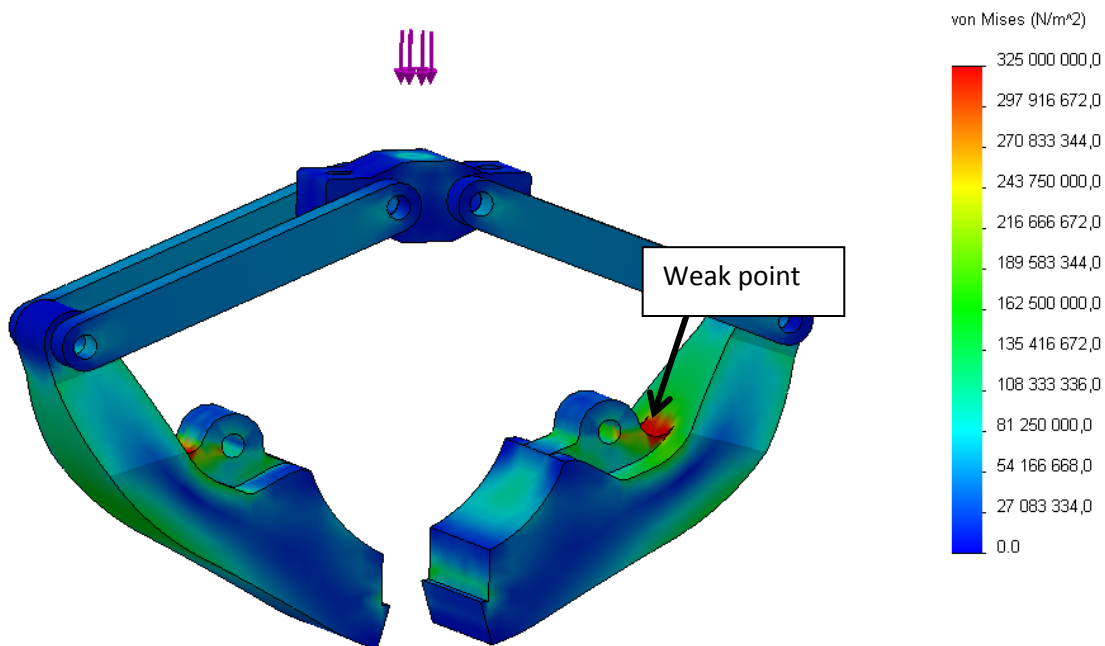
Fig 3.13 Von Mises plot. The lower clamp is provided with an eye for attaching the upper clamp segment. The analysis indicates that this region gives an increased stress level.

The factor of safety plot was made and indicates that most of the mechanism have a factor of safety above 4 globally (Fig 3.14). The FOS is determined from the yield limit and the von Mises stress.
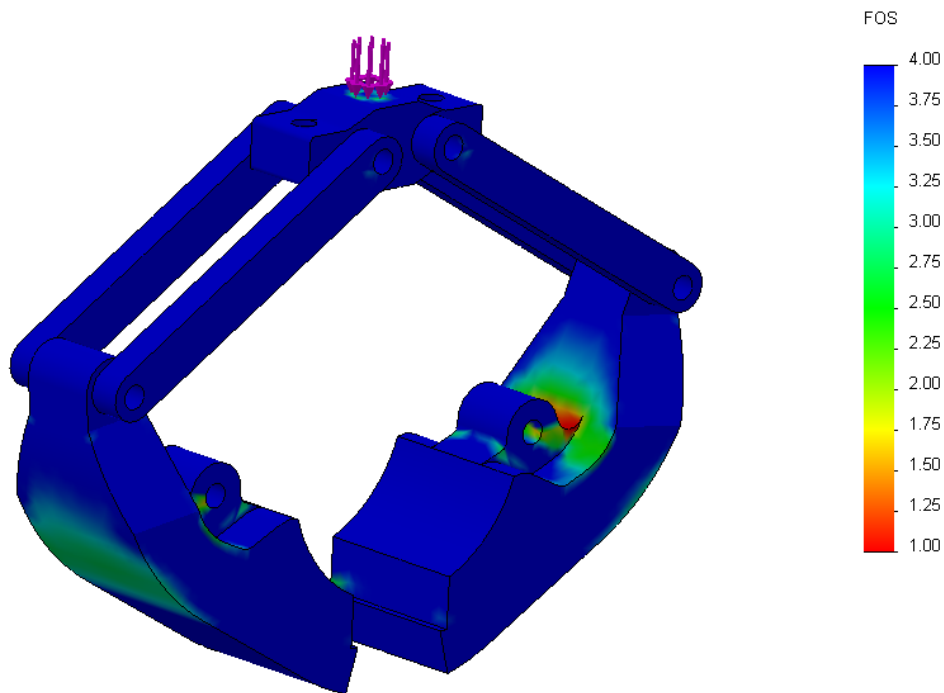
Fig 3.14 A factor of safety plot of the mechanism.

3.1.5 COMMENTS ON THE RESULT

The highest stress values are considered as local stress. These stresses will not give large deformations to the structure and can normally be ignored since the cap is only subjected to static loads. The nominal stress values for the whole cross section are described as global stress and this is critical when dimensioning components that only undergo static loads. If the cap was subjected to dynamic loads, much more concern needs to be taken on the local stress areas [33]. Yielding will occur when the component is exceeding the yield strength of the material. The local stress levels can be reduced by the use of a larger radius and round of notches and edges. Also the geometry can be up-scaled to provide a lower stress concentration.

The result gave a positive indication of the design, meaning that it could potentially withstand the operational loads. A further investigation was carried out to provide more sufficient and accurate data for dimensioning the design.

3.2 DESIGN OF THE LOCKING MECHANISM

The previous chapter gave a positive indication regarding the strength of the mechanism. In this chapter will the pin bolts, linkages and power screw be controlled against appropriate failure modes. As mentioned before the joints in the mechanism will undergo some frictional loss. The same goes for the threads and collar bearing on the power screw. Investigation of these losses is important to assure that the force applied is sufficient. If the frictional force is small, it needs to be assured that the applied force is not too high so that a component gets overloaded. Therefore, the frictional loss was first determined when designing the locking mechanism since it will cause an increment of the applied load by the power screw.

3.2.1 *DETERMINATION OF THE FRICTIONAL LOSS IN THE MECHANISM JOINTS*

Friction will occur in the mechanisms linkage pin joints and in the pin bolt that attaches the lower clamp segments to the upper clamp segment. This needs to be accounted for and will cause the applied force to be larger in order to produce the same required clamp force. The friction coefficient can vary for metal surfaces sliding against each other, depending on the surface roughness, lubricant and material properties. It was assumed that the pin joints are treated with some kind of lubricant when assembled and the lubricant would stay on the joints surfaces after the cap has been deployed subsea. When the cap is submerged, the seawater will not act as a lubricant to the pin joints. The two sliding surfaces will squeeze away the water when they are slided.

Another aspect is that the determination of the frictional loss in the pin joints only account for the frictional loss when the shaft (pin) and Bearing (pin opening) (Fig. 3.15) are sliding against each other. The determination does not account for the face-to-face frictional loss at the ends of the joint. It is not a straight forward task to establish a reasonable frictional coefficient because there are many uncertain factors.
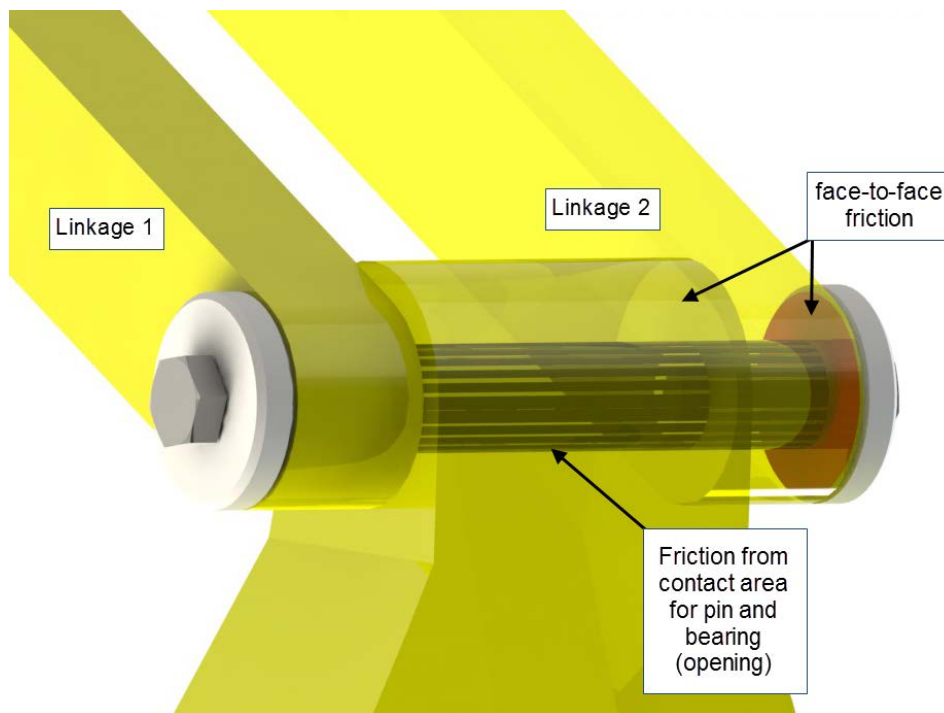

Fig. 3.15 *The different areas that will contribute for frictional loss of the pin joint.*

Steel against steel contact with lubricated surfaces typically has a friction coefficient between 0.03-0.12 when sliding against each other [34]. There is a difference of friction coefficients for a static and a sliding (dynamic) contact situation (Fig 3.16). A stationary object that is initiated in movement has a greater friction coefficient compared to an object that is already sliding (moving). When investigating the mechanism, the mechanism is in a moving situation, since it is in the end of the locking cycle and the clamps initiate contact with the hub and cap profile. Therefore, the frictional situation can be looked on as dynamic. For the determination of the friction in the pin joints, a friction coefficient of 0.1 is taken as a basis. It should be noted that this is an assumption and it exists some uncertainties related to the value.
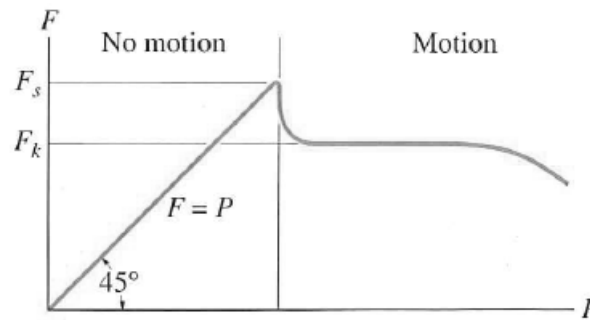
Fig 3.16 F_s is the limiting static frictional force and when the object is exceeding this force, movement occurs. The force F_k will act when the two bodies already are sliding against each other, [35].
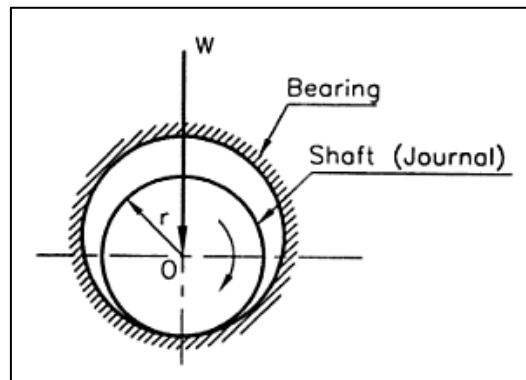
Fig 3.17 The stationary part is called the bearing (linkage) and the rotating element is called the journal (pin). The journal is a drive fit in the bearing and is therefore slightly less in diameter than the bearing [36].

When a journal revolves in a bearing due to friction between two rubbing surfaces, the friction force starts opposing the motion, hence some power is lost. A reasonable assessment of the frictional resistance can be based on the laws of dry friction. This means that the calculations of the pins are based on a bearing that is not lubricated or as in this case, only partially lubricated. The law of dry friction has been found to be approximately true by experiments [37].

The law of dry friction [37]:

1. The friction force is directly proportional to the normal reaction between the surfaces for a given pair of materials and the frictional force acts tangential to the contacting surface in a direction opposite to the relative motion.
2. The friction force depends on the material of which the contact surfaces are made of.
3. The friction force is independent of the area of contact.

4. The force of friction is independent of the velocity of sliding. This law is not true in strict sense as it has been found that the friction is dependent slightly with the increase in velocity.
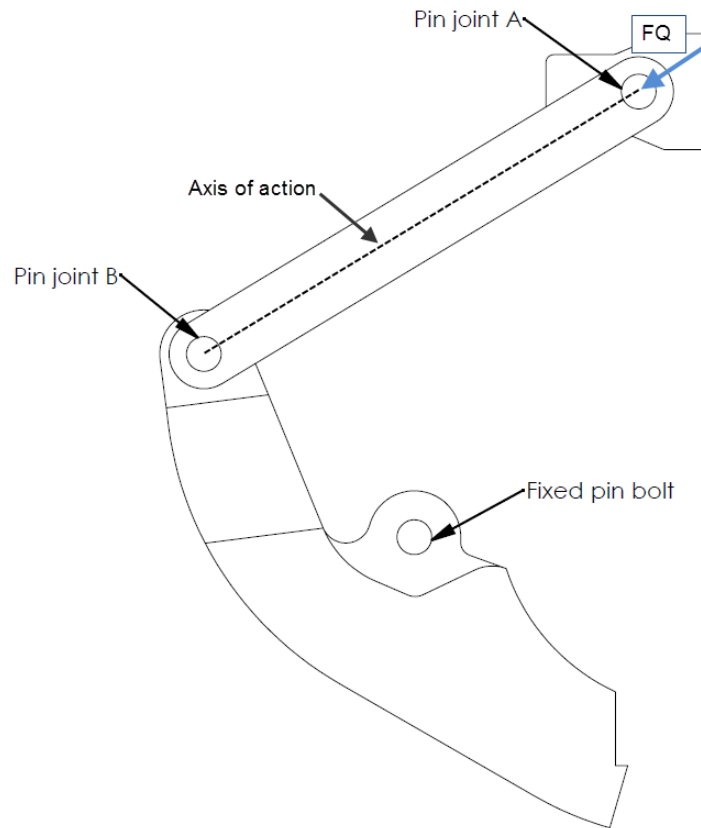

***Fig 3.18** When the force F_Q is applied to the linkage it has an axis of action that goes through the middle of the linkage breadth.*

Due to friction at pin joints A and B, the line of action of the load F_Q will not remain along the longitudinal axis AB. When accounting for friction, an axis of friction can be generated where the force $F_{Q'}$ acts along. The frictional axis can be determined by considering a friction circle at each pin-joint.
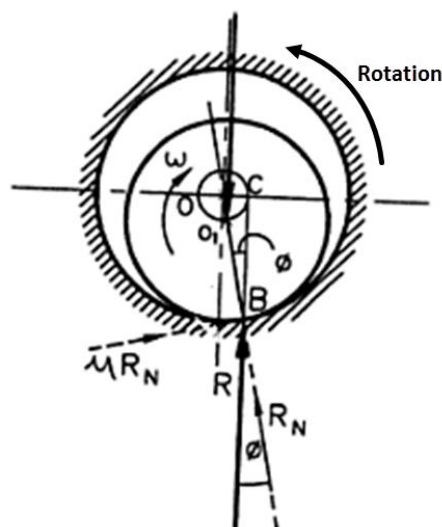
***Fig 3.19** The pin diameter is small in size to more clearly illustrate the effective contact area that is located at point B [36].*

If a linkage revolves in clockwise direction as shown in fig 3.19, the pin joint starts to climb up the bearing in the opposite direction. This is due to friction between two rubbing surfaces, the friction starts opposing the motion. When a shaft rests in its bearing, the load F_Q acts through the centre of gravity, then the normal reaction of the bearing acts in line with F_Q in the vertically upward direction. When the linkage is revolved, the linkage is still in equilibrium under the action of load F_Q, with normal (reaction) force R_N and the frictional force μR_N, which is tangential to the contact surface.
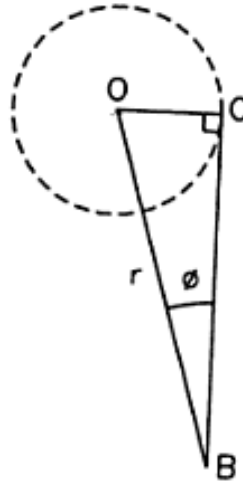
Fig 3.20 OC is perpendicular to the force R, with O as centre and OC as radius of the friction circle. B is the contact point showed in figure 3.19. $\emptyset$ is the angle of friction and r is the pin joint radius [38].

R is a resultant reaction force of R_N and μR_N, which is inclined at an angle ϕ to R_N (Fig 3.19).

OC= μR_N, this is known as the radius of the frictional circle of a pin joint [38].

Due to friction between the two rubbing surfaces, the resultant force on the pin joints is tangential to the friction circle and parallel to the force F_Q. Thus, the axis of action line will shift to new position called axis of friction (Fig 3.21).
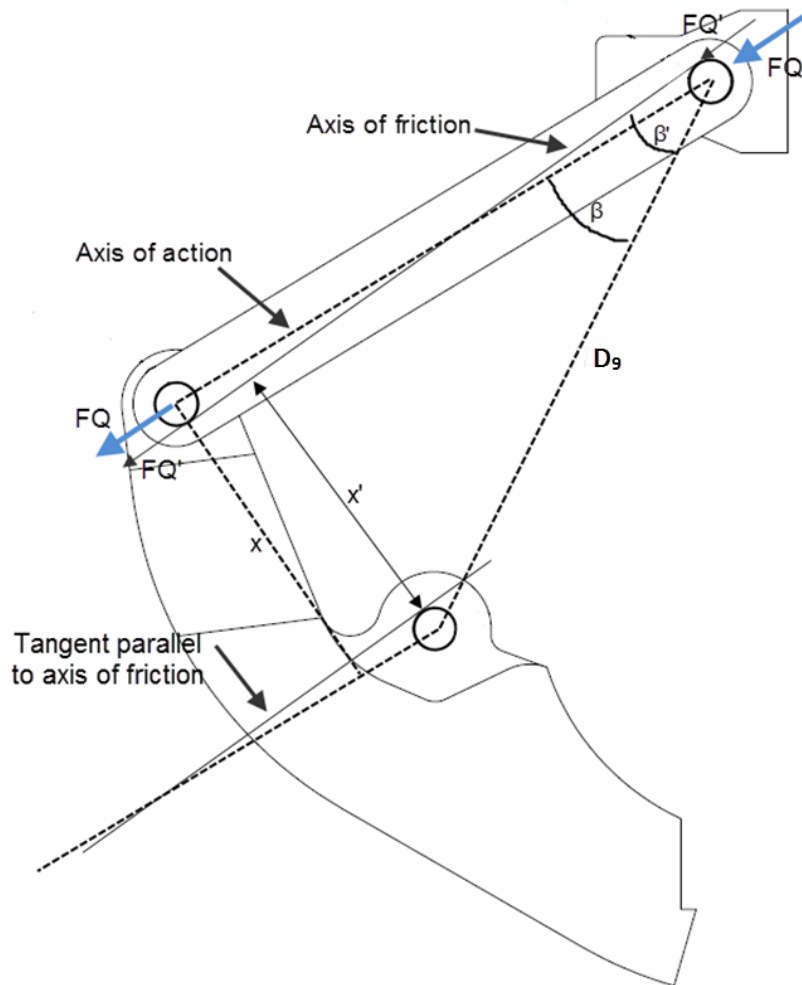
Fig 3.21 *The axis of friction is illustrated and result in a new $F_{Q'}$ and an angle β' which account for the frictional loss. The lever arm also gets a new moment arm with a length of x'.*

The three pin joints needs to be evaluated in order to find out which way the pin is "climbing" in the bearing.
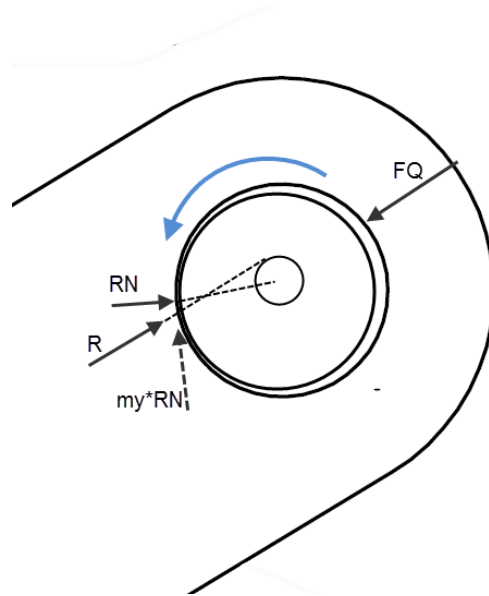
Pin joint A:

Fig 3.22 The frictional circle and the associated forces in pin joint A.
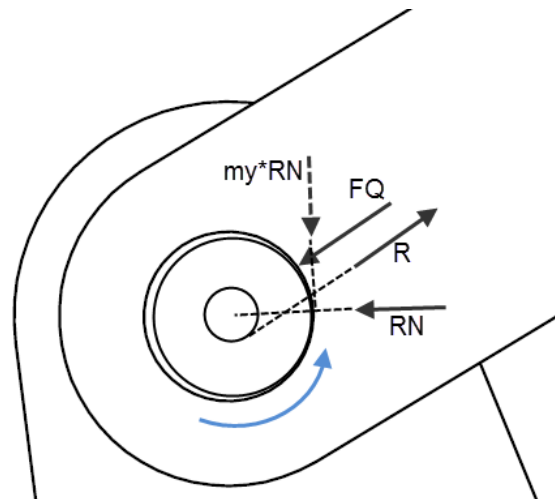
Pin Joint B:

Fig 3.23 The frictional circle and the associated forces in pin joint B.

Pin bolt:
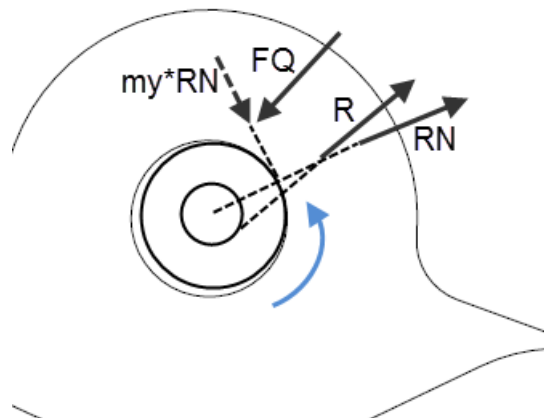
Fig 3.24 The frictional circle and the associated forces in pin bolt

The diameter of the pin was determined to be 36mm (chapter 3.2.2). The loading condition for the pin that attaches the lower clamp segment to the upper clamp segment has not been investigated. As a basis, the same diameter for this pin is selected.

Table 3.3 *Inputs for determining the frictional effect in the mechanism*

Description	Variable	Value	Unit
Lever arm length	D_7	229.1	mm
Linkage length	D_8	438	mm
Normal distance between pin joint B and clamp pin bolt.	D_{11}	240.7	mm
Radius of pin joint	R_{pj}	18	mm
Required clamp force	F_3	344.832	kN
Friction coefficient for pin joints	μ_{pj}	0.1	-
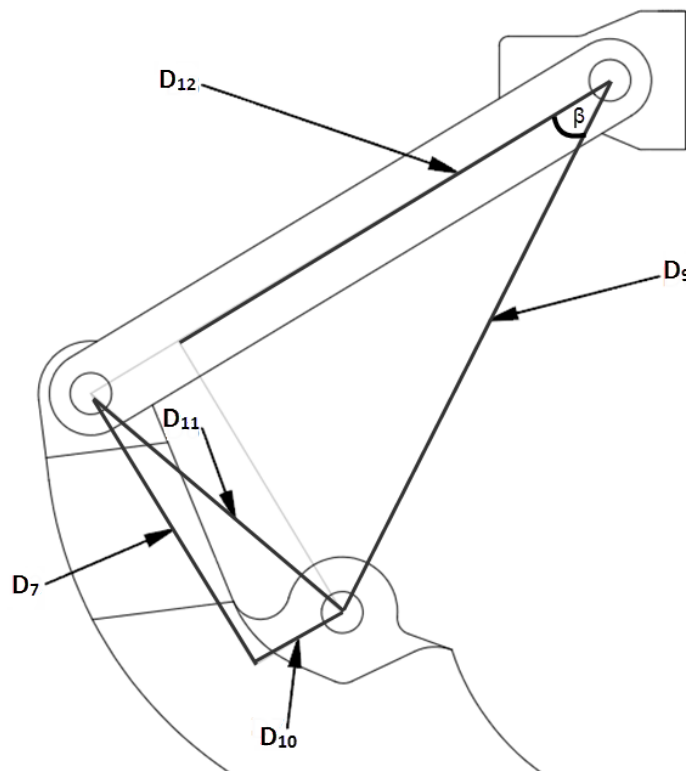
Fig 3.25 *Distances necessary to determine the angle* β.

The angle between D_9 and D_{12} is β. To find this angle the distance D_{10} and D_{12} (Fig 3.25) needs to be calculated first:

$$D_{10} = \sqrt{D_{11}^2 - D_7^2}$$

$$D_{10} = \sqrt{240.7^2 mm - 229.1^2 mm} = 73.82 mm$$

Determination of the length D_{12} is done by subtracting the D_{10} from D_8:

$$D_{12} = D_8 - D_{10}$$

$$D_{12} = 438 mm - 73.82 mm = 364.18 mm$$

When D_{10} and D_{12} are determined, the angle β can be found:

$$\beta = \tan^{-1}\left(\frac{D_7}{D_{12}}\right)$$

$$\beta = \tan^{-1}\left(\frac{229.1mm}{364.18mm}\right) = 32.17°$$

The radius of the friction circle at the pin joints is calculated:

$$r_{pj} = \mu_{pj}R_{pj} \tag{3.1}$$

$$r_{pj} = 0.1 \cdot 18mm = 1.8mm$$

The inclination of the friction axis and the linkage own axis is β-β', To determine the inclination, the distance D_9 (Fig 3.25) needs to be found first:

$$D_9 = \sqrt{D_7{}^2 + D_{12}{}^2}$$

$$D_9 = \sqrt{364.18^2mm + 229.1^2mm} = 430.249mm$$

Since the inclination between the axis of action and friction axis is determined by the friction circle radius for joint A and B, the following equation is true:

$$\tan(\beta - \beta') = \frac{2r_{pj}}{D_9}$$

$$\beta - \beta' = \tan^{-1}\left(\frac{2 \cdot 1.8mm}{430.249mm}\right) = 0.479°$$

The inclination of the friction axis β' is calculated:

$$\beta' = \beta - 0.479°$$

$$32.17° - 0.479° = 31.69°$$

The distance x' can be determined (Fig 3.21):

$$x' = \sin(\beta')\, D_9$$

$$x' = \sin(31.69°) \cdot 430.249mm = 226.02mm$$

As a result from the frictional loss, the lever arm has decreased in length which will require a higher force to be applied on the mechanism to get the same clamp force.
As performed earlier in chapter 3.1.2, a moment equation can be established around P_1 (Fig 3.5) with x' as the new lever arm length:

$$0 = -F_{Q'} \cdot x' + F_3 \cdot D_6$$

$$0 = -F_{Q'} \cdot 226.02mm + 344.832kN \cdot 183.9mm$$

$$F_{Q'} = 280.571kN$$

The $F_{Q'}$ is calculated to be 280.571kN. This is the force that needs to be applied normal to the two linkages, which gives a force of 140.285kN per linkage.
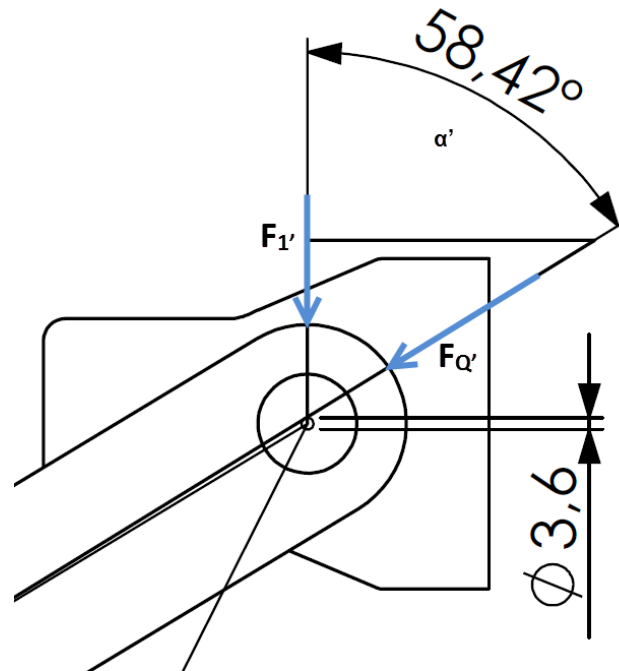

<u>*Fig 3.26*</u> *The angle α' is used to determine the applied vertical force F1'.*

The vertical force $F_{1'}$ which is necessary to be applied by the power screw can be determined:

$$F_{1'} = \cos(\alpha')F_{Q'}$$

$$F_{1'} = \cos(58.42°) \cdot 280.571kN = 146.932kN$$

$$F_{1',total} = 2F_{1'} \rightarrow 2 \cdot 146.932kN = 293.9kN$$

The new calculated vertical force $F_{1'}$ result in a total load $F_{1',total}$ of 293.9kN that needs to be applied by the power screw. A frictional coefficient of 0.1, gave an increment of 7.8kN which is a 2.7 percentage increment due to the frictional loss. Cautions should be taken as there are uncertainties related to this determination. It has not been accounted for frictional loss at the planar faces of the joint that revolves to each other's surfaces and it should be noted that it exist uncertainties to the frictional coefficient value.

It would be beneficial to compare the result with an FEA model. Ansys Classic have the ability to implement coupling constraints that can account for frictional loss. This is accomplished by using MPC184 elements and a revolute joint between the moving components. Because of the limited time in this master thesis, this was not prioritized.

3.2.2   *PIN JOINTS*

The pin joint design was investigated so that satisfying results for shear failure and bending failure could be obtained. The Eurocode 3 standard is used to justify the dimensions. The EC3 standard is based on nominal stress while traditional dimensioning technic is based on allowable stress. In other words, the EC3 neglect the peak stresses and allow for a higher utilization of the material. The different failure modes are still tested with traditional dimensioning technic. Allowable stress analysis is simple and approximate because factors as principle stresses and stress concentrations are neglected. Uncertainties exist of the obtained result when using allowable stress, therefor a higher factor of safety is needed.
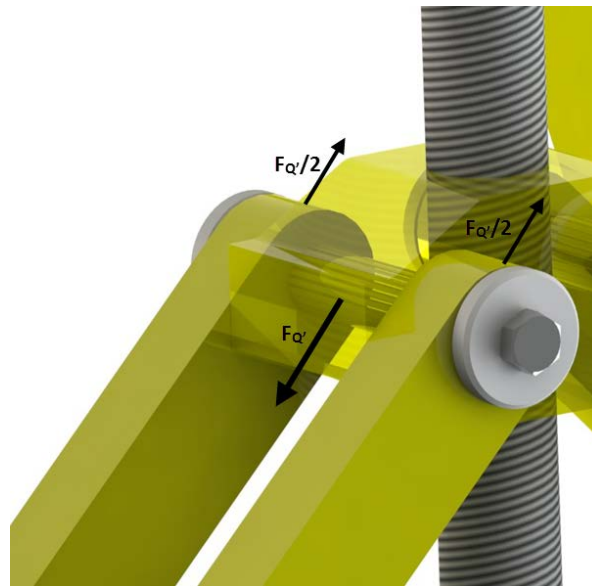

***Fig 3.27** The first trail design consisted of two linkages and a pin that goes through the joint with a bolt and washer attached at both ends.*

***Table 3.4** First trail values for the linkages and pin joints*

Description	Variable	Value	Unit
Linkage breadth	b	60	mm
Linkage thickness	t_l	40	mm
Horizontal plate thickness	t_h	100	mm
Applied force	$F_{Q'}$	280.571kN	kN
Nominal diameter	d_n	30	mm

The force $F_{Q'}$ was established from chapter 3.2.1 where the applied normal force on the linkage was calculated when accounting for frictional loss in each joint.

BENDING FAILURE

The pin has some clearance in the pin hole, therefore it is subjected to a bending stress. It is assumed that the load acting in the horizontal plate and lower clamp segment eye is uniformly distributed, but uniformly varying in the two linkages (Fig 3.28).
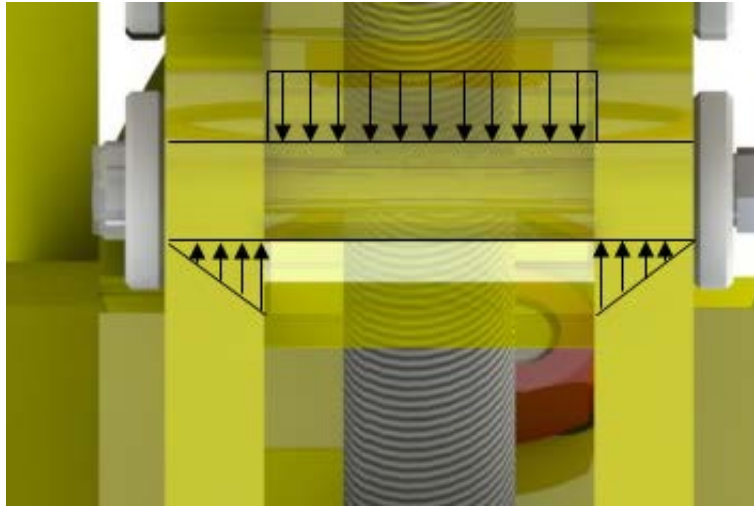
Fig 3.28 The distributed load diagram of the pin.

The largest bending moment will be developed in the middle of the pin. To calculate this, the pin is split in half. The position of the resultant force of the triangle load distribution is assumed to be 1/3 of the length from the inside of the linkage. For the evenly distributed loading, the resultant force is assumed to be in the middle (Fig 3.29).
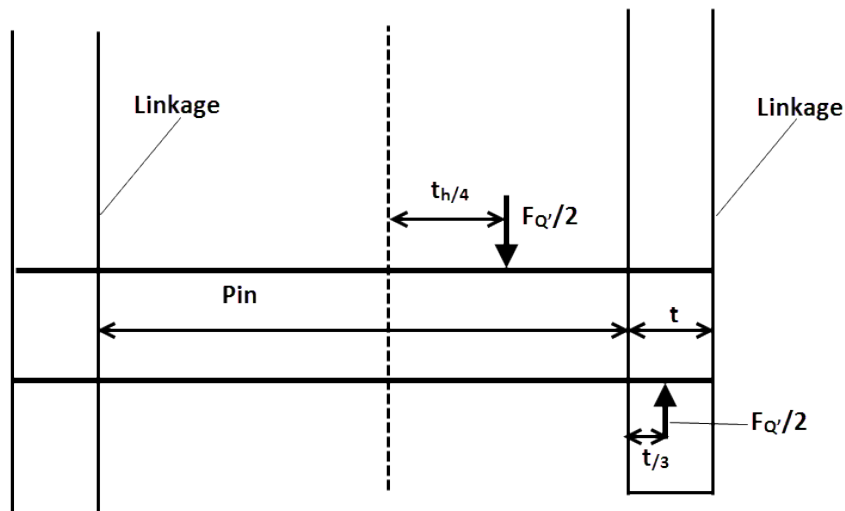

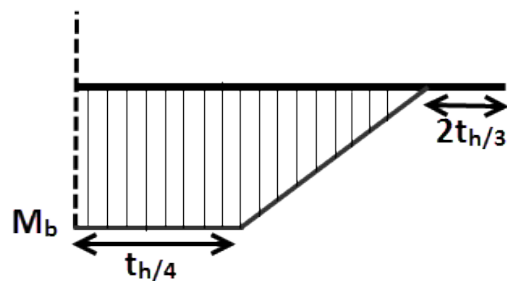*Fig 3.29 The positions of the applied load on the pin.*

Fig 3.30 A bending moment diagram. The maximum moment is assumed to be at the middle of the pin.

From the above assumption, the bending moment can be calculated:

$$M_b = \frac{F_{Q'}}{2}\left[\frac{t_h}{4} + \frac{t_l}{3}\right]$$

$$M_b = \frac{280.571\text{kN}}{2}\left[\frac{100mm}{4} + \frac{40mm}{3}\right] = 5.378kNm$$

y is the distance from the surface to the centre of the pin's cross section:

$$y = \frac{d_n}{2} \rightarrow \frac{30mm}{2} = 15mm$$

The moment of inertia of a cylindrical beam is calculated:

$$I = \frac{\pi d_n^{\,4}}{64} \rightarrow \frac{\pi 30^4 mm}{64} = 39760.8mm^4$$

The bending stress is calculated:

$$\sigma_b = \frac{M_b y}{I}$$

$$\sigma_b = \frac{5.378kNm \cdot 15mm}{39760.8mm^4} = 2028.9MPa$$

The obtained bending stress was unacceptable high and a new design was needed to be considered in order to achieve a lower bending stress in the pin.
It was considered to change the pin design because of the threaded hole in both ends that resulted in less material in the cross section and further resulted in a lower section modulus.
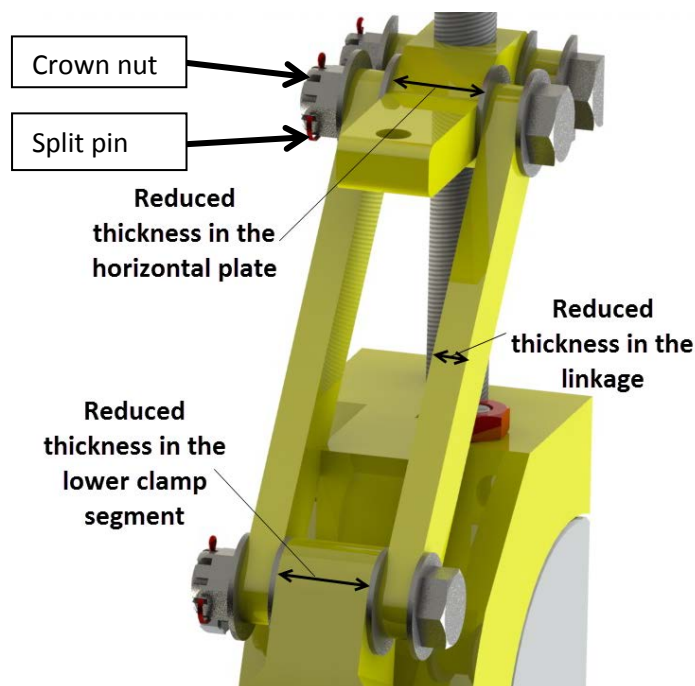

Fig 3.31 The new proposed solution for the pin bolts.

The new design needed to achieve a lower bending stress in the pin. Instead of threaded holes at each end, the pin was replaced with a pin bolt that is tightened with a nut. To obtain lower bending stresses, a diameter of 36mm was selected, which is a standard bolt dimension (Fig 3.31). The joint connection was also provided with four 5mm washers and a crown nut. The crown nut will make it easy to assemble the bolt and maintain the right tolerance between the linkages, so it can rotate freely. To lock it in the desired position, the crown nut was provided with a split pin. The thickness of the horizontal plate and lower clamp segment was reduced to 80mm instead of 100mm. The thickness of the linkage was reduced to 31mm (Fig 3.31).

Fig 3.32 The final solution. A pin with a circular bracket and a socket head cap bolt.

After a closer reflection of the selected design, a second new proposal was made. It was a disadvantage to reduce the thickness of the horizontal plate and the lower clamp segment eye since it exist a risk of stress concentrations in these regions. Threaded holes at the end of a pin did not affect the strength of the pin as much as first assumed. When looking at the load and bending moment diagram of the pin joint connection, it can be seen that both ends of the pin is subjected to a minor bending moment and a shear force that acts at the linkage-eye transition (Fig 3.28 – 3.30). At the same time, the section modulus is maintained relatively high when making a hole in the cross section of a cylinder.

The new design existed of three parts, the pin body, a circular bracket and a head cap bolt. The pin needs to be customized and manufactured with good tolerance. The design has the advantages of being easy to assemble and assures for a rotation. The cylindrical bracket makes a close fit in to the pin rod which prevents it from rotation. It is fitted with a socket head cap bolt that assure that the bracket is hold in place. The design is simple and provides a minimal length of the joint. The dimension of the circular bracket has not been evaluated but it is assumed that most of the loads will be transferred normally to the pin and a marginal load is acting in the perpendicular direction of the linkage load. When implementing the new pin, the thickness of the horizontal plate and the clamp segment eye could be increased to 104mm.

The thickness of the linkages can be calculated with equation 3.2, where γ_{M0} is the material factor that has a value of 1.05 [39].

$$t_l > \sqrt{\frac{F_{Q'}\gamma_{M0}}{R_{eH}}} \tag{3.2}$$

$$\sqrt{\frac{280.571\text{kN} \cdot 1.05}{325 MPa}} = 30.1 mm$$

A thickness of 31mm was selected. The new obtained dimensions can be used to calculate a new bending moment and bending stress for the pin:

$$M_b = \frac{280.571\text{kN}}{2}\left[\frac{104mm}{4} + \frac{31mm}{3}\right] = 5.097kNm$$

$$\sigma_b = \frac{\frac{280.571\text{kN}}{2} \cdot \left[\frac{104mm}{4} + \frac{31mm}{3}\right] \cdot 18mm}{\frac{\pi \cdot 36^4mm}{64}} = 1112.8MPa$$

$$n_y = \frac{827MPa}{1112.78MPa} = 0.7$$

The result of the design modification gave a much lower bending stress value. However, a safety factor of 0.7 is unacceptable. Therefore, the bending moment was assessed with the EC3 standard.

For bending of bolt jointed connections the following expression needs to be valid:

$$M_b \leq M_{Rd} = 1{,}5W\frac{R_{eH}}{\gamma_{M0}} \tag{3.3}$$

$$1.5 \cdot \frac{\pi}{32} \cdot 36^3mm \cdot \frac{827MPa}{1.05} = 5.412kNm$$

The result indicates an allowable bending moment of $5.412kNm$. The bending moment M_b is within this allowable limit. The calculated safety factor can be ignored since the bending moment satisfy the EC3 requirement.

SHEARING FAILURE

The pin bolt is subjected to shear stresses in two sections at the pin (Fig 3.33).
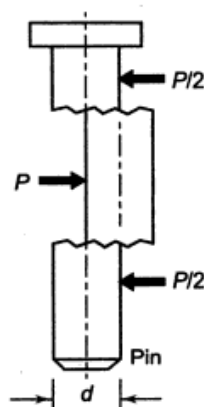

Fig 3.33 The load P causes two sections of the pin to undergo shearing [40].

The shear stress was calculated:

$$\tau = \frac{F_{Q'}}{2\left(\frac{\pi}{4}d_n{}^2\right)} \rightarrow \frac{280.571\text{kN}}{2 \cdot \left(\frac{\pi}{4} \cdot 36^2mm\right)} = 137.8MPa$$

The allowable shear stress was set to $0.5R_{eH}$. The safety factor against shearing could be determined:

$$n_y = \frac{0.5R_{eH}}{\tau} \rightarrow \frac{0.5 \cdot 827MPa}{137.82MPa} = 3$$

The cross section area of the 36mm diameter pin is 1017.88mm². The bolt is controlled against shearing considerations with the EC3, the γ_{M2} is a material factor. The following expression needs to be valid:

$$F_{Q'} \leq F_{v,Rd} = 0.5A\frac{R_m}{\gamma_{M2}} \tag{3.4}$$

The equation 3.4 is multiplied with 2 since the bolt has two shearing sections.

$$F_{v,Rd} = 2 \cdot 0.5 \cdot 1017.88mm^2 \cdot \frac{1034MPa}{1.25} = 842kN$$

The result indicates that the bolt has more than enough capacity against shearing. The EC3 standard also provides an interaction equation for the shearing and bending moment that needs to be valid:

$$\left(\frac{F_{Q'}}{F_{v,Rd}}\right)^2 + \left(\frac{M_b}{M_{Rd}}\right)^2 \leq 1 \tag{3.5}$$

$$\left(\frac{280.571\text{kN}}{841.990kN}\right)^2 + \left(\frac{5.097kNm}{5.412kNm}\right)^2 = 0.998$$

The result fulfils the requirement from equation 3.5. Still, it is recommended to increase the diameter of the shaft so that the result is somewhat lower than the obtained value (0.998).

3.2.3   *LINKAGES*

The linkage was investigated so that it could obtain a satisfying result for crushing and buckling failure. The base material will not be assessed for shearing considerations as rapture of one of the linkages by pure tension, edge shearing or tearing since the linkages are not be subjected to large tensile forces (only compression). The Eurocode 3 standard is used to justify the dimensions.

CRUSHING FAILURE

The bearing pressure was evaluated. This is the pressure between the pin and the base material causing compression stresses. The area that is resisting the pressure is called the projected area (Fig 3.34).
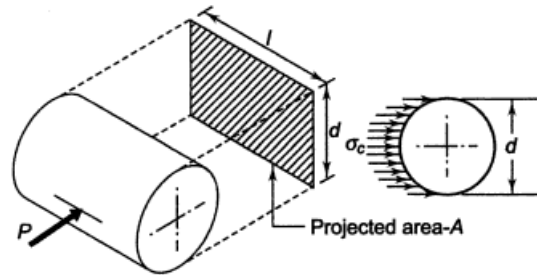
Fig 3.34 The load P generates a compression stress that is divided over a projected area [40].

The compression stress is determined:

$$\sigma_c = \frac{force}{projected\ area} = \frac{F_{Q'}/2}{t_l d}$$

$$\sigma_c = \frac{280.571\text{kN}/2}{31mm \cdot 36mm} = 125.7MPa$$

$$n_y = \frac{325MPa}{125.7MPa} = 2.6$$

In accordance with general dimensioning technic the crushing failure has a safety factor of 2.6.
To find out if the crushing failure is in accordance with the EC3, the following equation needs to be valid:

$$F_{Q'} \le F_{b,Rd} = 1.5 t_l d \frac{R_m}{\gamma_{M0}} \tag{3.6}$$

The equation 3.6 is multiplied with 2 since the connection consist of two linkages.

$$F_{b,Rd} = 2 \cdot 1.5 \cdot 31mm \cdot 36mm \cdot \frac{325MPa}{1.05} = 1036.3kN$$

The calculated force F$_{b,Rd}$ is much higher than the force $F_{Q'}$, and the crushing failure is in accordance with the EC3.

The horizontal plate and lever arm also have holes for the pins. These could also be controlled against crushing failure. This was not performed since the linkages have a much smaller thickness. Therefor the above calculations provided good enough data to justify the other components against crushing failure.

It should be noted that a diameter of pin hole needs to be slightly larger than 36mm which is the diameter of the pin. This to obtain some clearance between the pin and the base material.

BUCKLING FAILURE

The linkages have the possibility to break because of buckling. It is essential to control the linkage for buckling since the result can be hazardous. The buckling of a column can lead to a sudden and dramatic failure of the mechanism and the breakdown can happen without notice. Buckling can occur if the linkages are exposed to a compression load in the longitudinal direction. It is assumed that the linkages are only exerted to axial end loads. The maximum axial load that a column can support when it is on the verge of buckling is called the critical load, F$_k$. Any additional loading will

cause the linkage to buckle and therefore deflect literally. The linkage will buckle about the axis of the cross section having the least moment of inertia.
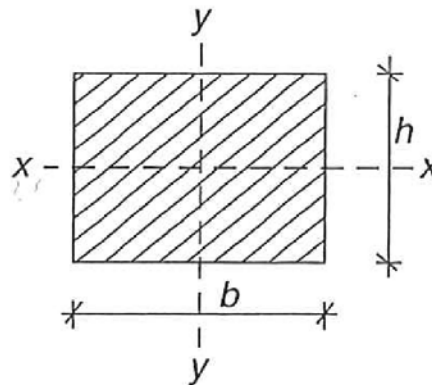

Fig 3.35 The x and y axis of the cross section, the linkage will buckle about the axis having the least moment of inertia [41].

The two moment of inertia's is determined:

$$I_x = \frac{1}{12} bh^3$$

$$I_y = \frac{1}{12} hb^3$$

For this linkage the cross section has a height of 31mm and a breadth of 90mm.

$$I_x = \frac{1}{12} \cdot 90\text{mm} \cdot 31^3\text{mm} = 0.22 \cdot 10^6\text{mm}^4$$

$$I_y = \frac{1}{12} \cdot 31\text{mm} \cdot 90^3\text{mm} = 1.88 \cdot 10^6\text{mm}^4$$

The x-axis gives the weakest moment of inertia and buckling will first occur about this axis. The linkage capacity against buckling decreases with a larger slimness ratio (equation 3.7). On the other hand, if the slimness ratio is small and below Eulers elastic limit, the linkage will undergo a larger compression stress that exceeds the linkages proportionality limit before the linkage will buckle and break. Buckling in this region is called plasticity-buckling because it allows buckling stresses exceed the elastic limit (Fig 3.36).
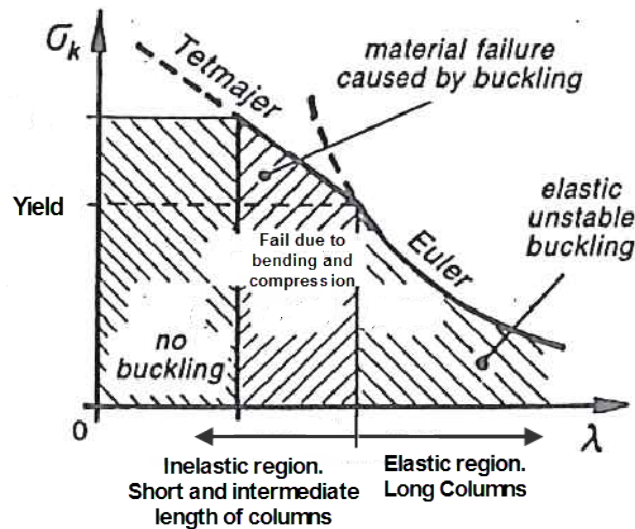
Fig 3.36 The relationship between Euler's and Tetmajer's regions [42].

For buckling about the y-axis which is in the direction of the cross section having the largest moment of inertia, the ends can be assumed to be constrained with a pin support in each end (Fig 3.37) When the linkage is assessed for buckling about the x-axis (weakest moment of inertia) the linkage can be assumed to have a fixed support in both ends which gives an effective length of 220mm (Fig 3.38)
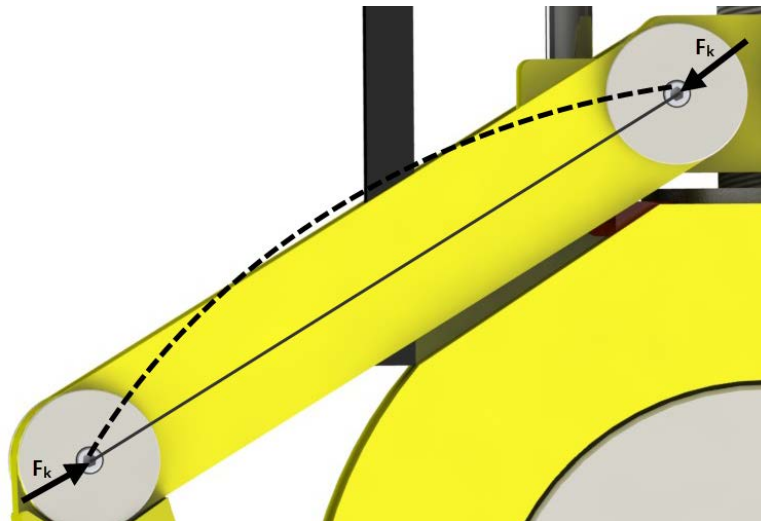

Fig 3.37 The buckling scenario for the y-axis, the linkage will act as a column with pin support in both ends. The effective length is the same as the actual length [43].

The slimness ration:

$$\lambda = \frac{l_k}{i} \tag{3.7}$$

The radius of inertia:

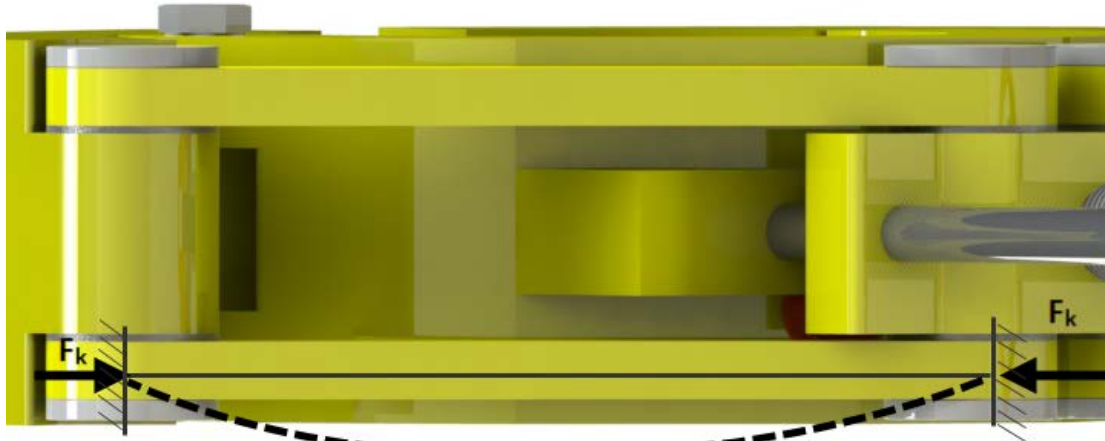$$i = \sqrt{\frac{I_0}{A}} \tag{3.8}$$

Fig 3.38 *When the linkage is controlled against buckling around the x-axis the linkage is assumed to be fixed in both ends. The effective length is half the actual length [43].*

The radius of inertia is determined:

$$i = \sqrt{\frac{0.22 \cdot 10^6 \text{mm}^4}{90mm \cdot 31mm}} = 8.88mm$$

To decide whether to use Euler's or Tetmajer's formula the slimness ratio needs to be determined:

$$\lambda = \frac{220mm}{8.88mm} = 24.775$$

The selected material for the linkages is S355. For high grade construction steel as S355 the Euler's formula is valid for $\lambda \geq 89$. Euler's formula is only applicable for values below the proportionality limit, therefore it will give wrong values in the inelastic region and wrong indications of the critical force.

In this case, Tetmajer's formula will be applicable since the slimness ratio is valid in the $10 \leq \lambda \leq 89$ range [45]. When the slimness ratio is in this area, the buckling stress is calculated by an equation for this specific material:

$$\sigma_k = 335MPa - 0.62\lambda \qquad\qquad (3.9)$$

$$\sigma_k = 335MPa - 0.62 \cdot 24.775 = 319.64MPa$$

The maximum applied force can be determined by multiply the cross section area with the stress:

$$F_k = A\sigma_k$$

$$F_k = 90mm \cdot 31mm \cdot 319.64MPa = 891.8kN$$

The maximum applied force before buckling occurs was found, the safety factor is determined:

$$n_b = \frac{F_k}{F_{Q'}/2}$$

$$n_b = \frac{891.796 kN}{280.571 \text{kN}/2} = 6.4$$

The applied load on the linkage is far below the critical load for buckling, with a safety factor of 6.6.

3.2.4 *POWER SCREW*

A mechanism is required to move the horizontal plate up and down. A power screw mechanism is suitable since it can transform turning motion into linear motion. The turning motion can easily be exerted by a ROV tool and the use of turning motion is therefore a favorable choice. Power screw mechanisms are simple and have few parts that reduce costs and increase the reliability. It can also be provided with self-locking. This is essential to prevent the clamp segments from opening on its own. The function of the self-locking is that when the rotational force on the screw is removed, it will remain motionless where it was left and not rotate backwards.
Normally, a power screw is self-locking and cannot be back-driven by the load, although this is not always the case. It is a risk that excessive wear or other factors could cause a failure of the nut. The wear of the nut should not be of main consideration in this case because the opening and locking of the connection is not to be performed repeatedly over the life cycle of the cap. But if the friction is not as high as intended, it could cause a back-driven effect of the screw. Since it inherent some possibility and risk for the power screw to be back-driven, the device should be equipped with a secondary locking.

Certain threads are used to repeatedly move or translate machine parts against heavy loads. For this task a stronger form for threads is required. Two of the most common used translation threads are square and acme. The square thread is the most efficient, but it is the most difficult to cut owing to its parallel side and it cannot be adjusted to compensate for wear [46]. The Acme form of thread has none of the disadvantages of the square form and has the advantage of being stronger. Trapezoidal metric thread form is almost the same as Acme threads except the thread angle is 30° instead of 29°. The Metric trapezoidal thread is a widely used thread for power screws and AKS own clamp connector is for instance equipped with this kind of threads. Therefore, Metric trapezoidal thread was the preferred choice for the power screw.

The required vertical force that needed to be applied by the power screw mechanism was determined to be 293.9kN (chapter 3.2.1). As a first trail value, a TR40x7 type trapezoidal thread was selected to be used, which is a single threaded screw with 40mm nominal diameter and a pitch of 7mm. An average value of 0.15 was used for the coefficient of friction at the thread surface [47]. This value was also used for the collar friction. From chapter 3.1.1 inconel 718 was selected as the power screw material.

Table 3.5 inputs related calculations for the power screw.

Description	Variable	Value	Unit
Thread friction coefficient	μ_t	0.15	-
Collar friction coefficient	μ_{Co}	0.15	-
Thread angle	θ	15	° (degrees)
median diameter	d_m	36.5	mm
Lead of thread	l_f	7	mm
Outer diameter of collar	D_o	85	mm
Inner diameter of collar	D_i	60	mm

As mentioned earlier, it is important to decide if the power screw is self-locking. This can be investigated by finding the friction angle which needs to be greater than the pitch angle ($\phi_f > \alpha_p$). If not, the mechanism could possibly be back-driven.

Finding the friction angle:

$$\tan \mu_t = \phi_f \rightarrow \tan^{-1}(0.15) = 8.53°$$

The lead is defined as the distance, measured parallel to the axis of the screw that the nut will advance in one revolution of the screw (Fig 3.39).
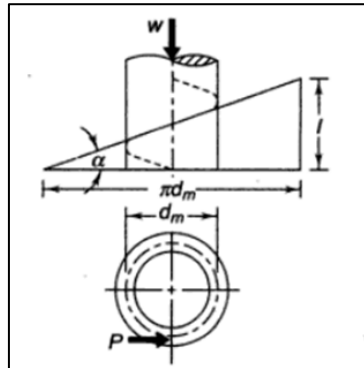

Fig 3.39 The pitch angle α makes an inclined plane that result in an inclination l [48].

Determining the pitch angle:

$$\tan \alpha_p = \frac{l_f}{\pi d_m} \tag{3.10}$$

$$\alpha_p = \tan^{-1}\left(\frac{l_f}{\pi d_m}\right) \rightarrow \alpha_p = \tan^{-1}\left(\frac{7mm}{\pi \cdot 36.5mm}\right) = 3.5°$$

The friction angle (8.53°) is greater than the pitch angle (3.5°) which means that the mechanism is self-locking. Equation 3.11 makes it possible to calculate the required torque that needs to be applied on the screw. Equation 3.12 is an expression of how much torque that is needed to overcome the collar friction.
The required torque to produce the force:

$$M_t = \frac{wd_m}{2} \frac{\left(\frac{\mu_t}{\cos\theta} + \tan\alpha_p\right)}{\left(1 - \frac{\mu_t}{\cos\theta}\tan\alpha_p\right)} \tag{3.11}$$

Accounting for friction at the collar:

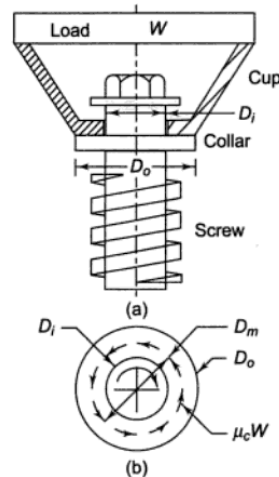$$(M_t)_c = \frac{\mu_{co}w}{4}(D_0 + D_i) \tag{3.12}$$

Fig 3.40 the collar friction is calculated with the mean diameter D_m [49].

The total torsional moment can be found by adding equation 3.12 with equation 3.11:

$$M_t = \frac{wd_m}{2} \cdot \frac{\left(\frac{\mu_t}{\cos(\theta)} + \tan(\alpha_p)\right)}{\left(1 - \frac{\mu_t}{\cos(\theta)}\tan(\alpha_p)\right)} + \left(\mu_{co}w \cdot (D_0 + D_i)\right)$$

The total torque is calculated:

$$(M_t)_t = \frac{293.864kN \cdot 36.5mm}{2} \cdot \frac{\left(\frac{0.15}{\cos(15°)} + \tan(3.5°)\right)}{\left(1 - \frac{0.15}{\cos(15°)} \cdot \tan(3.5°)\right)}$$
$$+ \left(\frac{0.15 \cdot 293.864kN}{4} \cdot (85mm + 60mm)\right) = 2.8kNm$$

The equation result in an applied torque of 2.8kNm to produce a axial force w of 293.9kN. It exists insecurity about the obtained result because of the uncertenties of the used frictional coeffecient. If another frictional coeffecient exist in reality, the required torsinal moment and axial load will also change. The critical part that will undergo the maximum stress values is the portion of the screw between the collar and the nut. In this region the power screw will undergo direct compression and torsinal stress due to the torque applied. The bottom of the screw is attached to a bearing that allow for axial movement which result in zero stress in the part of the screw that is below the nut.
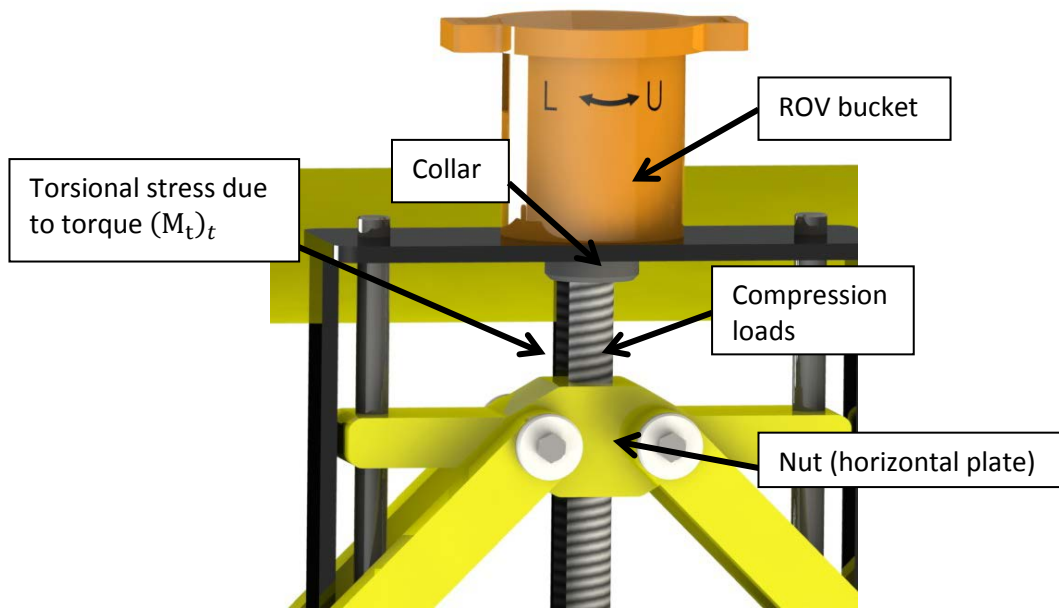
Fig 3.41 The loading scenario of the screw.

The direct compressive stress in the screw is given by:

$$\sigma_c = \frac{w}{\left(\frac{\pi}{4}d_c^2\right)}$$

(3.13)

The core diameter d_c also called the minor diameter is calculated by subtracting the tread lead from the nominal diameter:

$$d_c = d_n - l_f \rightarrow 40mm - 7mm = 33mm$$

The compression stress is determined:

$$\sigma_c = \frac{293.864kN}{\left(\frac{\pi}{4} \cdot 33^2 mm\right)} = 343.581 MPa$$

The torsional shear stress is determined:

$$\tau = \frac{16(M_t)_t}{\pi d_c^3}$$

(3.14)

$$\tau = \frac{16 \cdot 2.77kNm}{\pi \cdot 33^3 mm} = 392.562 MPa$$

The principal shear stress is determined:

$$\tau_{max} = \sqrt{\left(\frac{\sigma_c}{2}\right)^2 + (\tau)^2}$$

(3.15)

$$\tau_{max} = \sqrt{\left(\frac{343.581 MPa}{2}\right)^2 + (392.562 MPa)^2} = 428.5 MPa$$

$$n_y = \frac{0.5 \cdot 827 MPa}{428.505 MPa} = 1$$

According to the maximum shear stress theory, the maximum stress is estimated to be 428.5MPa, which gives a safety factor against yielding of 1. This is an unacceptable low safety factor and a new screw dimension needs to be selected. A new screw with a nominal diameter of 52mm and fine type threads with a lead length of 3mm was selected. The advantage with fine threads compared to normal threads is that a less torque is needed to be applied to get the desired load w.

The new core diameter d_c is 49mm. The median diameter is determined:

$$d_m = \frac{(52mm + 49mm)}{2} = 50.5mm$$

Pitch angle:

$$\alpha_p = \tan^{-1}\left(\frac{3mm}{\pi \cdot 50.5mm}\right) = 1.08°$$

The collar bearing was increased in size and the new design has an outer diameter of 115mm and an inner radius of 75mm.

The torque that needs to be applied on the screw is calculated by equation 3.11 and 3.12:

$$(M_t)_t = \frac{293.864 kN \cdot 50.5mm}{2} \cdot \frac{\left(\frac{0.15}{\cos 15°} + \tan(1.08°)\right)}{\left(1 - \frac{0.15}{\cos 15°} \cdot \tan(1.08°)\right)} + \left(\frac{0.15 \cdot 293.864 kN}{4} \cdot (115mm + 75mm)\right) = 3.4 kNm$$

With the new dimension of the power screw and the collar bearing, a torque of 3.4kNm needs to be applied. As mentioned before uncertainties exist for the frictional coefficient which has a great impact of the applied torque and output force.

SHEARING FAILURE

By inserting equation 3.13 and 3.14 in 3.15, the maximal shear stress can be determined:

$$\tau_{max} = \sqrt{\left(\frac{\frac{293.864 kN}{\left(\frac{\pi}{4} \cdot 49^2 mm\right)}}{2}\right)^2 + \left(\frac{16 \cdot 3.389 kNm}{\pi \cdot 49^3 mm}\right)^2} = 166 MPa$$

According to the maximum shear stress theory, a maximum stress of $166 MPa$ was found.

$$n_y = \frac{0.5 \cdot 827 MPa}{166 MPa} = 2.5$$

The new selected screw dimension resulted in an acceptable stress level which gave a safety factor of 2.5.

The threads of the screw, which are engaged with the nut, are subjected to transverse shear stresses. The screw will tend to shear of the threads at the core diameter under the action of load w, the shear area of one thread is $\pi d_c t$. t is the thickness of a thread and is one half of the pitch length since it is single threaded. z is the amount of threads in the nut and is calculated by dividing the thread pitch on the length of the nut. The nut length is 100mm. The transverse shear stress in the screw is given by:

$$\tau = \frac{w}{\pi d_c t z} \tag{3.16}$$

Determining the amount of threads:

$$z = \frac{100mm}{3mm} = 30$$

Determining the thickness of the threads:

$$t = \frac{3}{2} = 1.5$$

From equation 3.16 the transverse shear stress in the threads can be calculated:

$$\tau = \frac{293.864kN}{\pi \cdot 49mm \cdot 1.5mm \cdot 30} = 42.4 Mpa$$

$$n_y = \frac{0.5 \cdot 827MPa}{42.42MPa} = 9.7$$

The transverse shear stress in the screw was found to be 42.4MPa giving a safety factor of 9.7. The transverse shear stress in the nut was determined in a similar way. Under the action of load w, the thread of the nut will tend to shear off at the nominal diameter. The shear area of one thread is $\pi d_n t$.

$$\tau = \frac{w}{\pi d_n t z} \tag{3.17}$$

The transverse shear stress is determined:

$$\tau = \frac{293.864kN}{\pi \cdot 52mm \cdot 1.5mm \cdot 30} = 40 MPa$$

$$n_y = \frac{0.5 \cdot 325MPa}{39.97MPa} = 4$$

The transverse shear stress in the nut was found to be 40MPa giving a safety factor of 4.

CRUSHING FAILURE

The bearing pressure between the contact surface of the screw and nut is an important consideration in the design.

$$s_b = \frac{4w}{\pi z\left(d_n{}^2 - d_c^2\right)} \tag{3.18}$$

$$s_b = \frac{4 \cdot 293.864 kN}{\pi \cdot 30 \cdot (52^2 mm - 49^2 mm)} = 41.2 Mpa$$

$$n_y = \frac{325 MPa}{41.16 Mpa} = 7.9$$

The bearing pressure between the contact surface was found to be 41.2MPa giving a safety factor of 7.9. The permissible bearing pressure depends upon the materials of the screw and the nut and the rubbing velocity [51]. The selected screw dimension give satisfied stress values that should manage to cope with the intended loads.

BUCKLING FAILURE

When the screw is rotated and the clamp segments have established contact, the power screw has a length of 225mm between the nut (horizontal plate) and the collar. This part of the screw can be considered as a column with fixed support at both ends. This scenario gives an effective length that is half the actual length.

The radius of inertia and slimness ratio is calculated from eqution 3.7 and 3.8:

$$i = \sqrt{\frac{\frac{\pi \cdot 49^4 mm}{64}}{\frac{\pi \cdot 49^2 mm}{4}}} = 12.25 mm$$

The slimness ratio is determined:

$$\lambda = \frac{112.5 mm}{12.25 mm} = 9.18$$

The transition slenderness ratio is calculated in order to determine if it is in the Euler region:

$$\lambda_{transition} = \sqrt{\frac{2\pi^2 E}{R_{eH}}} \tag{3.19}$$

$$\lambda_{transition} = \sqrt{\frac{2 \cdot \pi^2 \cdot 205 GPa}{827 MPa}} = 69.95$$

Tetmajer's formula was not used since it was not found data for the inconel 718 material. Instead Johnson equation was used since it allow for inserting the material properties. The slimness ratio clearly indicates that the power screw is in the region where Eulers equition is not valid.

The critical buckling stress is calculated:

$$\sigma_k = R_{eH} - \frac{R_{eH}^2}{4\pi^2 E} \left(\frac{l_k}{i}\right)^2 \tag{3.20}$$

$$\sigma_k = 827 MPa - \frac{827 MPa^2}{4 \cdot \pi^2 \cdot 205 GPa} \cdot \left(\frac{112.5 mm}{12.25 mm}\right)^2 = 819.873 MPa$$

The critical force is determined:

$$819.873 MPa \cdot \frac{\pi \cdot 49^2 mm}{4} = 1546 kN$$

$$n_b = \frac{1546 kN}{293.864 kN} = 5.3$$

The critical buckling force is 1546kN which gives a safety factor against buckling of 5.3. This is acceptable.

3.2.5   *ROV BUCKET WITH SUPPORT BRACKET*

A new design proposal was generated for the supporting structure of the ROV bucket, guide bars and power screw (Fig 3.42 and Fig 3.43).
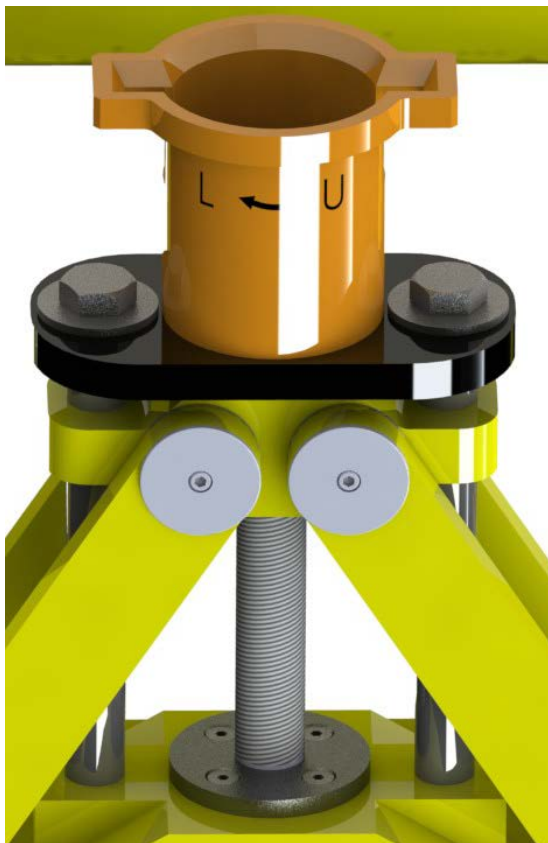
Fig 3.42 Support bracket for the ROV bucket. Mechanism in open position.

Fig 3.43 Support bracket for the ROV bucket. Mechanism in closed position.

When dimensioning the bracket and the two guide bars, it is important to clear out what kind of forces that will act in these components. It is assumed that the worst loading scenario for the bracket is when the clamp segments are tightened. When the power screw rotates, it will experience frictional loss at the collar surfaces. These forces result in an exerted bending moment located where the two guide bars are attached. The upper part of the screw will undergo a compression force. This force will also result in a bending moment where the guide bars are attached. Due to friction in the

nut's threads, the nut will try to rotate in the same direction as the screw is rotating. This will result in an applied force perpendicular to the bars length. Due to limited time in this master thesis these forces has not been determined and the dimensions of the support bracket has not been analysed. The ROV bucket is a standardized component and has been implemented in the design without modifications.

A secondary release is considered possible with this design. If a contingency situation ever occurs, a ROV can be equipped with an angle grinder and the two guide bars can be cut, then the mechanism should be released. This is possible since the two guide bars are in tension when the mechanism is in closed position.
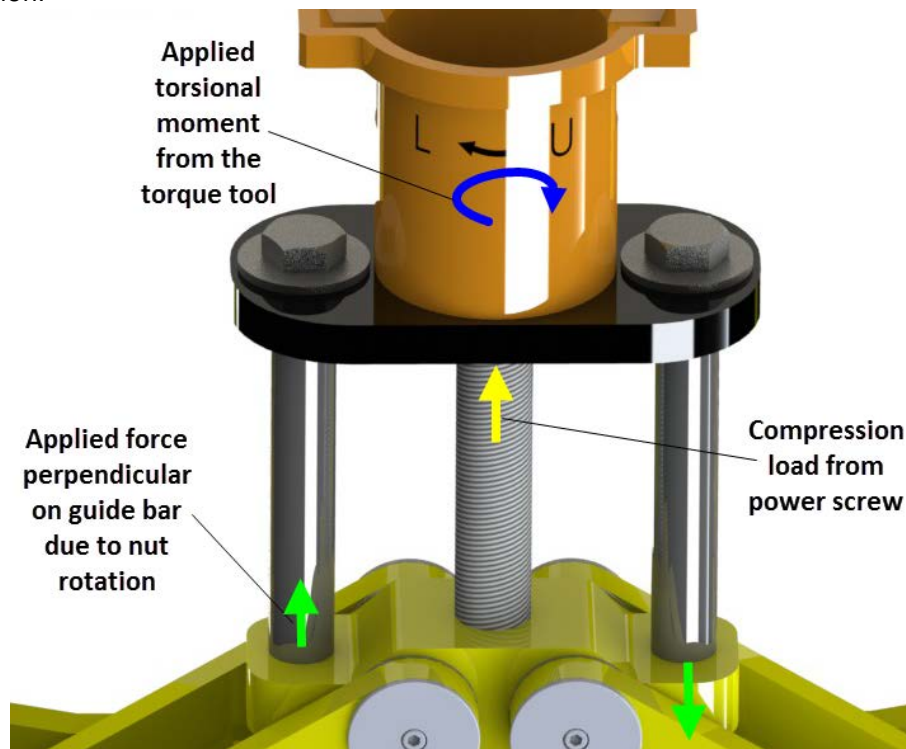

Fig 3.44 The loading scenario of the support bracket.

Another consideration is when the cap has been installed and is to be retrieved from the hub. In this situation the upper part of the power screw will be subjected to tensional loads. This has not been considered in the design, but should be relatively easy to implement. A simple solution for this could be to have a journal bearing at the bottom of the power screw.

3.3   DESIGN OF CONNECTION COMPONENTS

The connection components are referred to as the clamp segments, the elastomer seal and the cap disc. The latter one has not been subjected to any design change as the design has been duplicated from the ROV clamp connector (chapter 1.1.4). As mentioned before, the most critical factor for a successful connection design is the amount of separation at the sealing area.

3.3.1   *CLAMP SEGMENTS*

The clamp segments profile has been adopted from the ROV clamp connector design. This applies to the clamp shoulder design and the radial thickness of the segment. The design of the lever arm and clamp segment hinge has been developed in this master thesis.
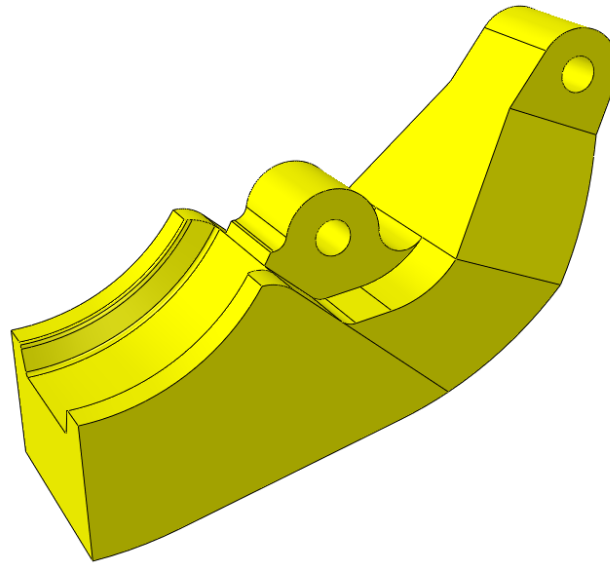
**Fig 3.45** **The first generated design of the clamp segment.**

Because of the advanced geometry and the short duration of this master thesis, hand calculations for verify and optimizing the clamp segment have not been carried out. However, a stress plot was generated and indicated areas that are subjected to global yielding.
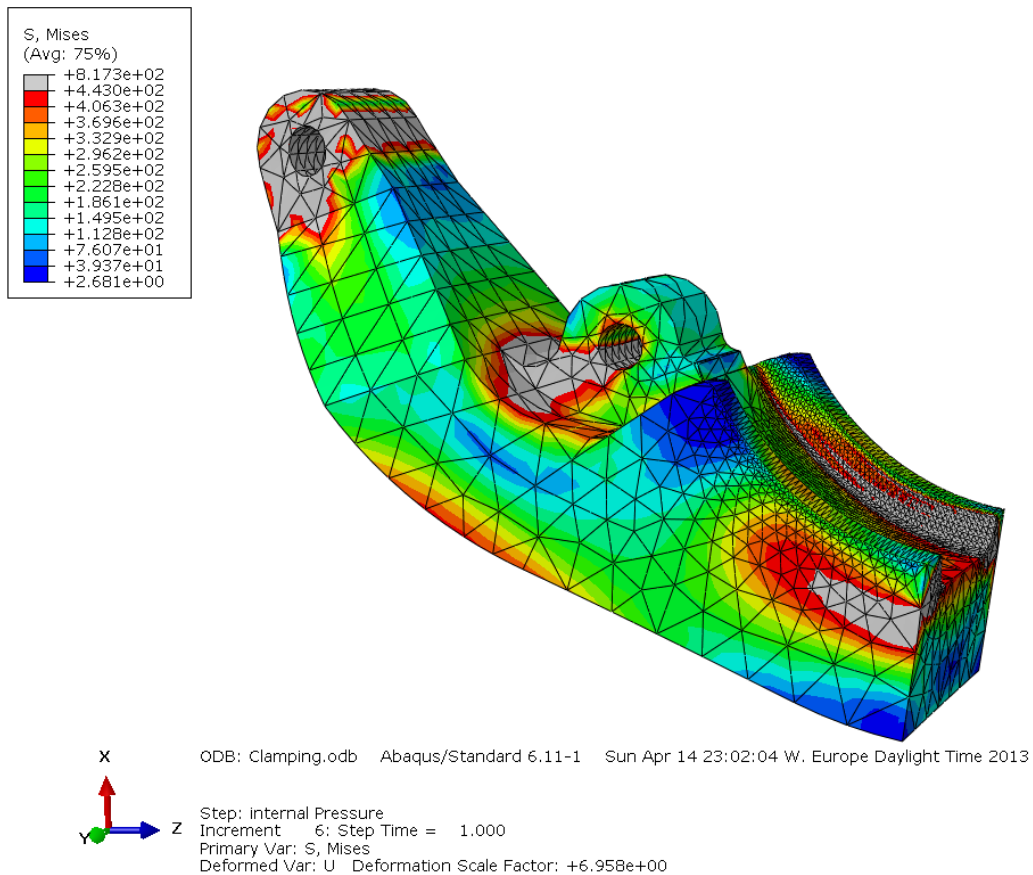

**Fig 3.46** **Von Mises plot of the clamp segment with a counter limit of 443MPa. It should be noted that the clamp force generated in this simulation was 420kN and therefor excessive high. A pressure of 345bar was used (Design pressure). The plot indicates high stress concentrations around the radii of the transition of the hinge and the lever arm and at the pin bolt hole for the linkages.**

Generally, changing to a larger radius in transition regions and to a larger cross section, will reduce the stress. Some improvements of the clamp segments were performed and resulted in the following design changes:

- The thickness of the segment is maintained up to the linkage connection.

- A larger radius at the hinge eye.

- The edge next to the upper clamp segment was altered to end up with a gap of 4 mm along the edge.
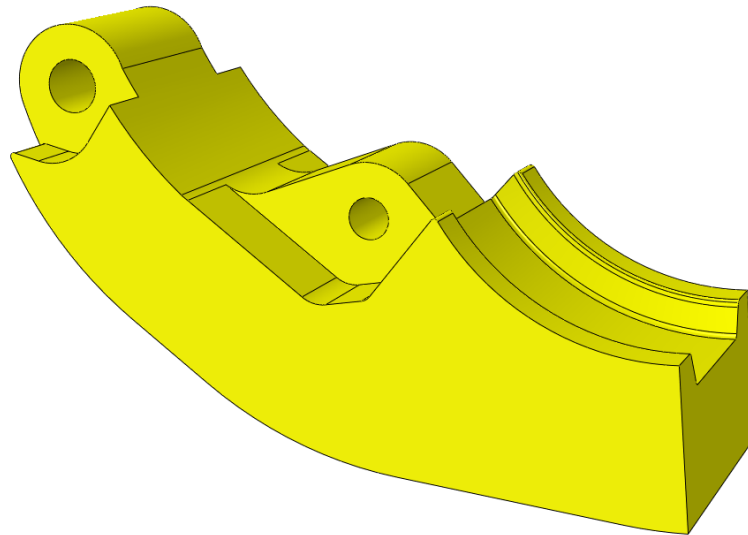

Fig 3.47 The clamp segment design after the design modifications.

The design change resulted in a lower stress level, but the design still needs to be improved in order to achieve even lower stress values. This is because the pin joint holes and the clamp segment shoulders still have some excessive stress levels.
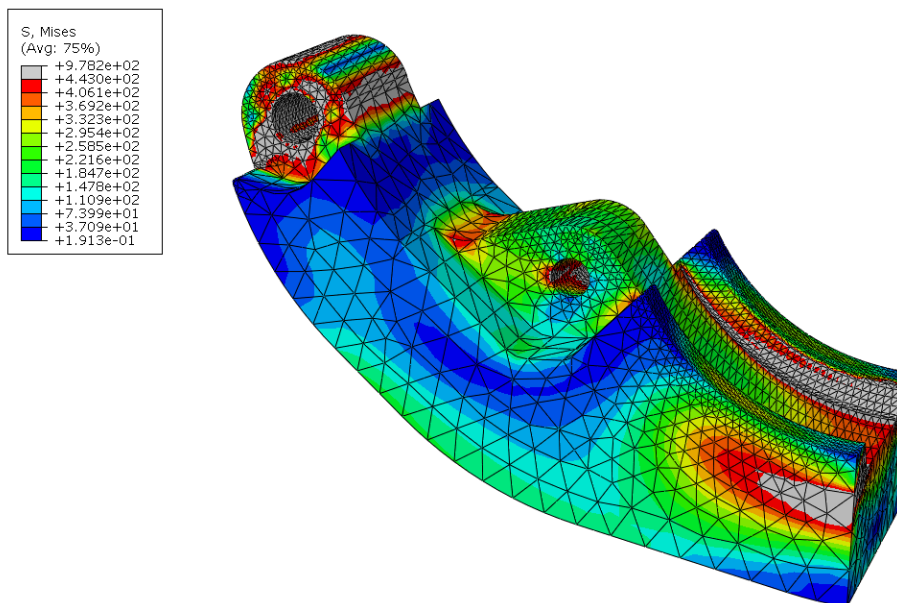

Fig 3.48 Von Mises plot of the clamp segment with a counter limit of 443MPa which is the material yield strength. In this simulation a clamp force of 345kN and a pressure of 517bar were used. The stress levels at the hinge eye and the linkage pin eye have decreased stress levels.

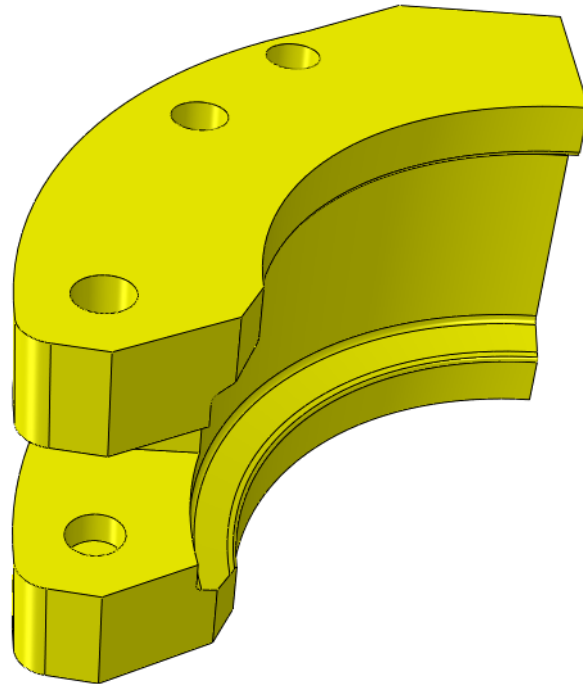The upper clamp segment was subjected to some improvements.

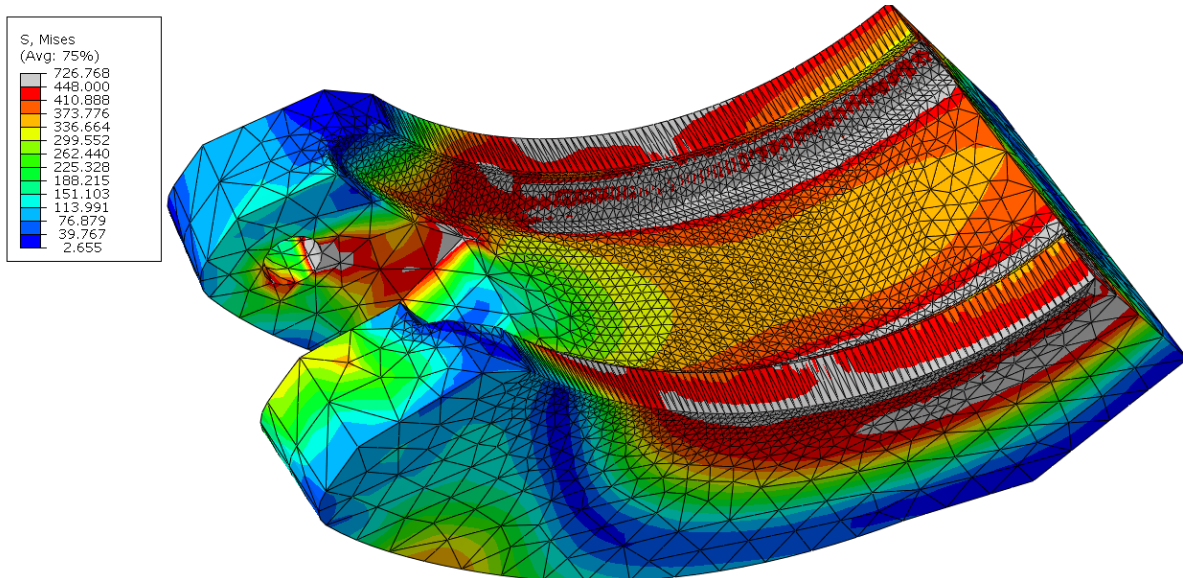*Fig 3.49 The first generated design of the clamp segment.*

Fig 3.50 Von Mises plot of the upper clamp, with the materials yield strength as the counter plot limit. It should be mentioned that the clamp force generated in this simulation was 420kN and is therefore excessive high. An internal pressure of 345bar was used.

The gap between the two bolt holes had an unnecessary large open area, this resulted in a higher separation at this region. To deal with this, more material was used between the gap which resulted in a lower separation value.
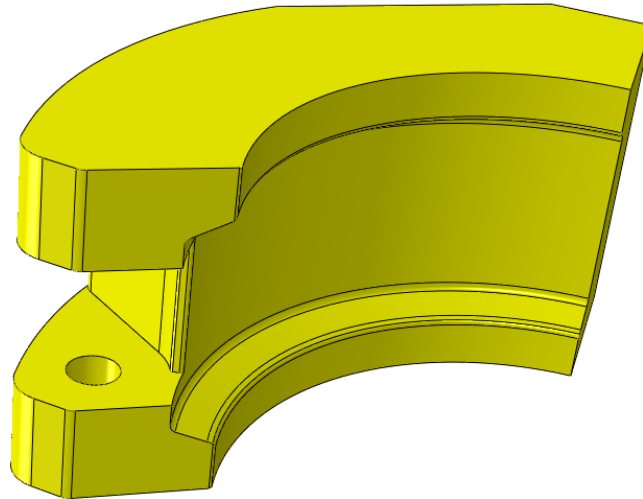
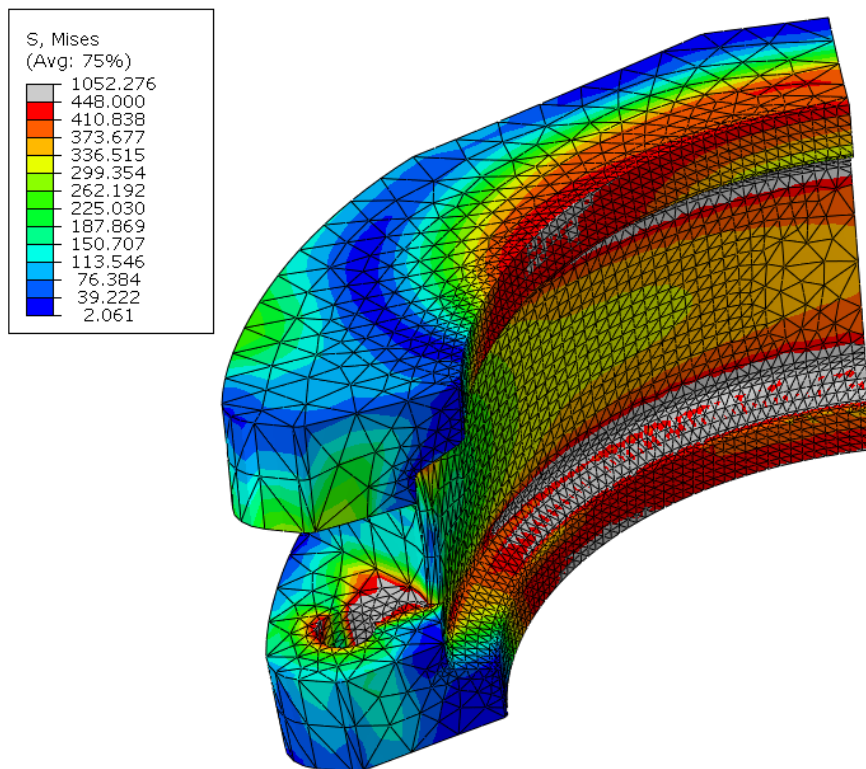*Fig 3.51 The improvements of the lower clamp segment*

Fig 3.52 Von Mises plot of the upper clamp segment with a clamp force of 345kN and a test pressure of 517bar. Regions of concern are the clamp shoulder and the pin bolt hole which is subjected to excessive stress levels.

3.3.2 *CAP DISC*

As mentioned before, the cap disc has not undergone any changes on its geometry throughout this project.
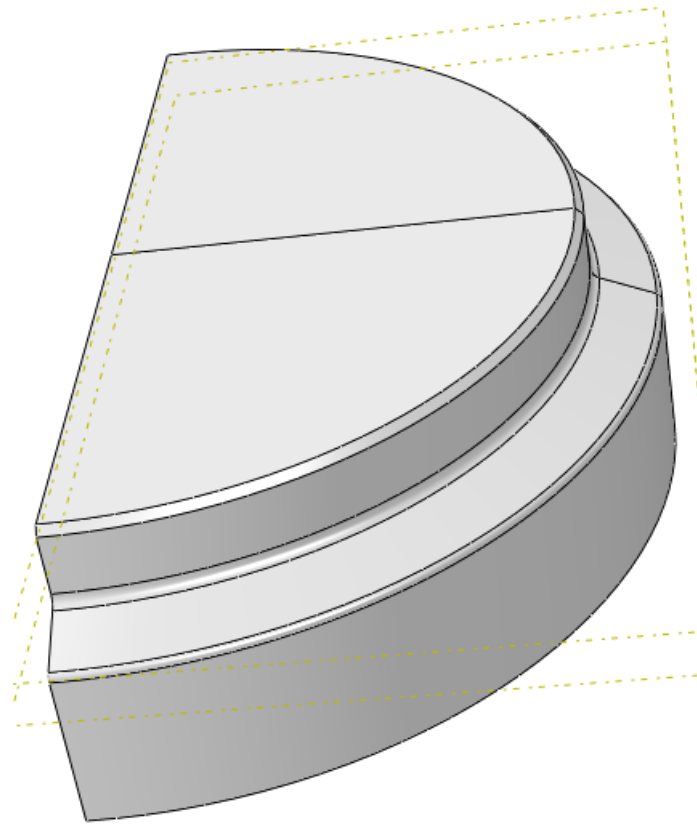

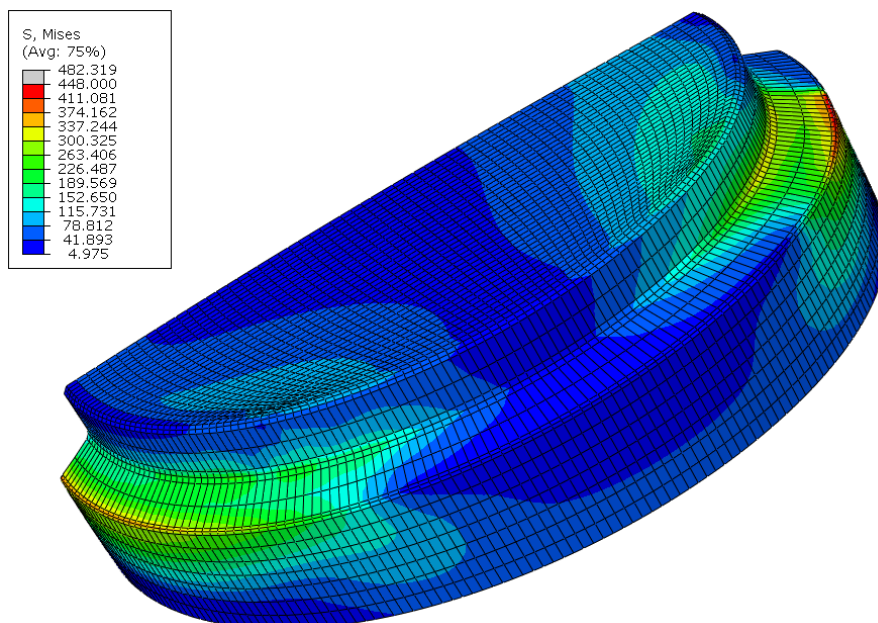*Fig 3.53* **The asymmetric geometry of the cap disc.**

Fig 3.54 **Von Mises plot of the cap disc with a clamp force of 345kN and a test pressure of 517MPa.**

The Von Mises plot indicates that the cap disc reach an acceptable stress level which means that the design tolerate the load it is exposed for.

3.3.3 DETERMINATION OF THE SEPARATION AT THE SEALING AREA

The cap will generate a clamp force that acts in the axial direction at each clamp shoulder when the connection is closed and tightened. This force preloads the segments and compresses the hub and cap disc. When the cap is subjected to an internal pressure, the pretension in the segments increases with an additional force and the two compressed parts will try to separate from each other. The pretension force can be determined and give indications about the separation at the sealed area. This has been performed by using the screw diagram where the clamp segments were treated as a bolt and the hub and cap parts between the clamp shoulders were treated as two compressed parts. It has also been accounted for the frictional loss that occurs at the wedge. From equation 2.1, the required clamp force was calculated to be at least 690kN, this value will be used as a basis in the calculations. The friction coefficient was set to 0.15, on the basis of previously calculations that AKS has performed on clamp devices with the same type of material.

Table 3.6 Inputs for the calculations.

| Description	Variabel	Value	Unit
Applied clamp force	F_0	689.663	kN
Clamp shoulder angle	α	24	Degrees
Total hydrostatic end force	H	3277.690	kN
Elastic Modulus	E	200	GPa
Cross section distance at clamp segment	D_c	114	mm
Inner radius	r_i	203	mm
Outer radius	r_o	290	mm
Hub face to cap disc contact area	A_h	25778	mm^2
Friction coefficient between clamp segment and hub/cap disc	μ_c	0.15	-
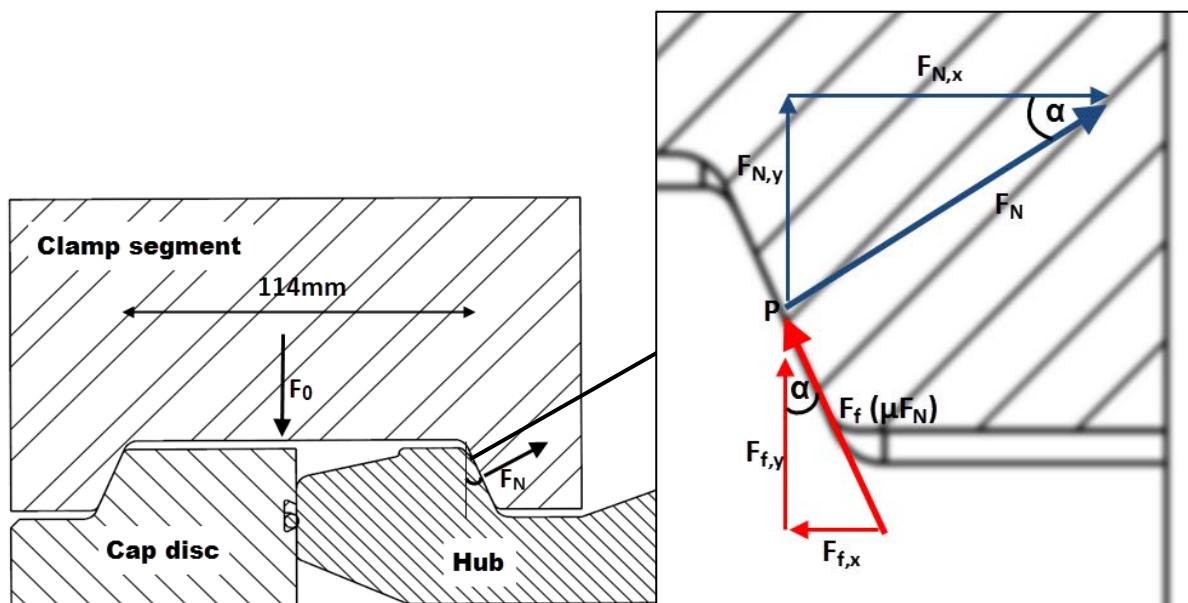
Fig 3.55 A section view of the connection, consisting of clamp segment, hub and cap disc. 114 mm was used as the length of the clamp segments for determining the elongation. The magnified figure show the forces associated with the clamping.

The normal force and the frictional normal force are always acting perpendicular to the contact surface and the frictional force F_f is acting tangential to the contact point. The normal force F_N is found by assessing the vertical forces acting on the inclined surface (y-direction). The pretension force is found by investigating the horizontal forces acting on the inclined surfaces (x-direction).
To find the normal force F_N, The sum of all vertical forces in point p is zero (Fig 3.55).

The y-component of the normal force:

$$\sin \alpha = \frac{F_{N,y}}{F_N} \rightarrow F_{N,y} = F_N \sin \alpha$$

The y-component of the friction force:

$$\cos \alpha = \frac{F_{f,y}}{F_f} \rightarrow F_f = F_f \cos \alpha = \mu_c F_N \cos \alpha$$

The vertical forces acting in point P:

$$F_N \sin(\alpha) + F_N \, \mu_c \cos(\alpha) - F_0/2 = 0$$

To determine the force F_N, it can be moved to the left side of the equal sign:

$$F_N = \frac{F_0/2}{(\sin(\alpha) + \mu_c \cos(\alpha))} \qquad \boxed{1}$$

The magnitude of the normal force can be determined:

$$F_N = \frac{689.663\text{kN}/2}{(\sin(24°) + 0.15 \cdot \cos(24°))} = 634.15 kN$$

The magnitude of the friction force can be determined:

$$F_f = F_N \mu_c$$

$$F_f = 634.15 kN \cdot 0.15 = 95.12 kN$$

The pretension force is found by summing up the forces acting in the x-direction.
The x-component of the friction force:

$$\sin \alpha = \frac{F_{f,x}}{F_f} \rightarrow F_{f,x} = F_f \sin \alpha = \mu_c F_N \sin \alpha$$

The x-component of the normal force:

$$\cos \alpha = \frac{F_{N,x}}{F_N} \rightarrow F_{N,x} = F_N \cos \alpha$$

In point P the sum of the horizontal forces (x-direction) are zero:

$$F_{ts} + F_{f,x} - F_{N,x} = 0$$

$$F_{ts} + \mu_c F_N \sin \alpha - F_N \cos \alpha = 0$$

$$F_{ts} = F_N (\cos \alpha - \mu_c \sin \alpha) \qquad \boxed{2}$$

The equation 1 is inserted into equation 2 and the pretension force can be calculated:

$$F_{ts} = \frac{F_0(\cos(\alpha) - \mu_c \sin(\alpha))}{2(\sin(\alpha) + \mu_c \cos(\alpha))}$$

$$F_{ts} = \frac{689.663\text{kN}(\cos(24°) - 0.15\sin(24°))}{2(\sin(24°) + 0.15\cos(24°))} = 540.6kN$$

The tension force can also be found by inserting the normal force value in equation 2:

$$F_{ts} = F_N \cos(\alpha) - F_f \sin(\alpha)$$

$$F_{ts} = 634.15kN \cdot \cos(24°) - 95.12kN \cdot \sin(24°) = 540.6kN$$

The tension after tightening of the clamp segments has been determined. When internal pressure is applied, the pretension in the clamp segment will increase and it will also tend to separate the sealed area.
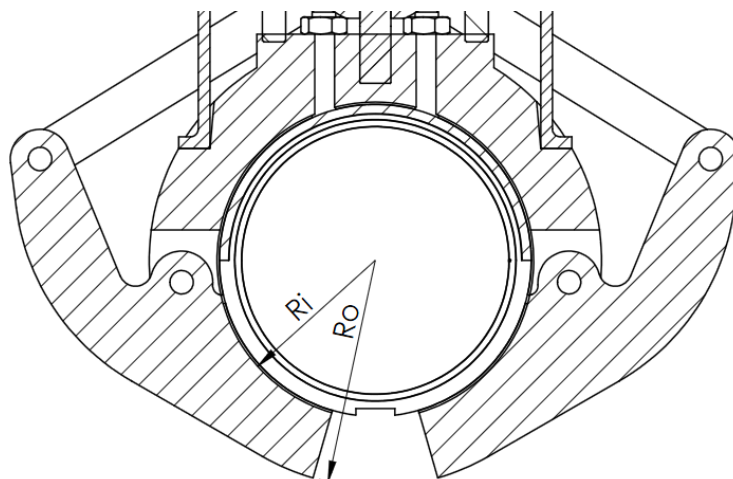

*Fig 3.56 **The inner and outer radius for the clamp segments for calculating the elongated area.***

The cross section area of the clamp segments is determined:

$$A_c = (r_o{}^2 - r_i{}^2)\pi$$

$$A_c = (290^2 - 203^2) \cdot \pi = 134746.051mm^2$$

The clamp segments area is reduced by an angle of 33° because of the gap between the two lower clamp segments and the loss of material around the hinge. This corresponds to a 9% reduction of the area.

$$A_c = 134746.051mm^2 \cdot 0.908 = 122349mm^2$$

The elongation in the cross section of the clamp segments is determined:

$$\delta = \frac{FDc}{EA} \tag{3.21}$$

$$\delta_1 = \frac{540.6kN \cdot 114mm}{200GPa \cdot 122349mm^2} = 0.00251mm$$

The elongation of the hub/cap disc contact area is determined:

$$\delta_2 = \frac{540.6kN \cdot 114mm}{200GPa \cdot 25778mm^2} = 0.01195mm$$

The additional force is determined:

$$F_a = H/(1 + \frac{\delta_1}{\delta_2}) \tag{3.22}$$

$$F_a = 3277.690kN/(1 + \frac{0.00251mm}{0.01195mm}) = 2708.89kN$$

Total tension load in segments:

$$F_{ts,total} = F_a + F_{ts}$$

$$2708.89kN + 540.6kN = 3249.49kN$$

The clamp force is determined:
$$F_c = F_{ts,total} - H$$

$$F_c = 3249.49kN - 3277.690kN = -28.69kN$$

The safety factor for the clamping force:

$$\eta_c = \frac{F_{ts,total}}{(F_{ts,total} - F_c)}$$

$$n_c = \frac{540.6kN}{(540.6kN + 28.69kN)} = 0.95$$

The clamp force is less than the resultant force from the internal pressure, this results in a separation between the cap disc and the hub.

$$Separation = \frac{F_{ts,total} \cdot 114mm}{EA_c} - (\delta_1 + \delta_2)$$

$$Separation = \frac{3249.49kN \cdot 114mm}{200GPa \cdot 122349mm^2} - (0.00251mm + 0.01195mm) = 0.001mm$$

The separation was found to be 0.001mm. A screw diagram was made to illustrate the cap connection. By studying the screw diagram, it can be seen that the clamp force is less than the applied load and separation occur.
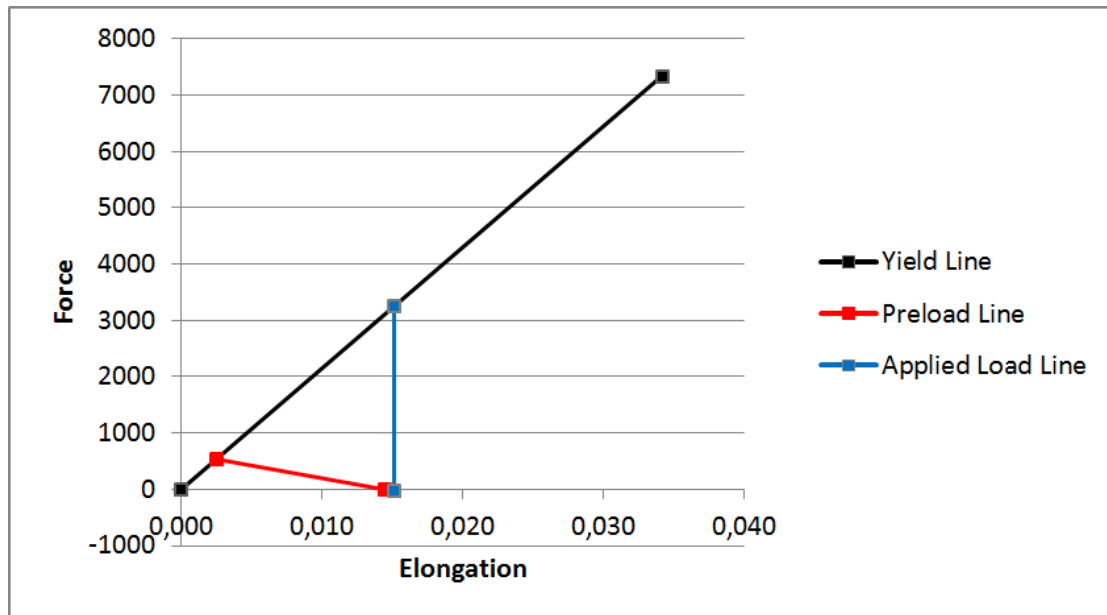
Fig. 3.57 A screw diagram was made to illustrate the preload force and the effect of the applied pressure. The diagram show how much of the load that is supported by the clamp and the contact area. It can be seen in the figure that the applied load causes a separation and the clamp force is not large enough to hold against the internal load.

When a connection with clamp segments is locked and the clamp segments are pretensioned, the connection will act as one unit. The blue line shows the internal pressure and how it affects the connection. The internal pressure forces the connection to separate. If the internal pressure is increased, then the blue line reaches the point where there is now clamping force in the connection. Beyond this point the connection will leak if the connection do not allow for any separation.
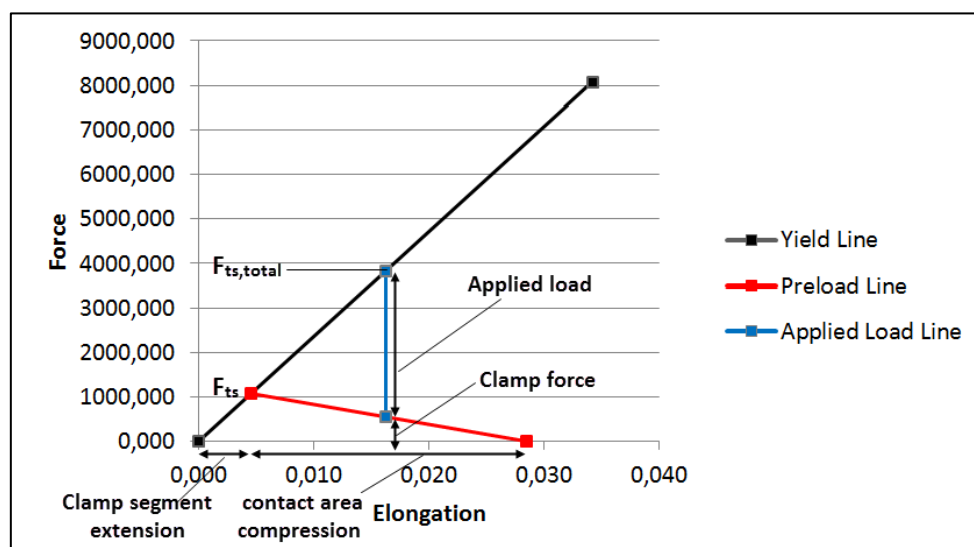

Fig. 3.58 Explanation of the screw diagram. In this diagram the connection have a clamp force and the sealing parts are in compression.
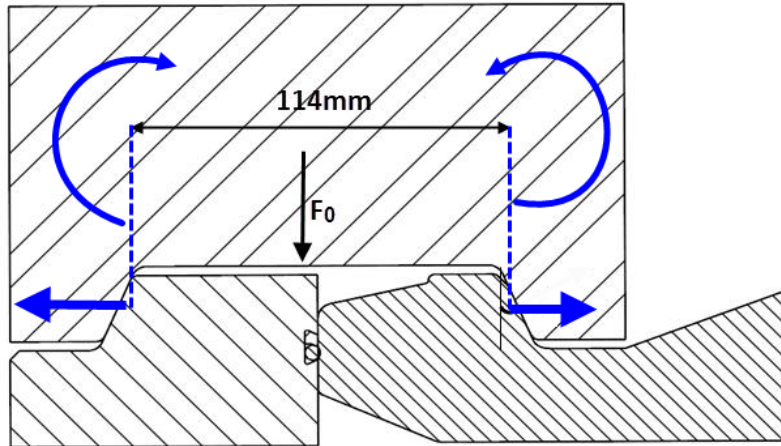
Fig 3.59 A bending moment generated at the clamp shoulders.

Additional to the elongation from the screw diagram, a bending moment is generated at the clamp shoulders. This will lead to an additional deflection that further will result in an even larger separation. A compensation for this will not be performed in this project and is therefore suggested as further work. By investigating equation 3.22, it can be seen that factors that can improve the clamp force and result in less separation will be to increase the area of the clamp segments and/or decrease the contact area of the cap disc and hub. These means will result in a larger additional force and the total pretension force will be greater.

3.3.4   SEAL SELECTION

The selection of a proper sealing is of major importance. This is considered as one of the most critical parts of the connection assembly as it takes part in preventing the connecting from leakage. The initial design used an elastomer seal that can tolerate an allowable separation of 0.3mm. The advantage of elastic sealing is that the more load or pressure that is exerted on one given interface, the more plastic deformation occurs and irregularities in the joint faces will be filled, prevents fluids from passing through the interface. An elastomer sealing does not require a high load to ensure a sealing function, assuming an adequate profile. The sealing that was selected as a basis is also equipped with a back-up ring to prevent gap extrusion of the seal profile.
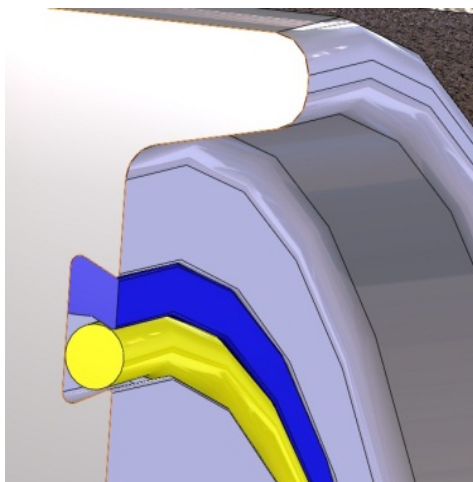

Fig 3.60 The elastomer seal provided with a back-up ring.
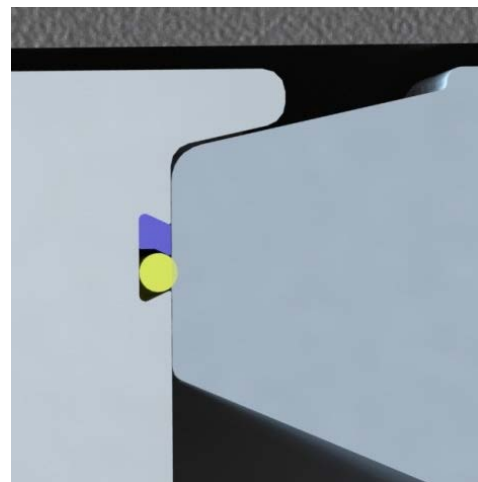

Fig 3.61 The cross section of the seal location, hub and cap disc.

The circumference diameter of the seal could possibly be changed to a smaller one (Fig 3.61). This could result in a smaller resultant force generated from the internal pressure and most likely a smaller separation. This can be considered if the design needs to be optimized further.

Seal Engineering is a supplier and manufacturer of seals, located in Fredrikstad. They are specialized in standardized and customized seal solutions for offshore equipment. They were contacted by telephone and e-mail regarding advice for selecting the most suitable seal type [55]. It was recommended to use a trapezoidal groove as the cap discs already have implemented in the design (Fig 3.60). This groove has the advantage of holding the seal in place which is required when the cap is relocated subsea. If a large enough breadth and depth size is selected for the groove, it should be possible to implement a large enough seal that could resist a separation of 0.31mm with the design pressure and 0.68mm with the test pressure (chapter 3.4.3).

A back-up ring of PEEK material was recommended in order to prevent extrusion of the elastomer seal. It was recommended to use the material RU5 for the elastomer seal. This material has great weathering, ozone and aging properties as well as a wide temperature range. It also has great resistance against mineral oils. The recommended seal solution does not distinguish far from the first selected design. Yet, the seal dimension most likely needs to be increased in size to compensate with the current separation values.

3.4   ABAQUS ANALYSIS

The finite element software Abaqus CAE (version 6.11-1) has been used for a static load study of the cap. The calculations and analysis so far has given positive results. The mechanism seems to provide enough force to lock the clamp segments and the locking mechanisms seems to tolerate the applied loads. The previous analysis was simple and generated unrealistic values for the clamp segment because of the boundary conditions. The advanced geometry and loading situation involve that the cap cannot be evaluated accurately with standard strength formulas. Therefore, a more comprehensive assessment is necessary to investigate if the cap maintain a leakage-tight connection and if the components withstand the applied loads.

Important areas to evaluate are global stress values and separation at the sealing area. Since the contact situation for the clamps are not the same around the circumference, it was not appropriate to simulate the cap as an axisymmetric model. An axisymmetric model would be an advantage because it would give a simple model to be computed. Instead, the cap was split in the middle plane since the design is asymmetric. This enabled a faster computation of the simulation to be solved.

3.4.1   *PARTITIONING AND MESH*

The network of elements and nodes that discretize a region is referred to as a mesh. The mesh density increases as more elements are placed within a given region. Results generally improve when the mesh density is increased in areas of high stress gradients. To assess improvement in regions where high stress gradients appear, the structure can be re-meshed with a higher mesh density at this location. The stress level is converging if the stress level is not changing considerably by increasing the element density.

When stress concentrations are present, it is necessary to have a very fine mesh at the stress-concentration region in order to get realistic results. It is important that the mesh density needs to be increased only in the region around the stress concentration and that the transition-mesh from the rest of the structure to the stress concentration is gradual. An abrupt mesh transition, in itself, will have the same effect as a stress concentration.

These factors are important to consider when selecting a proper geometry and mesh for the analysis, both to simplify the parts and to select the most appropriate element type and size. The goal is to make an accurate model with a quick as possible computation time. The more elements and nodes that are used in a model, the more time consuming the run time will be.

To establish the geometry in Abaqus, the different components were made as Parasolid files in SolidWorks and then further imported to Abaqus as a solid part. Abaqus automatic meshing feature uses tetrahedron (C3D10) elements by default. These elements use 10 nodes and have the advantage of being geometrically versatile. Another option is to use hexahedron elements (C3D8R). This will give a better result because it usually provides a solution that have the same accuracy but with a prominent reduced computation time. The hexahedron element uses 8 nodes.

CAP DISC

The cap disc was split in half so that it was suitable for the asymmetric model. The bolt holes, the peripheral groove for the elastomer sealing and the lip edge were removed from the geometry to obtain a less complex model. In order to mesh the part in hex elements, the cap disc was portioned in several sections. The element size was set to 10mm globally and 4mm in regions that most likely will undergo stress concentrations. These regions are contact surfaces and regions that have a radius. The part was divided in 62 848 elements and 57 311 nodes.
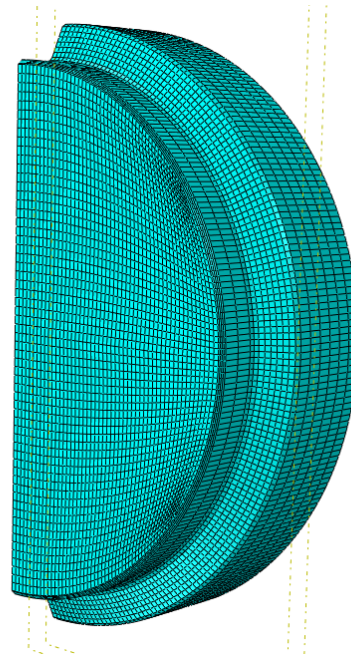

Fig 3.62 The mesh density of the cap disc.

HUB

The hub was split in half and globally meshed with an element size of 19mm. The contact region to the cap disc and the backside of the hub neck was meshed with an element size of 2mm. The front of the hub neck geometry had small radius that required a small element size to be meshed. This region was meshed with an element size of 0.5mm to avoid problems during the simulation. The top of the hub neck was meshed with an element size of 4mm. The meshed part resulted in a number of 8 130 elements and 9 579 nodes.
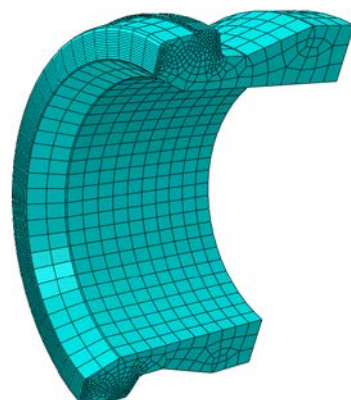

Fig 3.63 The mesh density of the hub.

LOWER CLAMP SEGMENT

The lower clamp segment was transferred into Abaqus from SolidWorks without any simplifications. Because of the complex geometry it was challenging to divide the part in hex elements and Abaqus self-generating mesh function was used where the part was divided in TET elements. The element size was set to 30mm globally and 4mm in the contact regions. The part was divided in 30 070 elements and 45 653 nodes.
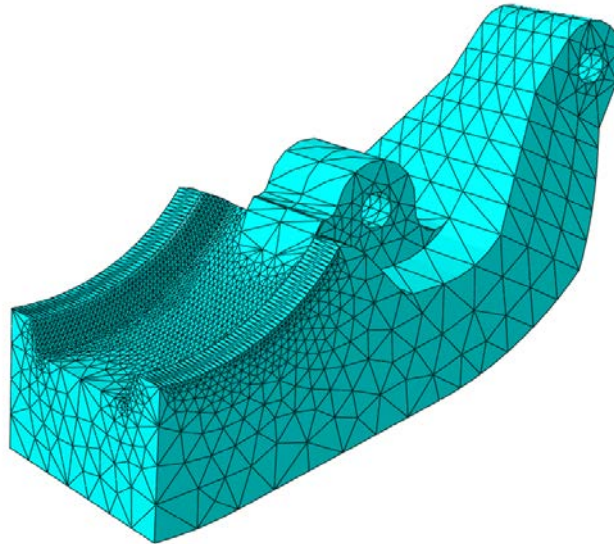
Fig 3.64 The mesh density of the lower clamp segment.

UPPER CLAMP SEGMENT

The upper clamp segment was split in half before it was meshed with the automatically mesh tool. As for the lower clamp segment, the automatically mesh tool was used for the upper clamp segment. The global element size was set to 25mm with a local element size of 4mm on the contact regions. The part was divided into 67 578 elements and 100 179 nodes.
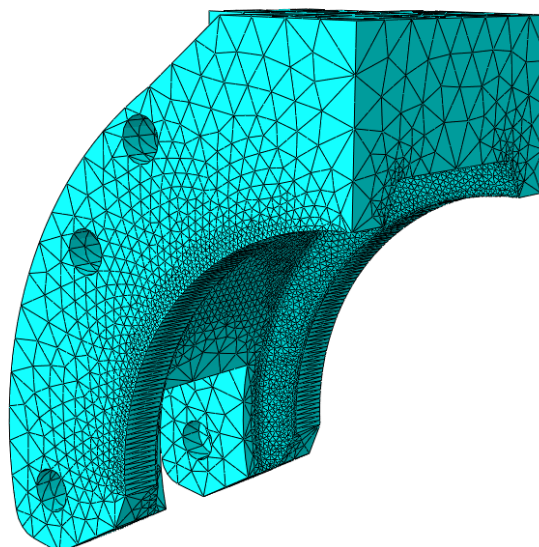

Fig 3.65 The mesh density of the lower clamp segment.

3.4.2   *ASSEMBLY AND BOUNDARY CONDITIONS*

The parts were assembled together with the front of the hub face coincident to the backside of the cap disc. The clamp segments were placed concentric to the hub and cap disc circumference, with the contact surfaces close to each other. It was important that the clamp shoulders were not in contact with the inclined hub/disc profile, as this could result in errors through the simulation if the parts interfered with each other before the clamping simulation started.
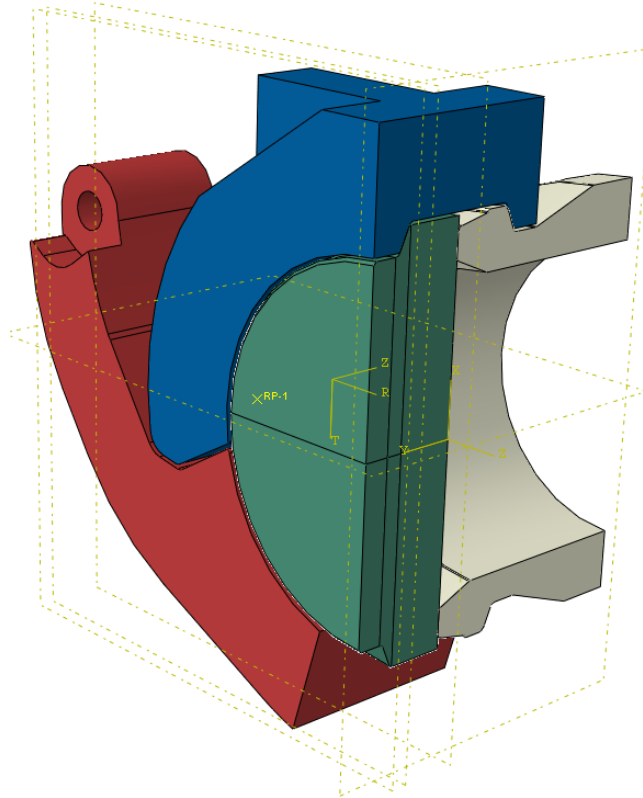
Fig 3.66 The components assembled together.

To simulate the clamping force, different solutions were considered. The best solution was found to be the use of a boundary condition where the lower clamp segment is rotated around the clamp hinge. This was done with the help of a cylindrical coordinate system established in the center of the joint and a coupling that only allowed for rotation around the joint-axis. To get the desired result, the total contact force generated between the surfaces was investigated. This force should be at least 345kN in vertical direction (Chapter 2.2.1). Another solution could be to add the applied force directly at the linkages attachment holes to simulate the clamping. This was not done because it would result in a model with a much longer computation time.
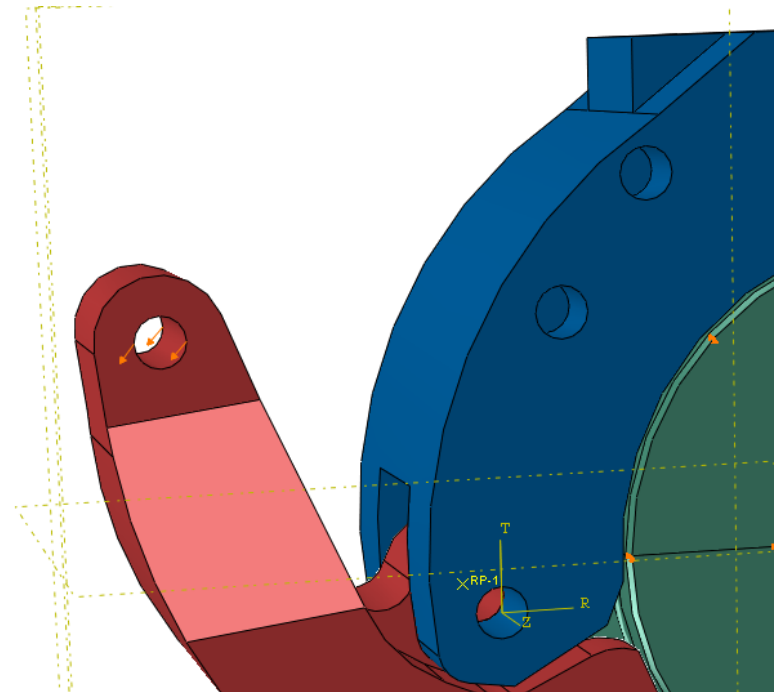
Fig 3.67 The clamp force was generated by applying rotation to the lower clamp segment.

Since the cap was split in half, the cut surfaces were given symmetric boundary conditions to achieve asymmetric properties. The back of the hub was constrained in all directions and acted as a rigid part. The cap disc front surface was constrained in y and x direction. It was not constrained in z-direction in order to close the cap disc to the front face to the hub during the clamping.
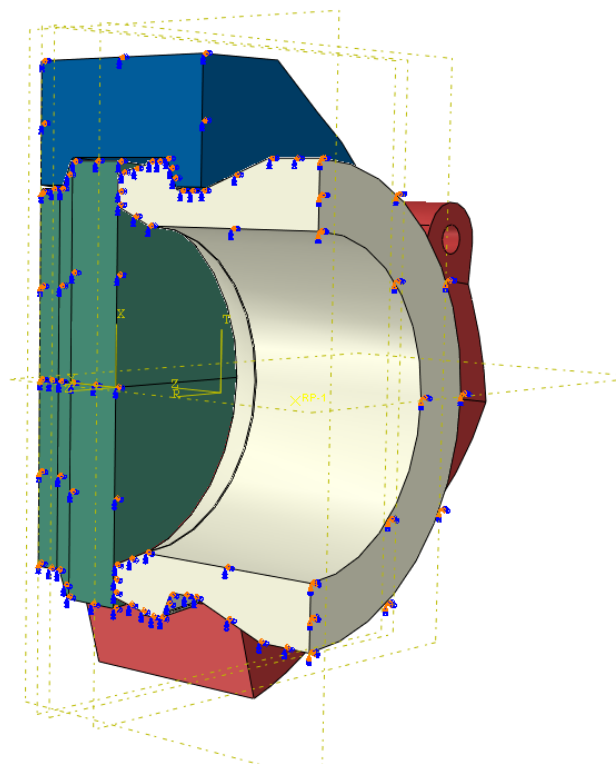
Fig 3.68 The boundary condition for the cap model.

All the internal surfaces were added a load of 34.5MPa. The pressure was distributed on all the internal walls to the hub and next to the circumference of the elastomer sealing.

Fig 3.69 The internal pressure.

All surfaces in the model that potentially could experience contact with each other were added a "surface to surface" contact interaction with a frictional coefficient of 0.1.

Fig 3.70 The Contact interactions. The regions that were added a contact interaction were the hub front face to the backside of the cap disc, clamp shoulder/hub neck surfaces and the plain surfaces for the clamp hinge.

To make the simulation solvable, it was necessary to divide the simulation in three steps: these consisted of:

- **Initial step**: all the contact interactions were created and the boundary condition for the symmetry, the hub and the cap disc were created.
- **Clamping step**: the rotation of the clamp segment and the associated boundary condition was created.
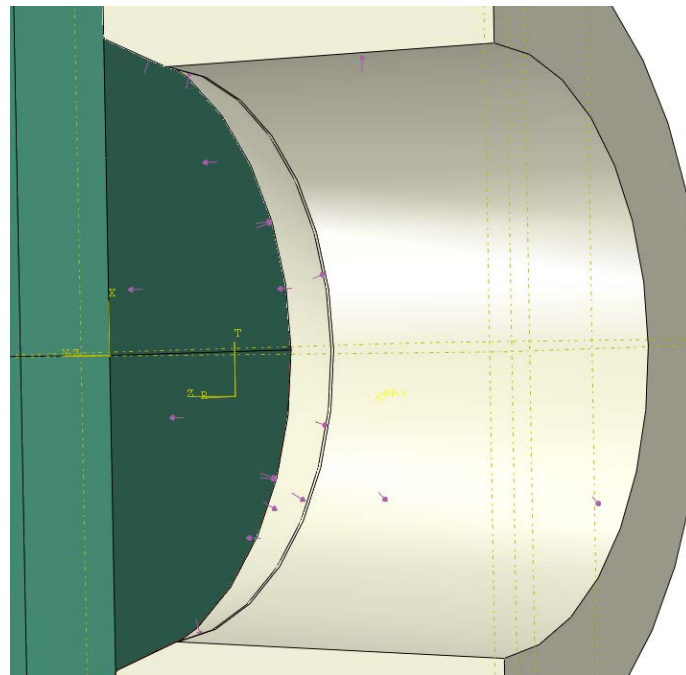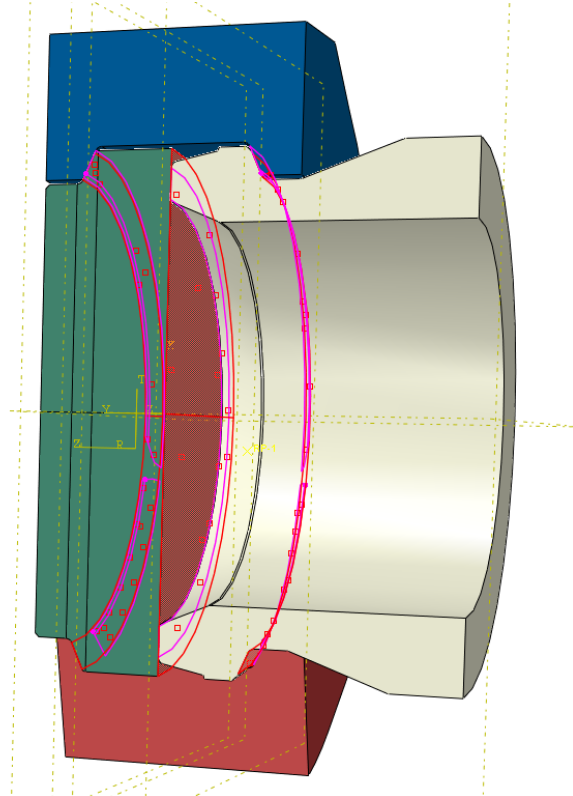- **Internal pressure step**: the internal pressure was created.

3.4.3   *ANALYSIS RESULTS*

To verify the simulation, it was first investigated how much total contact force that was generated between the clamp segment and the cap disc/hub profile. This indicates whether the rotation of the lower clamp segments generated the right clamp force. The result was satisfying and gave a clamp force of 345kn.
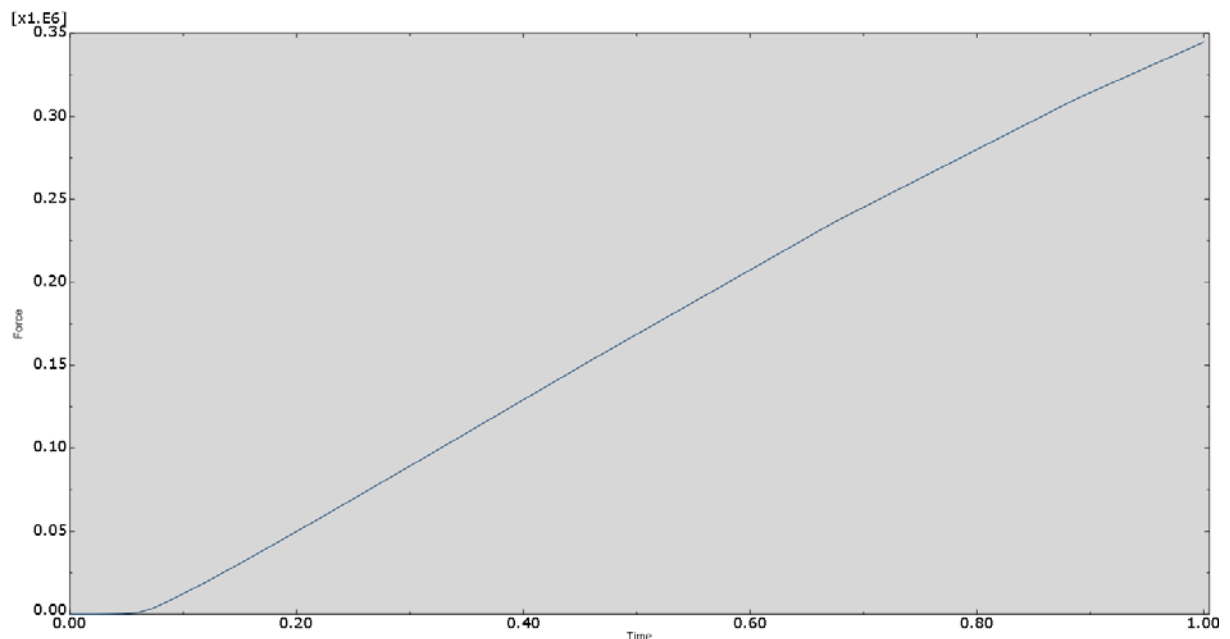
Fig 3.71 The total contact force between the hub/disc profile and the clamp segment provided a force of 345kN.

As mentioned in chapter 3.3.1, the cap was subjected to some regions with global yielding. Some minor design changes were performed to compensate for this. However, these changes were not sufficient and a further optimization of the design will be a part of recommendation for further work.
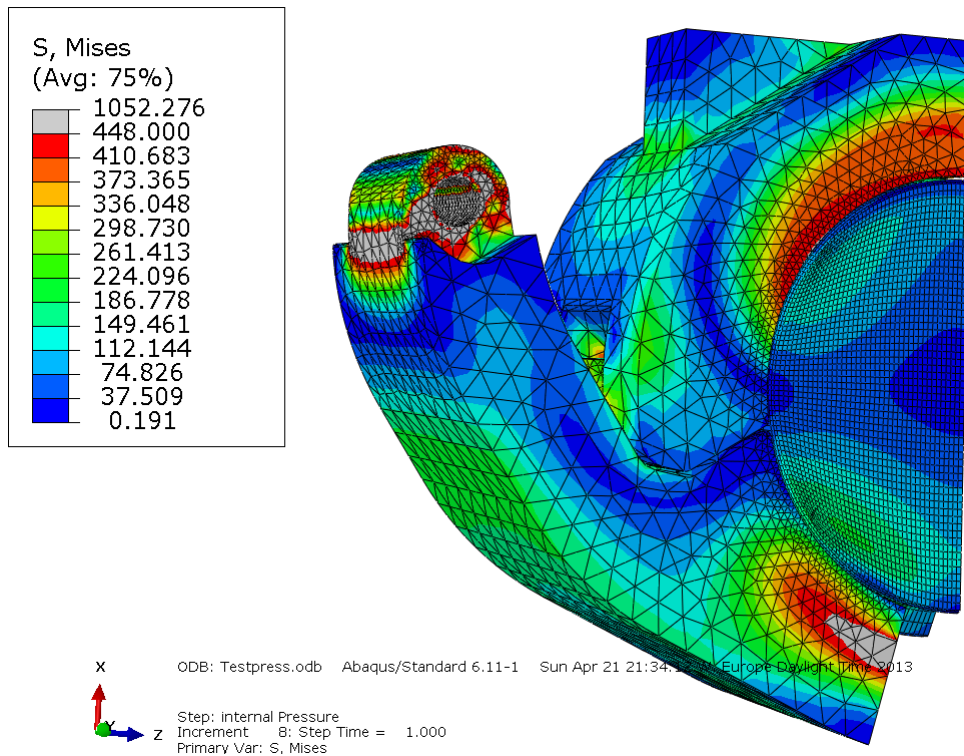
***Fig 3.72** The attachment hole for the linkages and the end of the lower clamp segment undergoes an excessive stress level.*
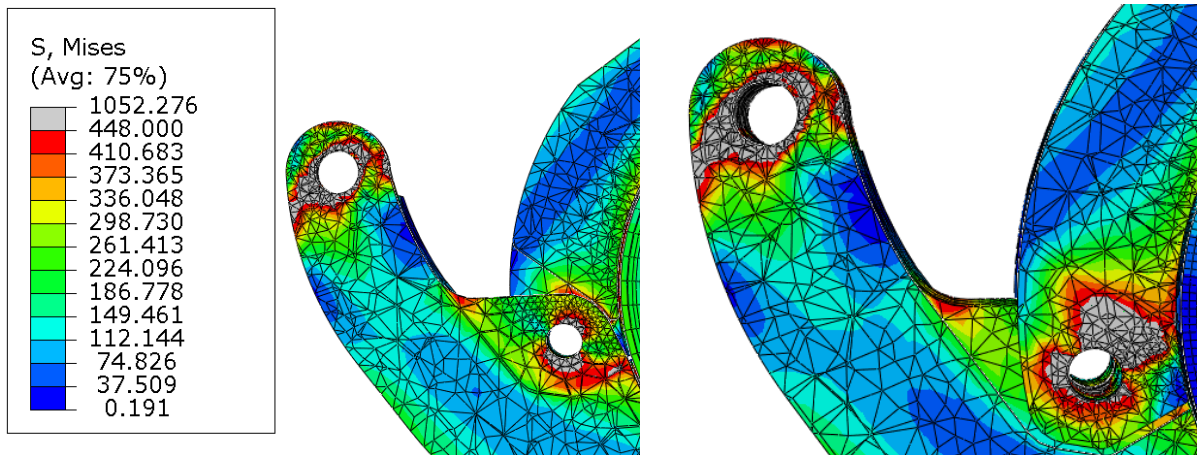
***Fig 3.73** Cross section of the clamp segment. The hinge hole on the lower clamp segment is subjected to global yielding.*

***Fig 3.74** Cross section of the clamp segments. The hinge hole on the upper clamp segment is subjected to global yielding.*

To deal with these high stress regions the radial diameter of the clamp segments can be increased in size and the bolt size for the hinge could also be increased. This will most likely cause the stress level to be decreased. A larger thickness around the linkage attachment hole can also be implemented in the design to reduce the stress.

DESIGN PRESSURE

To investigate the separation in the region where the elastomer sealing is placed, a circular path was created in the same perimeter as the seal diameter.
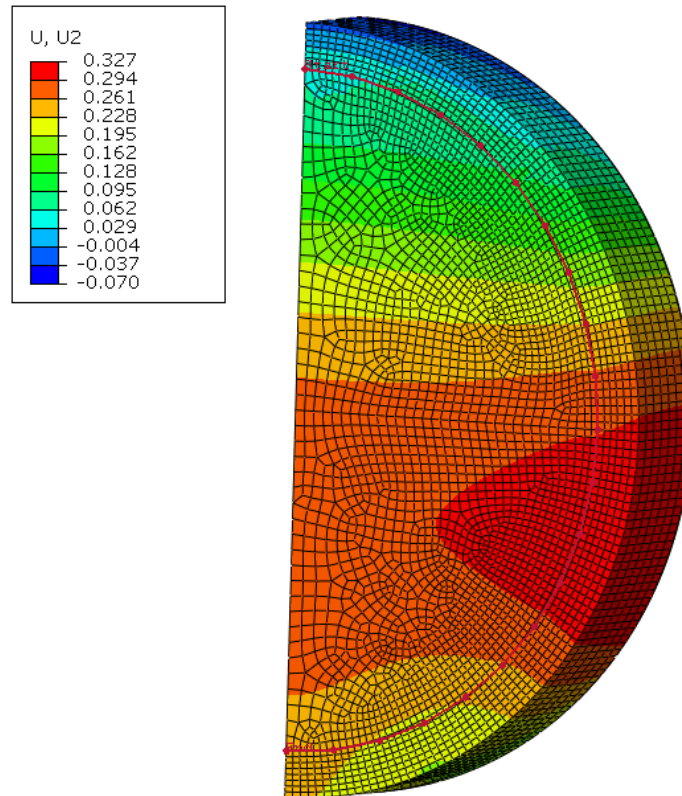
Fig 3.75 *A deformation plot of the cap disc that show a small deformation at the top of the disc and larger deformation at the middle and the bottom.*
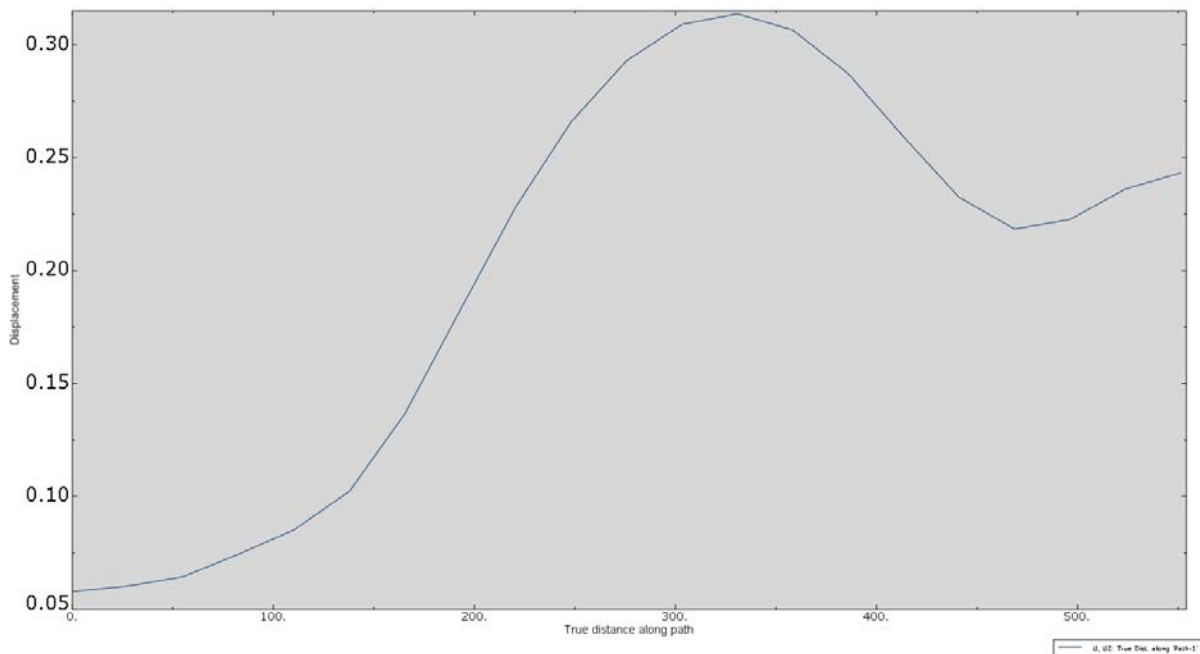
Fig 3.76 *A plot of the deformation through the path. The deformation has a peek nearly at the middle of the circumference where it has a separation of 0.31mm. The peak separation is located right below the clamp segment hinge.*

The analysis show that the deformation is less on the hub face compared to the cap disc face. This is because of the clamp segments that does not maintain a full support of the connection around the whole cap disc circumference. The areas with lack of support will be exposed for a larger separation.

These areas are found in two places, at the clamp segments hinge and at the bottom of the connection where it is no segments to support.

TEST PRESSURE
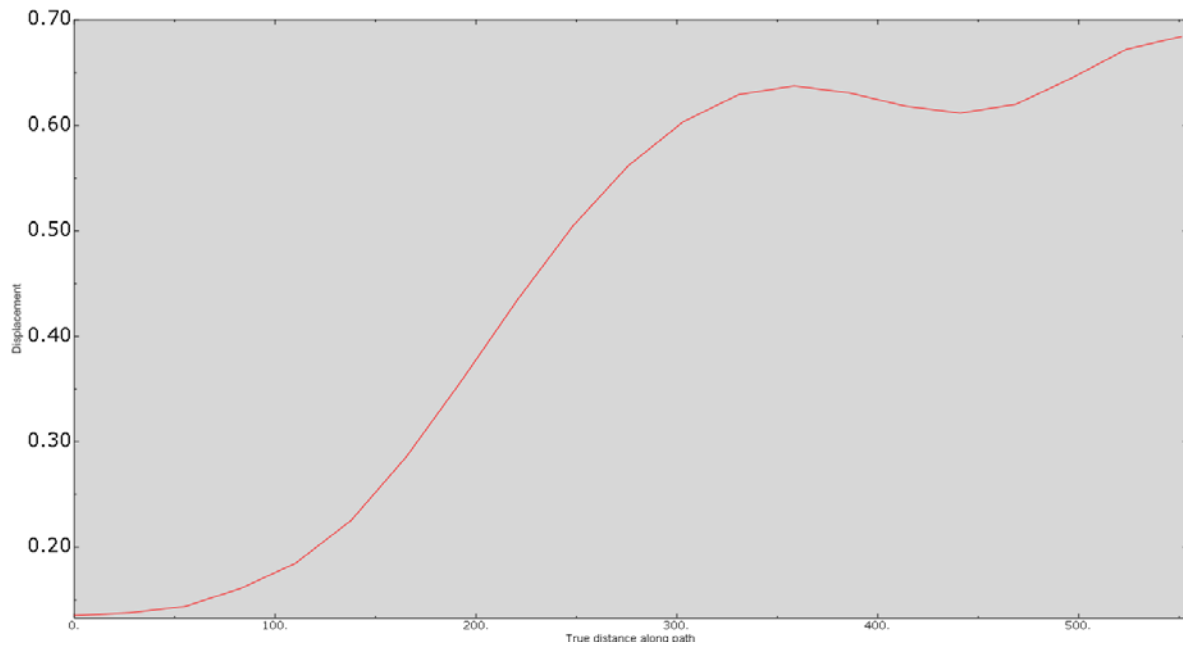
__Fig 3.77__ The deformation obtained at the seal region with test pressure, a maximum separation of 0.68mm was obtained at the end of the clamp segment.

The cap disc has a different behaviour when it is exposed for the test pressure. The peak separation changes location. The location of the peak stress is at the bottom of the clamp segment and not close to the clamp hinge as it was for the design pressure.

3.5   PRESENTATION OF THE FINAL DESIGN

The new design has been submit to some changes compared with the preliminary design. Most of these changes have been carried out in order make a stronger design.
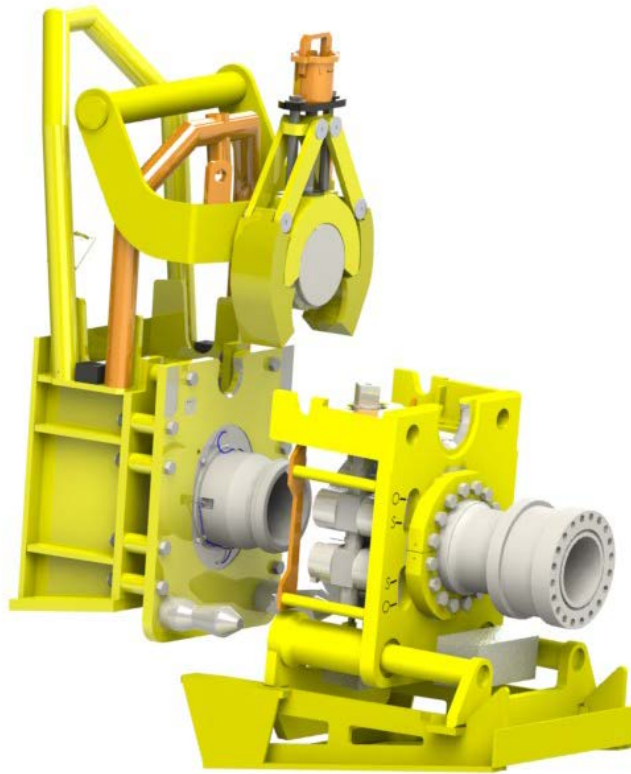
***Fig 3.78** The cap is being landed on the porch. It is intended that the cap utilizes the existing guiding structure on the porch.*
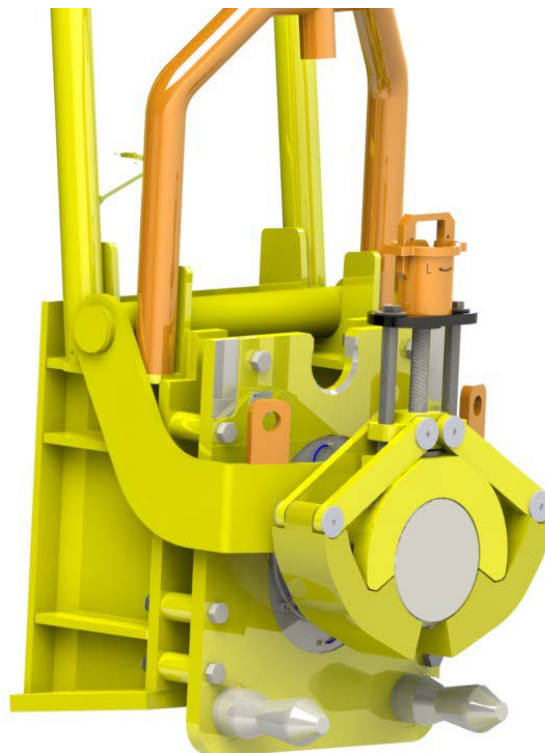
***Fig 3.79** The temporary pressure cap mounted on the IB hub.*
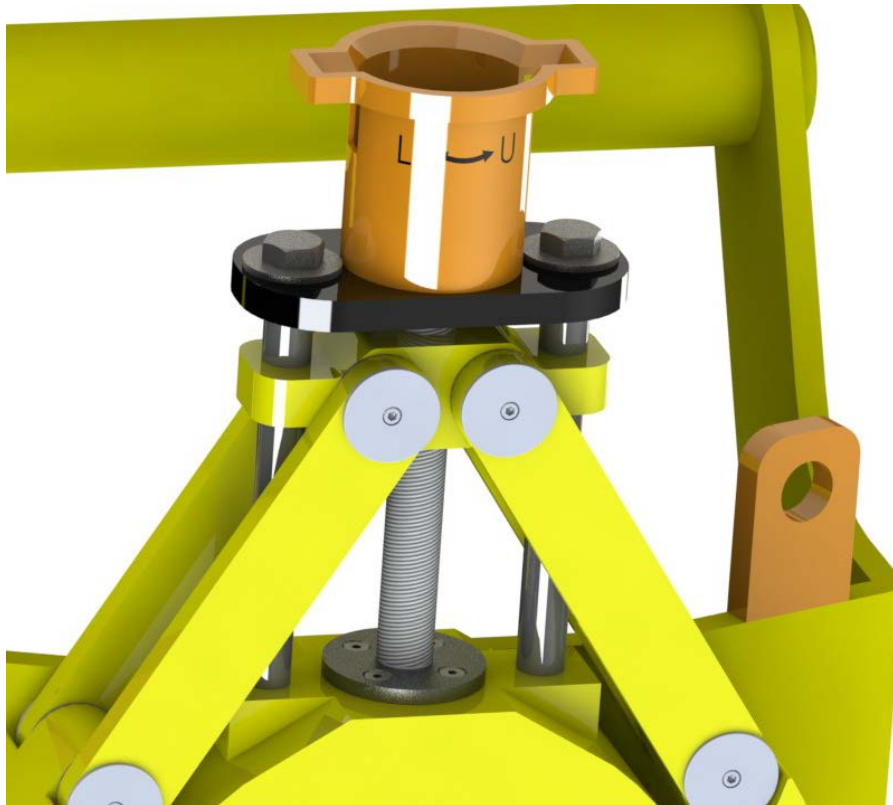
Fig 3.80 Frontside of the locking mechanism. The cap is in open position.
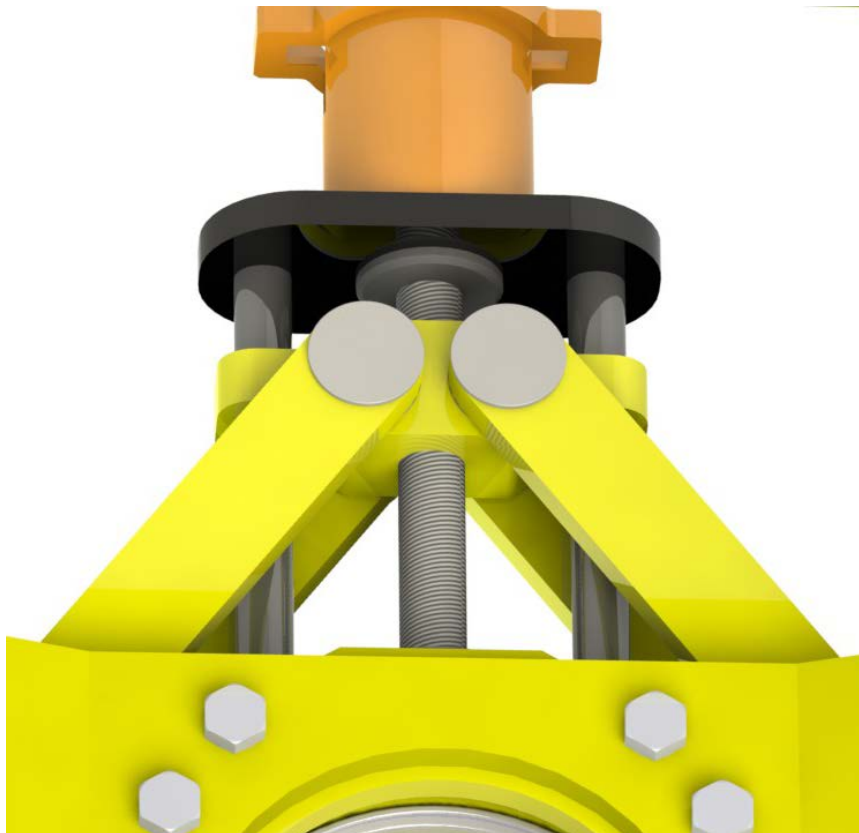
Fig 3.81 The backside of the locking mechanism.
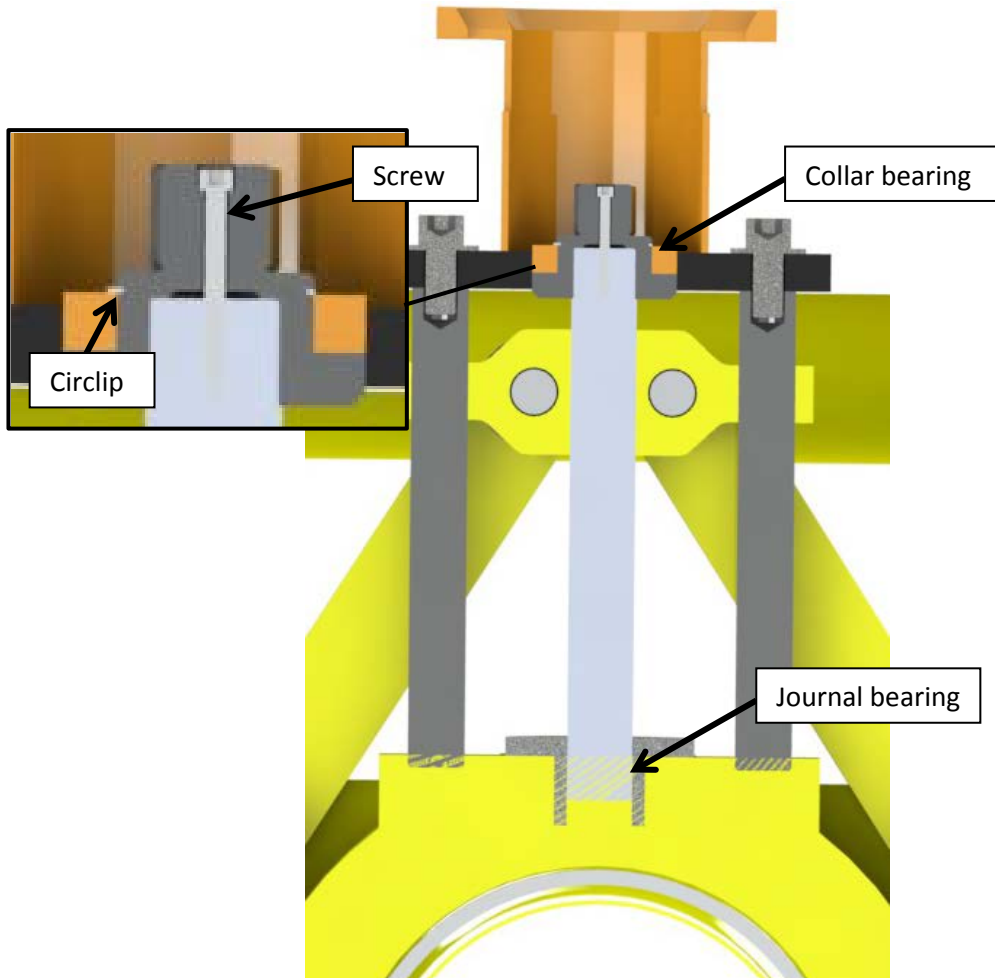
Fig 3.82 A section view of the locking mechanism in open position. The power screw has a collar bearing at the top and a journal bearing at the bottom.
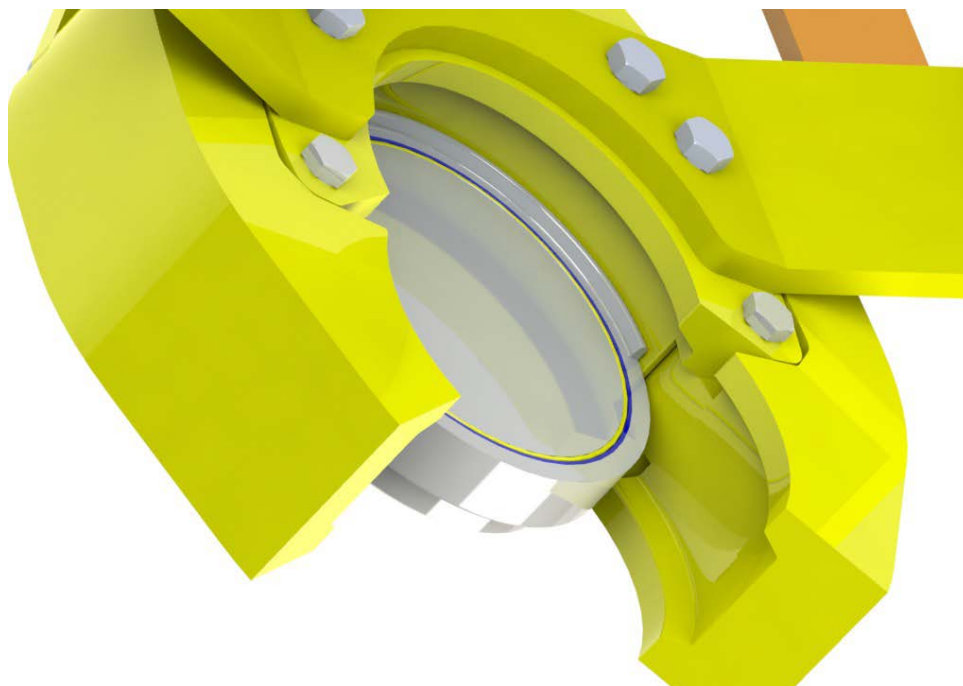
Fig 3.83 Backside of the cap.

4   EVALUATION AND DISCUSSION

4.1   PROJECT EVALUATION

This master thesis was initiated with a literature study to obtain suitable mathematical formulas and general information for dimensioning the different components. Several of the findings provided a step by step approach that was convenient when designing some of the components against static loads.

When the investigation of the preliminary design started, the clamp force was determined before the applied load for the locking mechanism was calculated. The hand calculated result was verified with a simplified light FEA model that had a fast computation time. The hand calculations, Ansys Classic and SolidWorks Simulation were in accordance with each other and provided confidence of the obtained values. Since the preliminary design was rejected, the modified design will be discussed further in the evaluation and discussion chapter.

It was intended that the cap was to be designed in accordance with the prevailing standards for subsea equipment and pressure containing components. Some rules and regulations have been collected from the standard. For instance the equation 2.1 for determining the clamp force was conducted from the ASME VIII Div. 2 standard and the test pressure was conducted from the API 6A (ISO 13628) standard. A comprehensive research is necessary when studying the different standards and understanding the prevailing directions and rules. Because of the relative short time duration of the master thesis, the design was generally controlled by allowable and principle stress theory. If the design is to be developed further, the regulations and rules from the prevailing standards need to be examined more closely.

It would be advantageous to spend more time with the work in Abaqus, so that the clamp segments could be more optimized. This would also be useful for the mesh optimization, especially for the lower and upper clamp segment.

4.2   DESIGN REVIEW

4.2.1   *CONNECTION COMPONENTS*

The clamp segment has been subjected to some modifications. After the preliminary design, the lower clamp segment got a longer lever arm implemented. The analysis indicated areas with high stress concentrations. These stress areas are around the clamp shoulders and the hinge hole, both for the upper and lower clamp segments. Stress concentrations can also be found at the linkage attachment hole. The stress concentrations were decreased by modifying the design with a larger thickness of the lever arm and a larger radius of the hinge-eye. However, more optimization is needed in order to achieve an acceptable stress level. Modifications that could improve the stress levels at the linkages attachment hole could be to increase the eye radius so that more material is placed around the hole. To cope with the stress at the hinge joint, the diameter of the joint can be increased as well as the radial diameter of the clamp segments.

Before a further optimization is carried out, it is considered necessary that the boundary condition for the lower clamp segment is realistic. This is relevant for the linkage attachment hole where it potentially can be a wrong translation of the applied rotation. A boundary condition that may be more realistic is to insert a coupling in the hole and apply a rotation to it, instead of applying the rotation directly to the cylindrical surfaces as it is done in the current model. A reference point can

also be inserted and the reaction force that occurs can be plotted. These reaction forces should concur with the calculated normal force for the linkages.

It has not been accounted for the frictional loss that occurs in the pin joints in the Abaqus model. This would be beneficial to examine since it could verify the hand calculations.
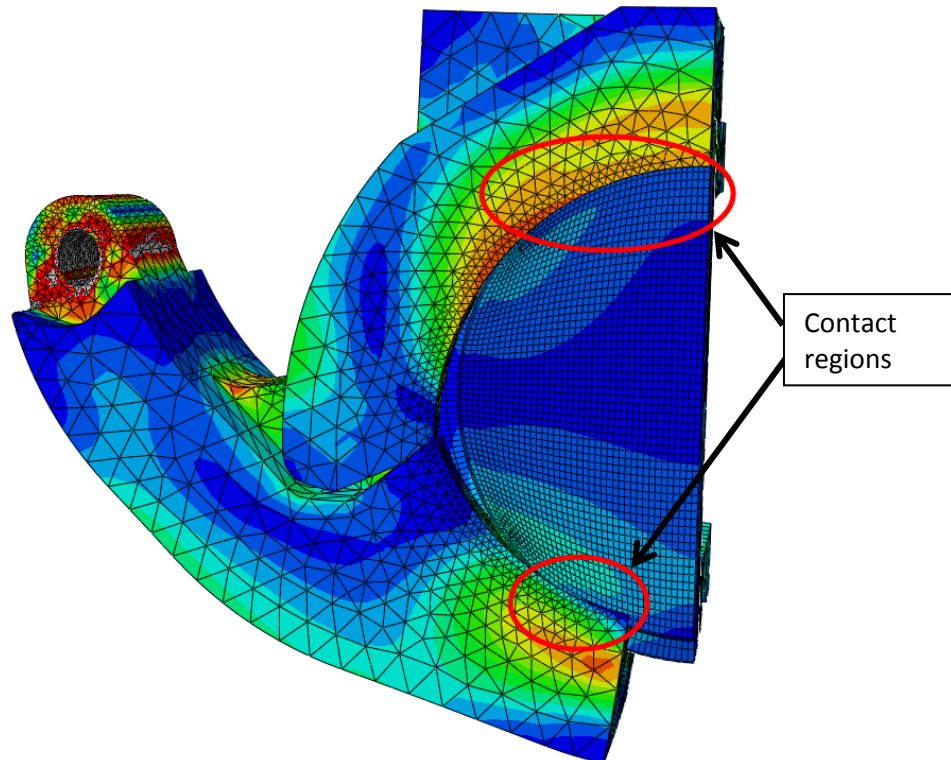
Fig 4.1 The region of the cap disc circumference next to the clamp hinge loses some contact. The plot is showed with a deformation scale factor of 13.6.

In chapter 2.3.1 it was assumed that most of the contact area of the connection was at the top of the upper clamp segment and at each end of the lower clamp segment. This assumption proved to be a reasonable match with the result from the analysis. This can be seen on the deformation plot (Fig 3.76) where the design pressure is applied. Less separation occurs at the top of the upper clamp segment and at the end of the lower clamp segments (Fig 4.1). This indicates that the connection has most of the contact area divided at the top and at the bottom of the connection.
The calculated separation that occurs at the seal region does not match the result from the analysis. The main contributor to this is assumed to be the screw diagram that do not account for the bending moment that occur by the clamp shoulders which further result in a deflection. Additionally, the formulas predict that it is an evenly divided contact area around the circumference of the connection. But in reality, most of the contact area is on a limited area.

When consulting with competent personnel regarding seal selection it was indicated that it was possible to acquire a custom made sealing solution that could withstand the separation that occurred at the design pressure and at the test pressure. Yet, the separation magnitude can possible be reduced by means of optimizing the clamp geometry and reduce the circumference diameter of the elastomer seal itself. Another aspect is that the hydrostatic external pressure increases with the water depth. A water depth of 1500m gives an external pressure of approximately 150MPa which corresponds to a differential pressure of only 195MPa. In reality it is the differential pressure that influences the separation of the sealing area. This means that with an increased water depth the separation would be less. The water depth for the HCS could vary from 100m to 1500m [29]. The cap

is required to be operated on all water depths and a conservative assessment of the separation behaviour that neglects the differential pressure is reasonable.

4.2.2   *LOCKING MECHANISM*

The locking mechanism has been accounted for the frictional loss in the pin joints and at the power screw. It was used a frictional coefficient of 0.1 for the pin joints and 0.15 for the power screw threads and collar bearing. Selecting a correct frictional coefficient is usually not a straight forward decision because it depends on many factors like wearing, material properties, lubrication and velocity. When it comes to a frictional coefficient for the power screw threads it was found that tests that has been performed previously at AKS resulted in a frictional coefficient of 0.1 [56]. This value should be used later when the frictional loss off the power screw threads needs to be calculated. It has not been accounted for the frictional loss between the guide bars and the horizontal nut. However, this frictional loss should have a minor change of the result.

The ROV bucket is a standard component and the design should be duplicated. The support bracket for the ROV bucket with the guide bars has not been investigated against static loads. This task is considered as fairly manageable to perform since the geometry is not complex. The horizontal plate was controlled against bending moment and shearing failure of the threads. Still, more investigation is required to dimension the horizontal plate completely against static loads.

The loading scenario for the release of the cap has not been investigated in this thesis. The power screw most likely needs a collar bearing at the bottom of the screw so that it can tolerate a compression in the lower part. This is considered as fairly easy to implement. The linkages needs to be dimensioned against rapture by pure tension, edge shearing or tearing since tension in the linkages are occurring. This is also considered as a fairly easy task to perform. If the cap concept is to be developed further, all the components needs to be assessed for this loading scenario.

5   CONCLUSION

This master thesis contains a description of the design of a new Temporary Subsea Installable pressure cap for Aker Solutions horizontal connection system. The main objectives were to investigate and design a locking mechanism and assess whether the connection components withstands the applied load, where a critical factor is the separation that occurs at the sealing area. After the preliminary design was assessed, it was rejected since it did not withstand the applied load and a new design proposal was generated.

Several components were designed against static loads that were performed through hand calculations and finite element analysis. The separation at the sealing area was found to be 0.31mm with the design pressure. More time is needed to get a satisfying design that could withstand the applied load within allowable limits.

The design presented in this thesis should be considered as a design with the potential to be a new temporary pressure cap.

5.1   RESULTS AND RECOMMENDATIONS

The most important results and findings are listed for the developed design:
- The power screw has been controlled for buckling, crushing and shearing failure. It has also been accounted for a frictional loss.
- The pin joints are controlled for bending moment and shearing failure. It has also been accounted for frictional loss.
- The linkages have been controlled for yielding, buckling and crushing failure.
- The horizontal plate (nut) has been controlled against bending moment and shearing failure at the threads.
- The clamp force has been determined and the required applied load by the power screw has been determined. The result has been verified through a FEA model in Ansys Classic and SolidWorks. The Power screw needs a torsional moment of 3.4kNm to produce a load of 294kN.
- A new ROV bucket support bracket design has been proposed and has potential to have a second contingency release.
- The maximum separation is found to be 0.31mm with the design pressure and 0.68mm with the test pressure. It should be possible to make a costume made seal that can withstand these separations values and it most likely exist possibilities to reduce the separation even more.

5.2   RECOMMANDATIONS FOR FURTHER WORK

The development of a new temporary pressure cap design is some steps forward in the development process. If the design is to be developed further, it is naturally to perform several tasks in order to end up with a more complete design:
- Perform an economical study for the cap where the development cost and sale prize can be estimated.
- Compare the calculated frictional loss of the pin joints with a FEA model.
- Dimension the ROV bracket with the guide bars against static loads.
- Perform an optimization study of the clamp segments to reduce the stress levels.
- Perform a convergence study of the FEA model to assure for a realistic result.
- Be sure that the boundary condition for the clamp force is realistic in the FEA model.
- Develop a guiding and aligning solution for the cap (This includes performing a tolerance study.)
- Investigate the intellectual property rights (IPR) considerations for the cap.

- Investigate whether the design could be scaled to other hub dimensions.
- Develop a mathematical model for the separation that occurs.
- Verify/Qualify the design in accordance with prevailing standards.
- Develop a solution for attaching the cap disc to the upper clamp segment.
- Investigate the static load scenario when the mechanism is to be released (dimensioning the components).
- Make manufacturing drawings of the components.
- Investigate the feasibility to use the cap on both flexible and rigid connections.
- Develop a guiding structure that enables it to be removed from the cap body (this could potentially enable a flexible termination to be landed while the cap is mounted to the IB hub).

6   REFERENCES

6.1   PRINTED SOURCES

[04] Yong Bai and Qiang Bai, Subsea Engineering Handbook, Gulf Professional Publishing, Burlington, USA, 2012, page 4-6,ISBN 978-0-12-397804-2

[05] Yong Bai and Qiang Bai, Subsea Engineering Handbook, Gulf Professional Publishing, Burlington, USA, 2012, page 11,ISBN 978-0-12-397804-2

[11] Yong Bai and Qiang Bai, Subsea Engineering Handbook, Gulf Professional Publishing, Burlington, USA, 2012, page 664-665,ISBN 978-0-12-397804-2

[15] N/A, Installation outline procedure HCS-U 12", Aker Solutions, Fornebu, Norway, page 27

[16] Kanitkar S. M., OMM IB PRESSURE CAP, Aker Solutions, Fornebu, Norway, page 6

[17] Dragland H. E., OMM 12" Temp. Pressure cap, Aker Solutions, Fornebu, Norway, page 10

[18] N/A, Connectors and Tie-In Systems (HCS), component description Aker Solutions, Fornebu, Norway, 2011, page 19

[19] Miklayev A., Omm, Torque tool, 17knm, - Display & cj operation & Maintenance manual rov tooling.

[21] Carlgren M., Omm, Stroke tool, HCS/HCM, 45t operation & maintenance manual Tie-In tooling.

[22] Haug H., First Pull in & Tie In of Skuld HCS Termination, power point, Norway, 09.09.2012, page 2

[25] Ulrich K. T., Eppinger S. D., Product design and development, McGraw-Hill, New York, USA, 2008, Page 74, ISBN 978-007-125947-7

[30] N/A, ASME VIII Rules for construction of pressure vessels, Division 2, New York, USA, 2011, page 418.

[31] N/A, ASME VIII Rules for construction of pressure vessels, Division 2, New York, USA, 2011, page 424.

[32] Terjesen G., Formler og tabeller, UMB, Ås, Norge, 2012, Page 5

[33] Waløen Å. Ø., Maskindeler, bind 1, Tapir forlag, Norway, 1994, page 116-119, ISBN 82-519-0920-1

[35] Hibbeler R.C., Statics and mechanics of materials, Printive Hall, Singapore, 2004, page 187, ISBN 013-129-011-8

[36] Phakatkar H.G., Theory of machines and mechanisms ll, Pragati books PVT. LTD, Pune, India, 2008, page 40, ISBN 818579095-7

[37] Phakatkar H.G., Theory of machines and mechanisms ll, Pragati books PVT. LTD, Pune, India, 2008, page 2, ISBN 818579095-7

[38] Phakatkar H.G., Theory of machines and mechanisms ll, Pragati books PVT. LTD, Pune, India, 2008, page 41, ISBN 818579095-7

[39] Terjesen G. Prosjektering av stålkonstruksjoner, tema: skrueforbindelser, IMT/UMB, Ås, Norway, 2012, page 11

[40] Bhandari V.B., Design of machine elements, Third edition, Tata McGraw-Hill publishing, New Delhi, India, 2010, page 97, ISBN 978-0-07-068179-8

[41] Vollen Ø., Mekanikk for Ingeniører, statikk og fasthetslære, 2. Edition, NKI forlaget, Bekkestua, Norway, 2010, page 337, ISBN 978-82-562-7152-8

[42] Giek K. and Giek R., Engineering formulas, Eight edition, McGraw-Hill, Germany, 2006, page P22, ISBN 0-07-145774-7

[43] Vollen Ø., Mekanikk for Ingeniører, statikk og fasthetslære, 2. Edition, NKI forlaget, Bekkestua, Norway, 2010, page 336, ISBN 978-82-562-7152-8

[44] Vollen Ø., Mekanikk for Ingeniører, statikk og fasthetslære, 2. Edition, NKI forlaget, Bekkestua, Norway, 2010, page 338, ISBN 978-82-562-7152-8

[45] Vollen Ø., Mekanikk for Ingeniører, statikk og fasthetslære, 2. Edition, NKI forlaget, Bekkestua,

Norway, 2010, page 343, ISBN 978-82-562-7152-8

[46] Bhandari V.B., Design of machine elements, Third edition, Tata McGraw-Hill publishing, New Delhi, India, 2010, page 185, ISBN 978-0-07-068179-8

[47] Bhandari V.B., Design of machine elements, Third edition, Tata McGraw-Hill publishing, New Delhi, India, 2010, page 194, ISBN 978-0-07-068179-8

[48] Bhandari V.B., Design of machine elements, Third edition, Tata McGraw-Hill publishing, New Delhi, India, 2010, page 188, ISBN 978-0-07-068179-8

[49] Bhandari V.B., Design of machine elements, Third edition, Tata McGraw-Hill publishing, New Delhi, India, 2010, page 193, ISBN 978-0-07-068179-8

[50] Bhandari V.B., Design of machine elements, Third edition, Tata McGraw-Hill publishing, New Delhi, India, 2010, page 195, ISBN 978-0-07-068179-8

[51] Bhandari V.B., Design of machine elements, Third edition, Tata McGraw-Hill publishing, New Delhi, India, 2010, page 196, ISBN 978-0-07-068179-8

[52] Dr D. M. McStravick, Mechanical Design applications, Power point, Rice University, Houston, USA, Spring 2007, page 17

[53] Dahlvig G., Christensen S. and Strømsnes G., Konstruksjonselementer 2. edition, gyldendal norsk forlag AS, Aurskog, Norway, 2005, page 91, ISBN 82-585-0700-1

[54] Terjesen G., Kompendium 4, utmatting av bolter, Norway, Page 11

6.2 MEDIA SOURCES

[13] Animated movie of the installation of the rigid HCS, Aker Solutions property

[14] Animated movie of the installation of the flexible HCS, Aker Solutions property

6.3 ONLINE SOURCES

[01] Norwegian continental shelf, Norwegian petroleum directorate, http://npd.no

[02] The publication "facts" chapter 3 -The petroleum sector – Norway's largest industry, Norwegian petroleum directorate, http://npd.no

[03] Who we are and what we do, Aker Solutions, http://www.akersolutions.com

[06] Subsea field, Oceanicconsultants-nigeria, http://www.oceanicconsultans-nigeria.com

[07] Subsea field, Exploration & production magazine, http://www.epmag.com

[08] Vertical connection system brochure, Aker Solutions, http://www.akersolutions.com

[09] Aker solutions connection systems, Aker Solutions, http://www.akersolutions.com

[10] Horizontal connection system brochure, Aker Solutions, http://www.akersolutions.com

[20] Torque tools and control systems, Velocious, http://www.velocious.com.au

[34] Table of friction coefficient, Engineering handbook, http://www.engineershandbook.com/

6.4 PERSONAL COMMINICATION

[12] 19.10.2012,Hogne Haug, Test engineer SIT, Ove Andreassen, Specialist engineer lifecycle technology, Anders Austad, tie-in and tooling specialist engineer, Meeting agenda: Gather information about HCS installation, recommendations for a new cap concept.

[23] 11.10.2012 Alexandre, Varasson, manager tender, Rodrigo Cabral, manager tender, Tristan Delahousse, tender manager, meeting agenda: Establish customer needs.

[24] 04.10.2012, Snorre Balkøy, Manager ROV/3D Studies, Meeting regarding concept design and offshore installation experience.

[26] 26.10.2012, Anders Rynning, senior engineer, email with information regarding hub dimension and design pressure.

[27] 26.10.2012 Lars Haga, manager tie-in product and technology, Anders Rynning, senior engineer, Per Höglund, product responsible for caps, Snorre Balkøy, Manager ROV/3D Studies, Agenda on

the meeting: concept brainstorming and concept selection.

[28] 14.11.2012, Martin Stegberg, manager tie-in department, contacted by telephone and e-mail regarding marginal values between porch and termination on HCS.

[29] 26.04.2013, Dag Emanuelsson, product manager for subsea caps, Conversation regarding water depth for HCS.

[55] 25.04.2013, Andre Putkowski, Representative from Seal Engineering, Communication by telephone and e-mail regarding seal selection.

[56] 17.04.2013, Møgedal Knut, First Chief Engineer tie-in, meeting regarding calculations results.

7   APPENDIX

7.1   APPANDIX 1, ANSYS CLASSIC SOURCE CODE FOR THE PRELIMINARY DESIGN

```
Finish
/clear
/COM,ANSYS RELEASE 14.0    UP20111024      17:39:45    10/31/2012
/TITLE,vertical force determination at lower clampsegment
!---------------------------------------------------------------------
! Data input
!---------------------------------------------------------------------
/prep7
ET,1,BEAM189
MP,EX,1,2.1E+11
MP,PRXY,1,0.3      ! Setting poissons-ratio for material 1 in x-y(and others by default)

SECTYPE,   1, BEAM, RECT, Horizontalplate, 0
SECOFFSET, CENT
SECDATA,30,150,0,0,0,0,0,0,0,0,0,0

SECTYPE,   2, BEAM, RECT, Momentarm, 0
SECOFFSET, CENT
SECDATA,60,38,0,0,0,0,0,0,0,0,0,0

SECTYPE,   3, BEAM, RECT, clamplug, 0
SECOFFSET, CENT
SECDATA,100,100,0,0,0,0,0,0,0,0,0,0

SECTYPE,   4, BEAM, RECT, clampsegment, 0
SECOFFSET, CENT
SECDATA,144.4,200,0,0,0,0,0,0,0,0,0,0


!---------------------------------------------------------------------
!  Establish data input for pin joint
!---------------------------------------------------------------------
K,1,  -420, 292,0,
k,2,  -420, 292,0,
k,3,    0, 292,0,
K,4,   420, 292,0,
K,5,   420, 292,0,
K,6,-332.8,-118.8,0,
K,7,-332.8,-118.8,0,
K,8, 332.8,-118.8,0,
K,9, 332.8,-118.8,0,
K,10,-248.4,  -28,0,
K,11, 248.4,  -28,0,
K,12,    0, -234,0,
K,13,    0, -234,0,
k,14,    0,    0,0

LSTR,    1,    3 !1
LSTR,    3,    4 !2
LSTR,    2,    6 !3
LSTR,    5,    8 !4
LSTR,    7,   10 !5
LSTR,    9,   11 !6

LARC, 10, 12, 14,248,4  !7
LARC, 11, 13, 14,248,4  !8

!********************* meshing****************
!LATT, MAT, REAL, TYPE, --, KB, KE, SECNUM !Associates element attributes with the selected, unmeshed lines.
!LSEL, Type, Item, Comp, VMIN, VMAX, VINC, KSWP !This function selects lines.

LESIZE,ALL,35, , , ,1, , ,1,

LSEL,S,LINE,,1,2,,
LATT, 1, ,1 , ,,,1
```

```
lmesh,all

LSEL,S,LINE,,3,4,,
LATT, 1, ,1 , ,,,2

lmesh,all

LSEL,S,LINE,,5,,,
LSEL,a,LINE,,6,,,
LATT, 1, ,1 , ,,,3

lmesh,all

LSEL,S,LINE,,7,,,
LSEL,a,LINE,,8,,,
LATT, 1, ,1 ,,,,4
lmesh,all


!lmesh,all


/ESHAPE,1
/REPLOT
!*********************Done meshing***************

nsel,s,,,1 ! selecting the two master nodes
nsel,a,,,50
cp,1,ux,all ! coupled in UX, relative to the Remote Force/Displacement coordinate system
cp,2,uy,all
cp,3,uz,all
cp,4,rotx,all
cp,5,roty,all

nsel,none

nsel,s,,,26 ! selecting the two master nodes
nsel,a,,,75
cp,6,ux,all ! coupled in UX, relative to the Remote Force/Displacement coordinate system
cp,7,uy,all
cp,8,uz,all
cp,9,rotx,all
cp,10,roty,all

nsel,none

nsel,s,,,51 ! selecting the two master nodes
nsel,a,,,100
cp,11,ux,all ! coupled in UX, relative to the Remote Force/Displacement coordinate system
cp,12,uy,all
cp,13,uz,all
cp,14,rotx,all
cp,15,roty,all

nsel,none

nsel,s,,,76 ! selecting the two master nodes
nsel,a,,,109
cp,16,ux,all ! coupled in UX, relative to the Remote Force/Displacement coordinate system
cp,17,uy,all
cp,18,uz,all
cp,19,rotx,all
cp,20,roty,all

!nsel,s,,,118 ! selecting the two master nodes
!nsel,a,,,140
!cp,21,ux,all ! coupled in UX, relative to the Remote Force/Displacement coordinate system
!cp,22,uy,all
!cp,23,uz,all
!cp,24,rotx,all
!cp,25,roty,all
```

```
/solu

FK,3,FY,-1642850,8

Ksel,s,,,1,2
Ksel,a,,,4,5
DK,all, , , ,0,,UX, , , , ,
ksel,none

Ksel,s,,,12,13
DK,all, , , ,0,,,UY , , , ,
ksel,none

Ksel,s,,,1,14,
DK,all, , , ,0,UZ,, , , , ,
ksel,none

Ksel,s,,,10
Ksel,a,,,11
DK,all, , , ,0,UX,UY,,ROTX,ROTY, ,
ksel,none

allsel,all
NLGEOM, off
SOLVE
FINISH
/POST1
/ESHAPE,1
/REPLOT
ETABLE,FXJ,SMISC, 14
ETABLE,FXI,SMISC, 1
ETABLE,SFYJ,SMISC, 19
ETABLE,SFYI,SMISC, 6
ETABLE,SFZJ,SMISC, 18
ETABLE,SFZI,SMISC, 5
ETABLE,MZJ,SMISC, 16
ETABLE,MZI,SMISC, 3
```

7.2　APPENDIX 2, ANSYS CLASSIC SOURCE CODE FOR THE MODIFIED DESIGN

```
Finish
/clear
/COM,ANSYS RELEASE 14.0   UP20111024     17:39:45   10/31/2012
/TITLE,vertical force determination on lower clampsegment
!----------------------------------------------------------------------
! Data input
!----------------------------------------------------------------------
/prep7
ET,1,BEAM189
MP,EX,1,2.1E+11
MP,PRXY,1,0.3      ! Setting poissons-ratio for material 1 in x-y(and others by default)

SECTYPE,  1, BEAM, RECT, Horizontalplate, 0
SECOFFSET, CENT
SECDATA,100,100,0,0,0,0,0,0,0,0,0,0

SECTYPE,  2, BEAM, RECT, linkage, 0
SECOFFSET, CENT
SECDATA,60,80,0,0,0,0,0,0,0,0,0,0

SECTYPE,  3, BEAM, RECT, torque arm, 0
SECOFFSET, CENT
SECDATA,100,150,0,0,0,0,0,0,0,0,0,0

SECTYPE,  4, BEAM, RECT, clampsegment, 0
SECOFFSET, CENT
SECDATA,112,200,0,0,0,0,0,0,0,0,0,0


!----------------------------------------------------------------------
! Establish data input for pin joints
!----------------------------------------------------------------------
K,1,  -55, 356.3,0,
k,2,  -55, 356.3,0,
k,3,    0, 356.3,
K,4,   55, 356.3,0,
K,5,   55, 356.3,0,
K,6,-430,130,0,
K,7,-430,130,0,
K,8, 430,130,0,
K,9, 430,130,0,
K,10,-248.4,  -28,0,
K,11, 248.4,  -28,0,
K,12,   -64.5, -225,0,
K,13,   64.5, -225,0,
k,14,   0,    0,0

LSTR,   1,    3 !1
LSTR,   3,    4 !2
LSTR,   2,    6 !3
LSTR,   5,    8 !4
LSTR,   7,   10 !5
LSTR,   9,   11 !6

LARC, 10, 12, 14,234  !7
LARC, 11, 13, 14,234  !8

!*******************Begynnelse meshing***************
!LATT, MAT, REAL, TYPE, --, KB, KE, SECNUM !Associates element attributes with the selected, unmeshed lines.
!LSEL, Type, Item, Comp, VMIN, VMAX, VINC, KSWP !This function selects lines.

LESIZE,ALL,35, , , ,1, , ,1,

LSEL,S,LINE,,1,2,,
LATT, 1, ,1 , ,,,1

lmesh,all

LSEL,S,LINE,,3,4,,
```

```
LATT, 1, ,1 , ,,,2

lmesh,all

LSEL,S,LINE,,5,,,
LSEL,a,LINE,,6,,,
LATT, 1, ,1 , ,,,3

lmesh,all

LSEL,S,LINE,,7,,,
LSEL,a,LINE,,8,,,
LATT, 1, ,1 ,,,,4
lmesh,all


!lmesh,all


/ESHAPE,1
/REPLOT
!**********************slutt***************

nsel,s,,,1 ! selecting the two master nodes
nsel,a,,,10
cp,1,ux,all ! coupled in UX, relative to the Remote Force/Displacement coordinate system
cp,2,uy,all
cp,3,uz,all
cp,4,rotx,all
cp,5,roty,all

nsel,none

nsel,s,,,6 ! selecting the two master nodes
nsel,a,,,37
cp,6,ux,all ! coupled in UX, relative to the Remote Force/Displacement coordinate system
cp,7,uy,all
cp,8,uz,all
cp,9,rotx,all
cp,10,roty,all

nsel,none

nsel,s,,,11 ! selecting the two master nodes
nsel,a,,,64
cp,11,ux,all ! coupled in UX, relative to the Remote Force/Displacement coordinate system
cp,12,uy,all
cp,13,uz,all
cp,14,rotx,all
cp,15,roty,all

nsel,none

nsel,s,,,38 ! selecting the two master nodes
nsel,a,,,79
cp,16,ux,all ! coupled in UX, relative to the Remote Force/Displacement coordinate system
cp,17,uy,all
cp,18,uz,all
cp,19,rotx,all
cp,20,roty,all

!nsel,s,,,118 ! selecting the two master nodes
!nsel,a,,,140
!cp,21,ux,all ! coupled in UX, relative to the Remote Force/Displacement coordinate system
!cp,22,uy,all
!cp,23,uz,all
!cp,24,rotx,all
!cp,25,roty,all

/solu
```
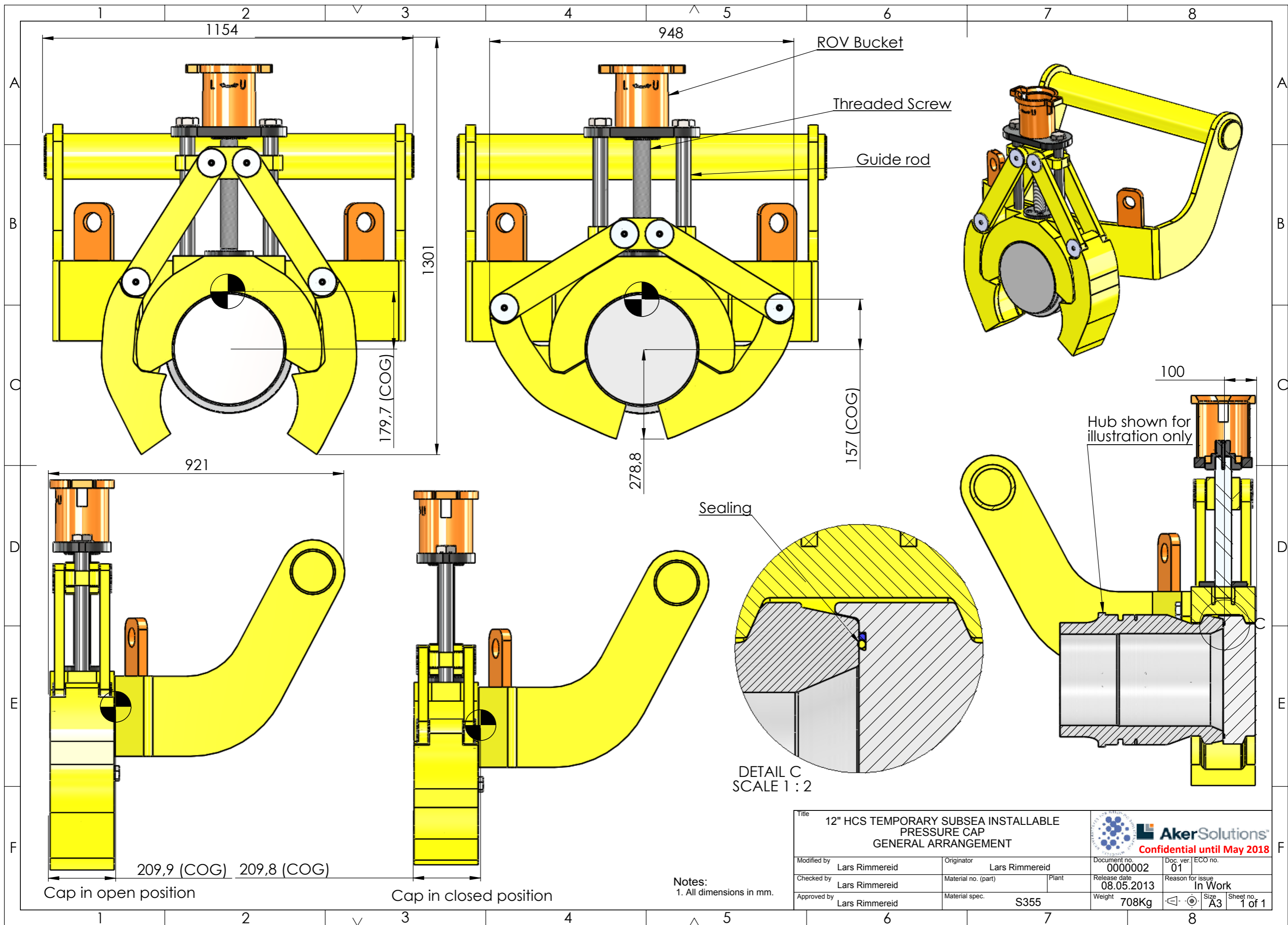
```
FK,3,FY,-286025

Ksel,s,,,1,2
Ksel,a,,,4,5
DK,all, , , ,0,,UX, , , , ,
ksel,none

Ksel,s,,,12,13
DK,all, , , ,0,,,UY , , , ,
ksel,none

Ksel,s,,,1,14,
DK,all, , , ,0,UZ,, , , , ,
ksel,none

Ksel,s,,,10
Ksel,a,,,11
DK,all, , , ,0,UX,UY,,ROTX,ROTY, ,
ksel,none

allsel,all
NLGEOM, off
SOLVE
FINISH
/POST1
/ESHAPE,1
/REPLOT
ETABLE,FXJ,SMISC, 14
ETABLE,FXI,SMISC, 1
ETABLE,SFYJ,SMISC, 19
ETABLE,SFYI,SMISC, 6
ETABLE,SFZJ,SMISC, 18
ETABLE,SFZI,SMISC, 5
ETABLE,MZJ,SMISC, 16
ETABLE,MZI,SMISC, 3
```
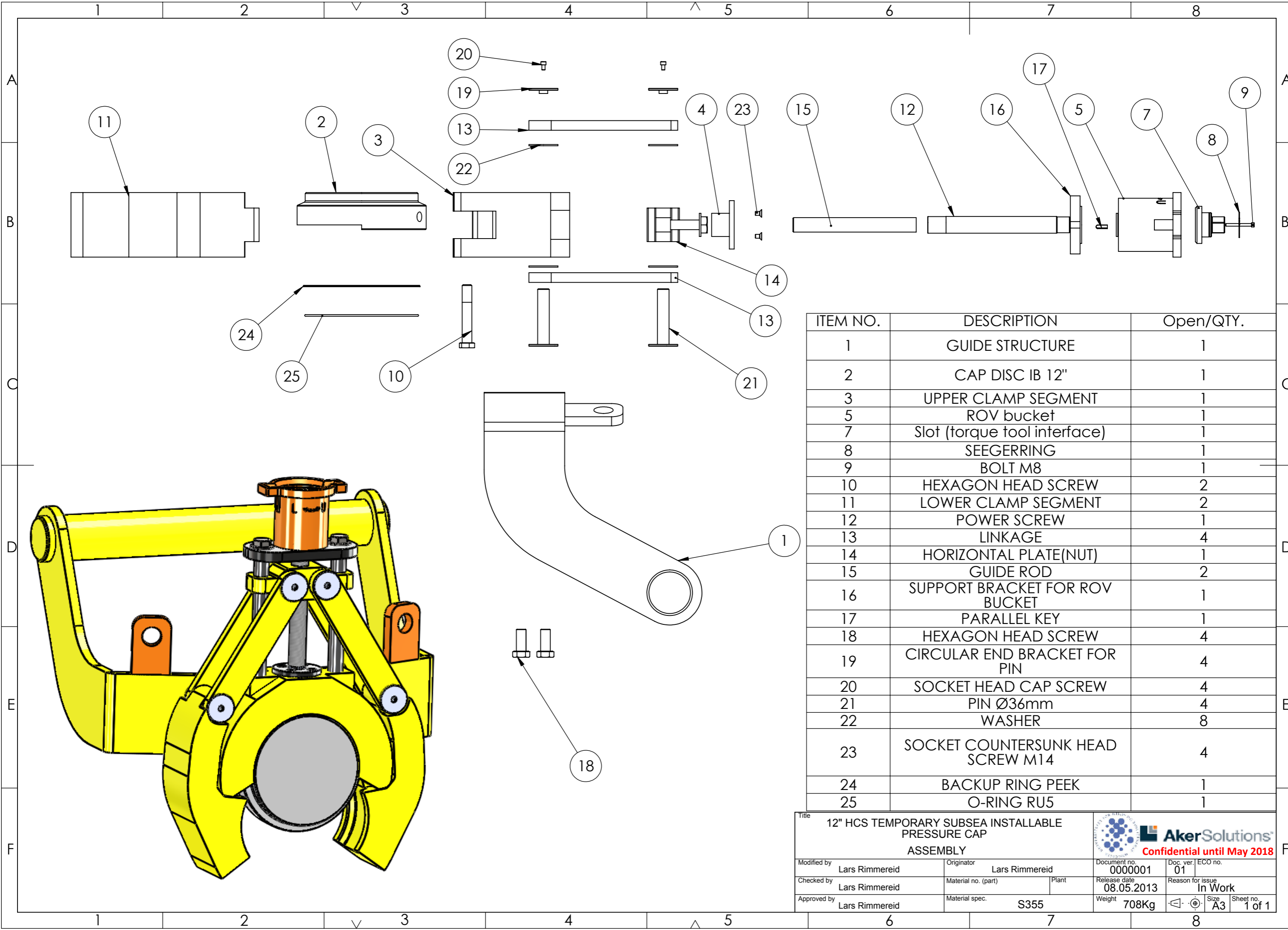
1154

948

ROV Bucket

Threaded Screw

Guide rod

1301

179,7 (COG)

157 (COG)

278,8

100

Hub shown for illustration only

921

Sealing

DETAIL C
SCALE 1 : 2

209,9 (COG)   209,8 (COG)

Cap in open position

Cap in closed position

Notes:
1. All dimensions in mm.

Title				
12" HCS TEMPORARY SUBSEA INSTALLABLE PRESSURE CAP GENERAL ARRANGEMENT				

Modified by Lars Rimmereid	Originator Lars Rimmereid		Document no. 0000002	Doc. ver. 01	ECO no.
Checked by Lars Rimmereid	Material no. (part)	Plant	Release date 08.05.2013	Reason for issue In Work	
Approved by Lars Rimmereid	Material spec. S355		Weight 708Kg	Size A3	Sheet no. 1 of 1

Aker Solutions

ITEM NO.	DESCRIPTION	Open/QTY.
1	GUIDE STRUCTURE	1
2	CAP DISC IB 12"	1
3	UPPER CLAMP SEGMENT	1
5	ROV bucket	1
7	Slot (torque tool interface)	1
8	SEEGERRING	1
9	BOLT M8	1
10	HEXAGON HEAD SCREW	2
11	LOWER CLAMP SEGMENT	2
12	POWER SCREW	1
13	LINKAGE	4
14	HORIZONTAL PLATE(NUT)	1
15	GUIDE ROD	2
16	SUPPORT BRACKET FOR ROV BUCKET	1
17	PARALLEL KEY	1
18	HEXAGON HEAD SCREW	4
19	CIRCULAR END BRACKET FOR PIN	4
20	SOCKET HEAD CAP SCREW	4
21	PIN Ø36mm	4
22	WASHER	8
23	SOCKET COUNTERSUNK HEAD SCREW M14	4
24	BACKUP RING PEEK	1
25	O-RING RU5	1

Title
12" HCS TEMPORARY SUBSEA INSTALLABLE PRESSURE CAP

ASSEMBLY

AkerSolutions

Confidential until May 2018

Modified by	Lars Rimmereid	Originator	Lars Rimmereid	Document no. 0000001	Doc. ver. 01	ECO no.
Checked by	Lars Rimmereid	Material no. (part)		Plant	Release date 08.05.2013	Reason for issue In Work
Approved by	Lars Rimmereid	Material spec. S355		Weight 708Kg	Size A3	Sheet no. 1 of 1